Open Ceramics 9 (2022) 100216

Contents lists available at ScienceDirect

Open Ceramics

journal homepage: www.sciencedirect.com/journal/open-ceramics

Review of space resources processing for Mars missions: Martian simulants, regolith bonding concepts and additive manufacturing

David Karl [a,*], Kevin M. Cannon [b], Aleksander Gurlo [a]

[a] Chair of Advanced Ceramic Materials, Institute of Materials Science and Technology, Technische Universitaet Berlin, Germany
[b] Department of Geology and Geological Engineering and the Center for Space Resources, Colorado School of Mines, Golden, CO, USA

ARTICLE INFO

Keywords:
space resources
In situ resource utilization (ISRU)
Mars regolith simulants
Materials processing
Regolith bonding concepts
Additive manufacturing

ABSTRACT

Scientific exploration of extraterrestrial planets has gripped human imagination since the advent of space travel. Human missions to Mars could produce insight into the essential questions of how, when and where life began on Earth. Such missions would only be feasible using local space resources materials, a concept called in situ resource utilization (ISRU). In the absence of organic materials from plants, the globally available oxidic surface minerals (regolith) are the only viable resource for large-scale construction efforts such as habitats, greenhouses, landing pads and equipment building. This review provides the first comprehensive literature review of ISRU materials research employing Martian simulants. It gives a detailed overview of all Mars simulants, their history, properties, and challenges, introducing a generational concept for simulants development. The available Mars simulant processing literature (including selected work on lunar simulants) is categorized into seven regolith bonding concepts. The state-of-the-art on additive manufacturing (AM) in ISRU research is discussed. Detailed feasibility assessments for all processing approaches are given, including overview graphs comparing the mechanical performance of each fusion concept with feedstock availability on the surface of Mars. Finally, major open questions and future challenges of materials processing for early Mars missions is examined.

1. Motivation for Mars missions

The origin of life has been described as the greatest scientific question of our times [1]. Humanity simply does not know how, where and when life started on Earth and little evidence exists to support the various theories that attempt to explain this puzzle. The prevailing assumption is that life is likely to have developed from inanimate matter, given the right circumstances such as time, high temperatures, liquid water and prebiotic chemistry [2]. While such claims are supported by the earliest evidence of life on Earth (~3.7–4.2 million-year-old fossilized microorganisms from early habitable environments in seafloor-hydrothermal vents [3]), the answer as to whether the formation of life is a commonplace or even deterministic process (and if it began on Earth), is unlikely to be answered on the basis of scientific evidence found on Earth alone. A good chance of learning where we ultimately came from might result from comparing Earth to Mars, an approach called comparative planetary evolution. While Earth's early record has been erased, Mars could offer direct evidence of the geochemical conditions prevalent on a prebiotic Earth [4].

Our current understanding of Mars is the result of numerous robotic missions, many of them spearheaded by the Mars Exploration Program (MEP) of the National Aeronautics and Space Administration (NASA), whose exploration programs are strongly focused on the search for life on Mars. A central MEP instrument for future mission planning is the Mars Exploration Program Analysis Group (MEPAG). MEPAG aspires to facilitate a process in which the scientific community reaches a consensus on the major goals for the scientific exploration of Mars. The MEPAG consensus for 2020 is summarized in four central goals: (i) to determine if Mars ever supported life or still supports life; (ii) to understand the processes and history of climate on Mars; (iii) to understand the origin and evolution of Mars as a geological system; and (iv) to prepare for human exploration of Mars [5].

After the Apollo program's end, a human mission to Mars has been viewed by many as the next logical step in exploring the solar system. The idea has captured our imagination and there are countless references in our past and present popular culture outlining such missions. For example, in recent years there has been a surge in best-selling books advocating Mars missions and discussing Mars settlement scenarios full of optimism about what might be possible [6–9]. However, conservative estimates by space agencies indicate the enormity of a scientific return

* Corresponding author.
E-mail address: david.karl@ceramics.tu-berlin.de (D. Karl).

https://doi.org/10.1016/j.oceram.2021.100216
Received 3 December 2021; Accepted 27 December 2021
Available online 30 December 2021

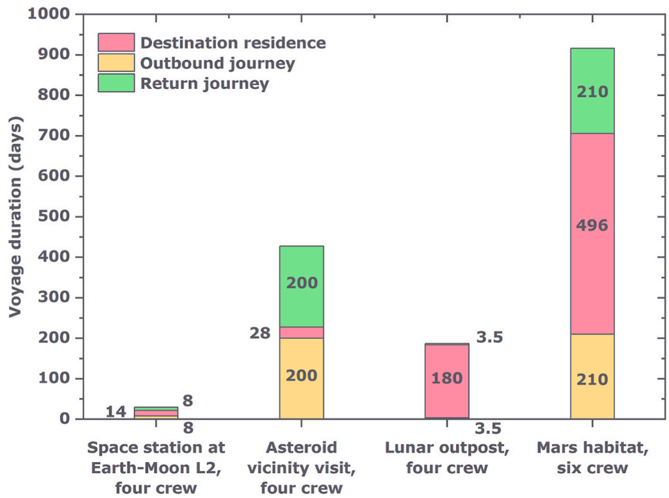

Fig. 1. Voyage duration of projected space missions. Data from Menezes et al. [10].

journey to Mars. In one such scenario, a notational crew of six astronauts would travel for 2 ½ years, with the ground crew needing to spend ~1 ½ years in a surface habitat under Mars gravity and radiation conditions. Because of the vast distances involved and the cost of launching supplies into space, it would be essential to make use of local resources, a concept known as in situ resource utilization (ISRU). ISRU is promulgated not only by NASA for Mars missions but also by the European Space Agency (mostly for Moon missions) and recently in the form of Space Resource Utilization (SRU) by numerous private companies in a buzzing new space sector.

2. Introduction to in situ resource utilization (ISRU) for space exploration

Earth-based space exploration is extraordinarily challenging and expensive, as all mass has to escape the gravity field of Earth and lifting propellant from Earth is a significant contributor to space exploration costs (99 units of mass are required to launch one unit of mass into space [10]). A central concept to reduce space exploration costs is called in situ resource utilization (ISRU). Sacksteder and Sanders define ISRU as "the collection, processing, storing and use of materials encountered in the course of human or robotic space exploration that replace materials that would otherwise be brought from Earth to accomplish a mission-critical need at reduced overall cost and risk" [11].

While futurists envision whole space economies from indigenous resources, space agencies make the point that ISRU is necessary to reduce the overall risk and cost of realistic space missions. In such a scenario, the cost of Earth-based materials and their space transportation has to be weighed against the cost associated with collecting, processing, storing, and using space resources. As a result of increased transport costs, the highest gains would be achieved the further away the resources were to be used [12].

The longest destination residence times envisaged for realistic space missions are for lunar outposts and Mars, rather than to the space station and asteroids (see Fig. 1); Space stations would include long residence times, but resources would all be non-local in origin. While a lunar outpost mission could have a residence time of 180 days, missions to Mars (such as missions proposed in the NASA Design Reference Architecture 5.0 [13]) would require a crew of six, with four astronauts staying in a surface habitat at 0.3 g and surface radiation conditions for ~500 Earth days. Such extensive residence times for Mars are inevitable because of the particular orbits of Earth and Mars, with the two coming closest to each other or 'at opposition' to each other only every 779.9 days.

Regarding transportation effort, mission scenarios for a lunar outpost would require the short outbound and return time of 3.5 days compared to 210 days outbound and return for Mars. Because there are significant costs associated with establishing ISRU, Donald Rapp, a leading ISRU researcher and co-PI of the Mars Oxygen In-Situ Resource Utilization Experiment (MOXIE) from Jet Propulsion Laboratory (JPL), concluded: "None of the lunar ISRU schemes appear to have a practical financial advantage and it appears to be better, cheaper, and simpler to bring

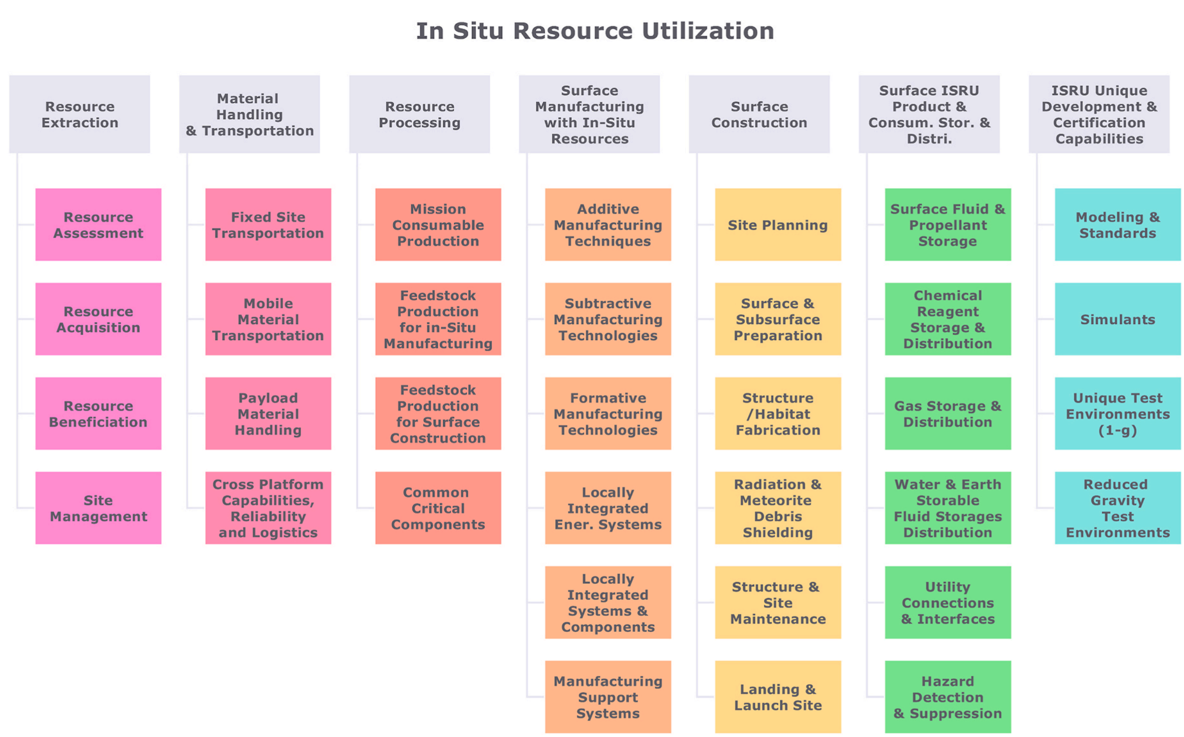

Fig. 2. NASA ISRU capabilities breakdown structure in 2005. Redrawn from NASA executive summary [14].

resources from Earth to the Moon – at least in the short run. By comparison, some forms of Mars ISRU have the potential for great logistic and financial benefit for human missions to Mars” [12].

Such considerations are reflected in a NASA executive summary report in 2005 by the leading ISRU proponents in the US [14]. The group led by Sanders and Duke defined the three primary objectives for Lunar ISRU as: (i) identification and characterization of lunar resources, focusing on the polar region; (ii) use of ISRU demonstrations on the Moon to prepare for human exploration of Mars; and (iii) development and evolution of Lunar ISRU to support continued presence on the Moon and cost-effective human space transportation. In the case of Mars, the three primary objectives for ISRU would be: (i) initial research/development of ISRU and characterization of resources on Mars focusing on water to prepare for human exploration; (ii) development and evolution of Mars ISRU capabilities to reduce costs, mass and risk of human missions making new exploration scenarios possible; and (iii) enabling human exploration beyond Mars. For both ISRU objectives, Sanders, Duke et al. have introduced a detailed breakdown structure of NASA’s ISRU capabilities (in 2005), indicating the space agency’s broad approach towards ISRU (see Fig. 2).

Also in this report, primary ISRU resources are summarized as solar energy, areas of near-permanent light and darkness, the vacuum and reduced gravity, atmospheric constituents, volatiles implanted by solar winds (hydrogen, helium, carbon, nitrogen etc. [15]), minerals dominated by silicates and oxides, metals, as well as water and raw regolith as a construction material [14]. In general, ISRU research brings together a wide range of issues. However, all have the primary aim of converting space resources into energy, breathable air, water for drinking, cleaning and agriculture, rocket fuel and construction/manufacturing materials.

2.1. *Why this review focuses on construction/manufacturing using regolith materials and early ISRU*

ISRU depends to a large degree on what kind of resources/materials are available at a given location. Up to this date, every landed mission to Mars encountered basaltic regolith, which is ubiquitous on the Martian surface. This Martian regolith seems to have a globally homogeneous component from basaltic crust with local to regional enrichments in secondary minerals, including sulfates, clays, carbonates, and feldspathic compositions. In the absence of organic building materials from plants, these oxidic surface minerals would be the only viable raw material for construction/manufacturing. What is more, the regolith is poorly sorted with grain sizes from dust to large boulders (which, in terms of raw material, might make crushing unnecessary).

Judging by power requirements and processing complexity, the direct utilization of regolith and rocks is preferable to the separation of elements for metals, oxides (glass, ceramics) and single elements [16], which is why this review focuses exclusively on early ISRU scenarios that employ the direct use of regolith as construction/manufacturing materials.

2.2. *The way we do ISRU materials research*

As real Martian regolith is unavailable, the general research approach for Earth-based ISRU research is to employ Martian regolith simulants. Such simulants and analog sites are terrestrial materials and locations that approximate key properties of Martian regolith and the Martian environment [17]. Up until now, due to the difficulty of emulating gravity, temperature, atmosphere and radiation conditions of the Moon or Mars, most ISRU material studies have relied on processing under terrestrial conditions (some notable examples are studies where sintering was done in non-terrestrial atmospheres, for example in vacuum [18,19], in hydrogen [20], in argon [21] and simulated Martian atmosphere [22]).

As non-refined simulants have been the major aspect that distinguishes an ISRU study from a terrestrial study, one could argue that the

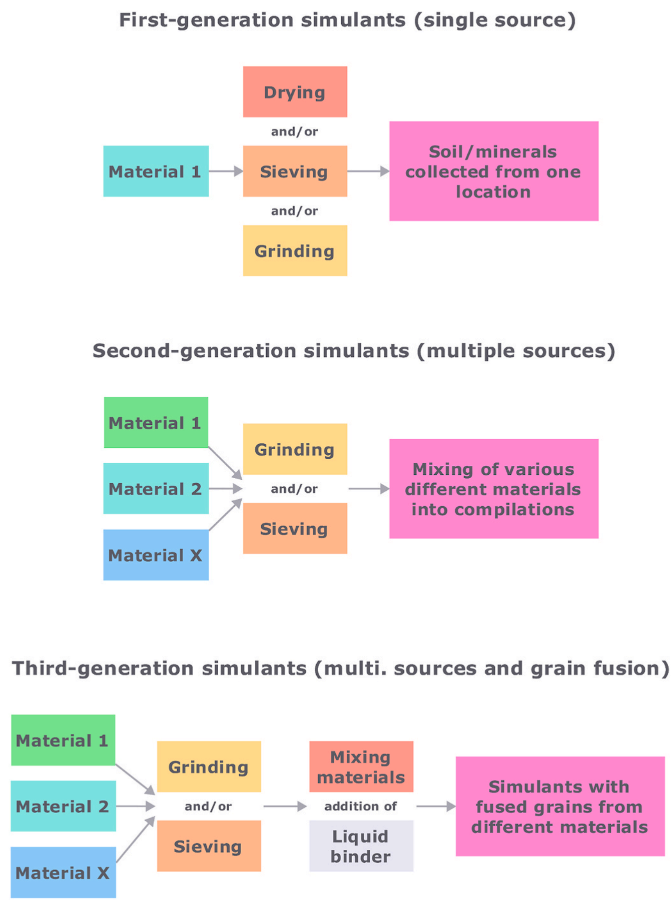

Fig. 3. Mars Regolith simulant generational concept proposed in this work.

quality of the simulant and the applicability of ISRU research to the real Martian environment depends to a large degree on the quality and properties of simulants, which is why the next section is dedicated to a detailed overview of regolith simulants, their concepts and properties.

3. Mars simulants

3.1. *Generational concept to categorize simulants*

Regolith simulants and analog sites can give a preview of the environment a space mission will encounter on Mars. For example, it is essential to know if the wheels on a rover have enough traction in a specific terrain [23] (besides analog sites, space agencies use extensive testbeds filled with simulants [24]). Another example is the calibration of scientific instruments on rovers using simulants [25]. Our knowledge of Mars, gained from remote research efforts by orbiters, landers and rovers, is continually evolving and is mirrored in simulant development [26]. Most notably, orbiter platforms have transformed our perception of Mars from a red basalt sandbox to that of a diverse world with environments, both modern and ancient, as varied as those found on Earth [27]. As simulant development has changed markedly over the years, becoming more complex and nuanced, the authors propose to categorize simulant design philosophies/concepts using a generational concept, dividing them into three generations laid out in Fig. 3.

First-generation simulants are materials from a single source, such as soils collected from one location (often such materials are further processed by grinding and sieving). The earliest simulant employing this concept was JSC Mars-1, a single source tephra from Hawaii [17]. There is a close relationship between the first-generation simulants and analog sites, which were often solids collected from such sites, e.g., JSC Mars-1, MMS. Second-generation simulants are compilations of different

Table 1
Comprehensive overview of Mars simulants and a selection of analog sites and rover testbeds.

First-generation simulants	Second-generation simulants	Third-generation simulants[a]	Mars-like terrestrial locations/analog sites and rover testbeds
JSC Mars-1 (Johnson Space Center Mars-1) - Allen et al., 1998 [17]. Columbia river basalt - Baker et al., 2000 [44].	**P-MRS** (Phyllosilicate Mars Regolith Simulant) - Böttger et al., 2012 [28]. **S-MRS** (Sulfatic Mars Regolith Simulant) - Böttger et al., 2012 [28].	**MGS-1** (Mars Global Simulant 1) - Cannon et al., 2019 [26,42]. **MGS-1C** (MGS Clay ISRU) - Exolith Lab data sheet Nov. 2018 [45].	Chilean Atacama desert (Yungay) Mars analog soil - Navarro et al., 2003 [43]. Rio Tinto River Basin - Fernández-Remolar et al., 2003 [46].
JSC Mars-1A (Johnson Space Center Mars-1A) - Orbitec data sh. 2008 [47].	Six simulants for biotoxicity study used by Schuerger et al., 2012 [48].	**MGS-1S** (MGS Sulfate ISRU) - Exolith Lab data sheet Jan. 2021 [49].	Navajo hematite concretions in Utah - Chan et al., 2004 [50].
MMS (Mojave Mars Simulant) - Peters et al., 2008 [51].	**JMSS-1** (Jining Martian Soil Simulant) - Zeng et al., 2015 [52].	**JEZ-1** (Jezero Delta Simulant) - Exolith Lab data sheet Feb. 2020 [53].	Acid–saline lakes of Western Australia - Benison and Bowen 2006 [54].
MMS-1 (Mojave Mars Simulant) - The Martian Garden data sh. 2019 [55]. **Salten skov I** - Nørnberg et al., 2009 [58].	**UC Mars1** (Uni. of Canterbury Mars Simulant) - Scott et al., 2017 [56]. **Y-Mars** (Yellowknife-Mars) - Stevens et al., 2018 [59].		Moon Plain area of Southern Australia - Clarke et al., 2006 [57]. **Mars PJ** (Peruvian Mars Analog) - Peeters et al., 2009 [60] and Valdivia-Silva et al., 2011 [61].
SSC1/2 (Surrey Space Centre) - Scott and Saaj 2009/2012 [62,63]. Fuller's Earth/Smectite clay - Gaier et al., 2010 [66].	**KMS-1** (Korea Mars Simulant) - Kang 2018 [64]. **Neu Mars1** (Northeastern University Mars1) - Guan et al., 2019 [67].		Dry Valleys of Antarctica - Tamppari et al., 2012 [65]. Great Salt lake, analog for martian hypersaline aqu. Sys. - Perl and Baxter 2020 [68].
ES-1/2/3/4 (Engineering Soil simulants) - Brunskill et al., 2011 and Oravec et al., 2021 [69,70].	**OUCM/EB/HR/SR-1/2** (Open University simulants) - Ramkissoon et al., 2019 [30].		**JPL Lab 82/107** (Jet Propulsion Laboratory) sand boxes - Perko et al., 2006 [71].
Source clay minerals used by Vaniman et al., 2012 [72] and El-Maarry et al., 2015 [73]. Quartz simulant used by Knak Jensen et al., 2014 [75].	**MMS-2** (Enhanced Mars Regolith Simulant) - The Martian Garden 2019 [74]. **JSC-RN** (Johnson Space Center Rocknest) – Clark (prev. Hogancamp) et al., 2019/20 [76,77].		**JPL MER Yard** at building 317 and **JPL Mars Yard** - Perko et al., 2006 [71]. **Astrium Mars Yard** in Stevenage (UK) - Gouache et al., 2011 [24].
HIT-M-1 (Harbin Institute of Technology Martian Simulant 1) - Zheng and Qiao 2020 [78].			**M90** (Jet Propulsion Laboratory) - Oravec et al., 2021 [70].

[a] Fusion of grains with a binder is specified in Cannon et al. [26] for MGS-1 family simulants. However, currently shipped simulants from Exolith lab do not contain the binder due to the increased effort required.

materials produced by directly mixing (often ground) materials mimicking mineralogical distribution and elemental abundances more closely – a concept introduced by P/S-MRS. The two simulants are mixtures of carefully curated minerals obtained from various locations [28]. Third-generation simulants follow the second-generation mixing concept and further enhance physical properties (texture and particle size distribution and geomechanical properties) by using a binder to fuse single grains from different materials into large multi-mineral granules. This recent approach was first introduced for asteroid simulants [29] and subsequently used for MGS-1 [26] (it should be noted that currently produced MGS-1 simulants from Exolith lab skip the fusion step due to the difficulty of implementing it at a large scale).

3.2. Comprehensive overview of Mars simulants

The authors could identify around 30 Mars simulants, and Table 1 gives a comprehensive overview of Mars simulants and a selection of analog sites (as well as testbeds).

This compilation builds on previous collection efforts for simulants by Ramkissoon et al. [30] and the Planetary Simulant Database website [31], combining the two sources into one table and adding recent simulants (as well as several rare simulants). The data for analog sites is a selection from Marlow et al. [25] and Martins et al. [32] with some additions (for a recent, comprehensive overview, see Martins et al.).

This large number of simulants is a result of what Witze describes for lunar simulants as a wild proliferation. Space agencies and researchers tend to make their own individual simulants. Witze even cites Edmunson's comment that "there are a lot of people out there creating their own simulant with no geology or materials-processing background" [33]. Edmunson had previously been part of NASA's 2010 lunar soil simulants team, which revised the development history and requirements for lunar simulants and introduced best-practice procedures for creating future simulants [34] that had been developed by Schrader et al. [35]. Metzger et al. later applied such best practice procedures for asteroid simulants, using a figure of merit system [36] that recently is being adapted as a more user-friendly set of "Regolith Simulant Report Cards" [37]. The 2010 lunar soil simulants team was led by Taylor, who, with co-workers, discussed quality and applicability for lunar simulants several times [38–40]. As no simulant can re-create all the physical and chemical properties of extraterrestrial materials [33], simulant development and use is always a trade-off, with high simulant fidelity being challenging and expensive. Talyor is cited as remarking "one size does not fit all" and insists that simulant materials should be used only for very specific purposes [38]. To support researchers in their choice of simulants (and to make sure simulants are used correctly), NASA's soil simulants team proposed a database [34]. One approach to such a database would be to classify simulant properties according to the attributes they best mimic. Such a classification applied to Mars analogs by Marlow et al. would be organized according to four high-level attributes: compositional, electrochemical, physical and environmental [41]. Marlow et al. further divided these into: (i) compositional according to mineralogical distribution, elemental abundances, presence of volatiles (water content, dissolved gases) and organic content; (ii) electrochemical with dielectric constant, redox potential, pH, magnetism (magnetic susceptibility and saturation magnetization); (iii) physical according to thermophysical (albedo, thermal inertia), mechanical (shear strength, slope stability) and bulk physical (particle size distribution, particle shape, density, porosity); and (iv) environmental according to temperature, aridity, wind and radiation.

A major challenge in creating such a database is missing data on many less-well-studied simulants. Knowledge of simulant properties is

Table 2
Simulants made available to a wide group of researchers.

Name and reference	Material origin/description	Simulation aim/based on	Remarks
JSC Mars-1 (Johnson Space Center Mars-1) - Allen et al., 1998 [17].	Weathered volcanic ash (<1 mm fraction) from Pu'u Nene cinder cone on Hawaii. 40–60 cm thick zone of altered ash was collected from 30 cm below ground.	General composition based on Phobos-2 ISM spectra of Olympus-Amazonis Martian bright region and compared to XRF data from Viking 1/2 and Pathfinder.	- First simulant made available in large quantities to a large group of researchers. - Distributed from JSC - Spectral analog. - 9100 kg produced.
JSC Mars-1A (Johnson Space Center Mars-1) - Orbitec 2008 [47].	Palagonitic tephra (volcanic ash altered at low temperatures) from JSC Mars-1 location.	Reproduction of JSC-Mars 1 by Orbitec and sold commercially (until 2017) in <1 mm and <5 mm fractions.	- High amounts of volatiles, roots and organics.
MMS (Mojave Mars Simulant) - Peters et al., 2008 [51].	MMS dust and MMS sand are from a mechanically crushed basalt flow mined by Tertiary Tropico Group in the western Mojave Desert (close to JPL).	Geotechnical global Mars simulant by JPL based on Viking 1/2, Pathfinder and Spirit/Opportunity (JPL tested various rovers and landers in the Mojave desert [25]).	- To overcome hygroscopicity of JSC Mars-1(A). - Available as dust, sand and whole rock. - Not available outside NASA.
MMS-1 (Mojave Mars Simulant) - The Martian Garden data sheet 2019 [55].	Cinder material with alteration minerals from near MMS location [26]. Available as coarse, unsorted, fine, superfine, planter.	Claimed to be a reproduction of MMS by the education company The Martian Garden and sold commercially since 2016 (starting as Kickstarter).	- Different mineralogy than original MMS [26] - Significant deviation in chemistry from MMS in the MMS-1 data sheet [82].
MMS-2 (Enhanced Mars Regolith Simulant) - The Martian Garden data sheet 2019 [74].	Superfine MMS-1 (77%[a]) is mixed with iron(III) oxide (10%), silica sand (8%), gypsum (4%)and magnesium oxide (1%) of unknown origin/ definition.	Chemical reproduction of average Mars surface (location unclear). Chemical table printed on MMS-2 could be from Opportunity "soil" measurements cited in Peters et al. [51].	- Claimed to be 90% chemical match to surface of Mars (reference Mars chemistry unclear).
JSC-RN (Johnson Space Center Rocknest) - Clark (prev. Hogancamp) et al., 2019/20 [76,77].	Mixture of sourced chemicals and MMS: $NaClO_4$ (1%), goethite (1.5%), pyrite (1%), ferric sulfate (1%), granular ferric oxide (7.5%), forsterite (10%), MMS (78%).	Chemical and mineralogical simulant for water-extraction studies based on Mojave Mars Simulant (MMS) and rover data.	- 1000 kg made. - Similar mineralogy and chemistry to RN soil characterized by Curiosity.

Table 2 (continued). Simulants made available to a wide group of researchers.

Name and reference	Material origin/description	Simulation aim/based on	Remarks
P-MRS (Phyllosilicate Mars Regolith Simulant) - Böttger et al., 2012 [28].	Crushed mineral fragments <1 mm supplied by Museum für Naturkunde Berlin and Dr. F. Krantz GmbH of gabbro (3%), olivine/dunite (2%), quartz (10%), hematite (5%), montmorillonite (45%), chamosite (20%), kaolinite (5%), siderite (5%), hydromagnesite (5%).	General composition of early basic conditions based on orbiter (Mars express/OMEGA) and rover missions (Spirit). Simulates rocks altered by pH-neutral hyd. fluids to clays of the smectite group. Siderite and hydromagn. sim. carbonates from precipitation/interaction between CO_2-rich atmos. with basaltic subsurface rocks.	- Initially developed by J. Fritz to calibrate the Raman spectrometer of the ExoMars mission. - Mainly used by DLR for astrobiology, water retention, BIOMEX space experiments [83]. - Briefly available from www.roboklon.com.
S-MRS (Sulfatic Mars Regolith Simulant) - Böttger et al., 2012 [28].	Crushed mineral fragments <1 mm supplied by Museum für Naturkunde Berlin and Dr. F. Krantz of gabbro (32%), olivine (15%), quartz (3%), hematite (13%), goethite (7%), gypsum (30%).	General composition of late acidic Mars conditions based on orbiter (Mars express/ OMEGA) and rover missions (Spirit). Simulates sulfate deposits in addition to ign. rocks and anhydrous iron oxides, including goethite and gypsum.	see **P-MRS**
MGS-1 (Mars Global Simulant 1) - Cannon et al., 2019 [26,42].	Crushed mineral fragments <1 mm from various locations (and commercial chemicals) fused by sodium metasilicate with a crystalline phase (65%) of plagioclase (27.1%), pyroxene (20.3%), olivine (13.7%), magnetite (1.9%), hematite (1.1%), anhydrite (0.9%) and amorp. phase (35%) of basaltic glass (22.9%), hydr. silica (5.0%), Mg-sulfate (4.0%), ferrihydrite (1.7%), Fe-carbon. (1.4%).	Global simulant aiming for high fidelity in mineral, chemical, volatile, and spectral properties based on windblown Rocknest soil at Gale crater analyzed by MSL Curiosity. Both crystalline and amorphous phases taken into consideration, geomechanical properties considered. New simulant design philosophy with fusing single minerals into solid cobbles (with a binder) to achieve a more natural texture and particle size distribution.	- Widely made available by CLASS Exolith Lab (UCF), also available from Colorado School of Mines as CSM-MGS-1. - Large quantities produced. - Slight adjustments in constituents for the shipped version (compare [26–42]). - Open standard. - First, third-generation simulant, expected to be used widely.
MGS-1C (Mars Global Simulant Clay ISRU) - Exolith Lab data sheet Nov. 2018 [45].	MGS-1 (60%) is mixed with not further specified smectite (40%) - most likely sodium montmorillonite from Wyoming (MX-80) [84].	Specifically designed for ISRU water extraction studies based on M-WIP/NASA Water ISRU study (case C) [85]. MGS-1C is enriched in hydrated clay minerals (smectite).	- Montmorillonite used instead of nontronite and saponite, which are more common smectites on Mars [86], but not commonly available on Earth.
MGS-1S (Mars Global Simulant Sulfate ISRU) - Exolith Lab data s. Jan. 2021 [49].	MGS-1 (60%) is mixed with polyhydrated sulfate gypsum (40%).	Specifically designed for ISRU water extraction studies based on M-WIP/NASA Water ISRU study (case B) [85].	- Total evolved water at 200 °C is 7.8 wt%.
JEZ-1 (Jezero Delta Simulant) - Exolith Lab data sheet Feb. 2020 [53].	Preparation as MGS-1 with olivine (32%), plagioclase (16%), glass-rich basalt (13.5%), pyroxene (12.0%), Mg-carbonate (11%), smectite (6.0%), Mg-sulfate (2.4%), ferrihydrite (2.1%), hydrated silica (1.8%), magnetite (1.1%), anhydrite (1.0%), Fe-carbonate (0.8%), hematite (0.3%).	Jezero Crater delta simulant based on orbital remote sensing. JEZ-1 has MGS-1 mineralogy with extra smectite clay, Mg-carbonate, and additional olivine (all detected from orbit).	- Jezero Crater delta to be investigated by NASA Mars 2020 rover. - Local simulant (not global).

[a] Simulant mixing ratios for all tables in wt%.

Table 3
Compilation of published properties of Mars simulants according to the concept introduced by Marlow et al. [25]. A dot indicates that data on this property has been published, while no dot indicates the apparent absence of such data.

	JSC Mars-1	JSC Mars-1A[a]	MMS	MMS-1[b]	MMS-2	JSC-RN	P-MRS	S-MRS	MGS-1	MGS-1C	MGS-1S	JEZ-1
Chemical properties:												
Mineralogical constituents	•	•	•		•	•	•	•	•	•	•	•
Chemical composition	•	•	•	•	•	•	•	•	•	•	•	•
Dielectric constant	•											
Redox potential	•	•		•					•			
pH	•	•		•					•			
Electrical conductivity	•											
Volatiles	•		•						•			
Mechanical properties:												
Cohesive strength	•		•									
Angle of internal friction	•		•									
Physical properties:												
Particle size	•	•	•	•	•	•	•	•	•	•	•	•
Particle shape	•	•	•	•					•			
Specific surface area	•								•	•		
Density	•								•	•		
Bulk density	•	•	•	•					•			•
Porosity	•											
Water content	•	•		•		•			•		•	
Spectral Reflectance	•		•						•	•	•	
Thermophysical properties:												
Albedo[d]												
Thermal inertia[d]												
Magnetic properties:												
Magnetic component	•		•									
Paramagnetism	•											
Magnetic susceptibility[d]												
Saturation magnetization												
Organic content:												
Loss on ignition	•		•			•			•	•	•	
Total organic carbon[d]												
Molecular abundances	•											
Culturable counts	•											
References:	[17,91]	[47,89]	[51]	[82,89]	[92]	[76,77]	[28] [c]	[28][c]	[26,84,89]	[45,84]	[49]	[53]

[a] Claimed by Orbitec to be the same.
[b] Claimed by The Martian Graden to be the same.
[c] LOI results for P-MRS and S-MRS were obtained from personal communication with Jörg Fritz.
[d] Properties that have not yet been reported for simulants.

inconsistent and no systematic approach has been taken to reporting simulant properties. Often only very basic properties for simulants have been reported, such as composition (mineralogical distribution and elemental abundances), while other characteristics are frequently unknown. Nonetheless, in the next section, an attempt is made to apply the system proposed by Marlow et al. to the most widely available simulants (see Table 3).

In recent years the situation for simulants has improved and there is growing awareness of the issues mentioned above. Space agencies and others have started controlled curation and distribution efforts for simulants. Notable examples are the international space analog rock store (Bost et al. 2013 [79]), the Canadian Space Agency (CSA) planetary analogue suite (Cloutis et al. 2015 [80]), ESA's sample analog curation facility with its sample analog collection ESA^{2}C (Smith et al. 2019 [81]) and the online Planetary Simulant Database (Cannon [31]) providing free information on simulants, thus meeting an important need for the ISRU community.

3.3. Composition and physicochemical properties of widely available simulants

Table 2 gives a comprehensive overview of the origin, mineral composition and simulation aim for simulants available to a large number of researchers either in the past or at present. Additional tables for less used simulants and analog sites mentioned in Table 1 can be found in 3.1.4.

While lunar simulants had been available at least since the 1980s, the first-generation of Mars simulants was introduced with JSC Mars-1 (see Table 2), the earliest professional Martian simulant [87]. In 1998 Allen et al. hand-collected a thin layer (from below a 30–40 cm overlying soil horizon) of altered basaltic tephra made of finely crystallized, glassy particles at the Pu'u Nene cinder cone on Mauna Kea Hawaii (see Fig. 4) [17].

After repeated drying and sieving, Allen et al. made this single-source simulant available to support scientific research, engineering studies and education. JSC Mars-1 filled a real need and became the best-established Mars simulant. As a result of the diligent initial characterization by Allen et al., as well as numerous studies, JSC Mars-1 is still the best-described simulant with multiple properties reported (see Table 3). However, with a mass loss of 7.8 wt% at 100 °C to 21.1 wt% at 600 °C (dominated by H_2O) [17], JSC Mars-1 volatile content diverges significantly from the water content of Martian soils as established in-situ by the Thermal and Evolved Gas Analyzer (TEGA) on Phoenix and the Sample Analysis at Mars (SAM) on Curiosity [77,88].

JSC Mars-1 was so successful that when the initial 9100 kg ran out, the company Orbitec was contracted to re-create the simulant, even though by that time, Mars surface missions had collected additional evidence that could have facilitated the development of a more up-to-date simulant. The second batch was collected from the same location and sold over the Orbitec website (until 2017) under the name JSC Mars-1A [47]. In general, it is assumed that JSC-Mars-1A has nearly identical simulant properties to JSC Mars-1, as it is obtained from the same source

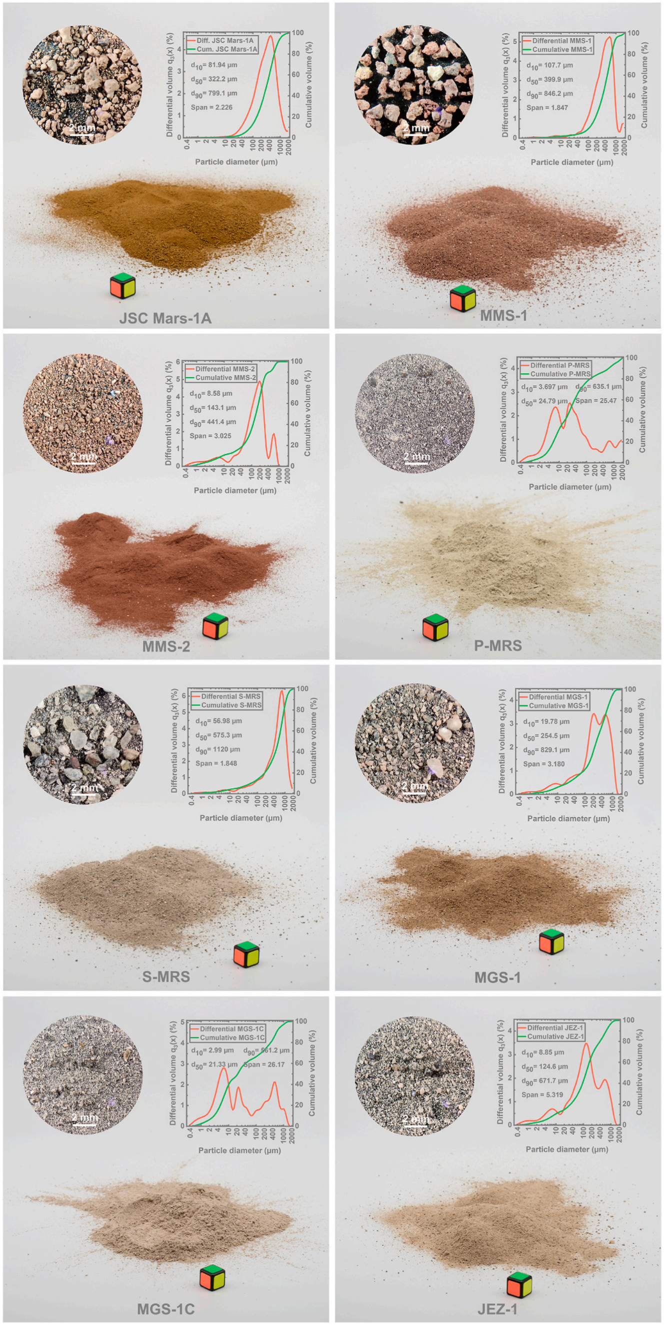

Fig. 4. Physical appearance and particle size distribution of numerous simulants available to a broad range of researchers. All simulants are depicted as-delivered. The depicted reference scale cube (and color target) has a 1 cm edge length. (For interpretation of the references to color in this figure legend, the reader is referred to the Web version of this article.)

[89]. However, Orbitec may not have taken as much care as Allen et al. in preventing contamination. The authors have observed that JSC Mars-1A contains what appear to be small plant parts (roots), which correlates with Wamelink et al. reporting the presence of small amounts of nitrate, ammonium and significant residual organics in JSC Mars-1A [90].

The first simulant established to overcome hygroscopicity of JSC Mars-1 was MMS (Mojave Mars Simulant), developed by Peters et al. in 2008 [51]. Like JSC Mars-1, a first-generation simulant, MMS was made for the Jet Propulsion Laboratory (JPL) according to a one-source concept using basalt mined in the western Mojave Desert (JPL tested various rovers and landers in the Mojave desert) and was based on Viking, Pathfinder and MER missions as well as on orbital data [51]. Peters et al. chose MMS because of its inert hygroscopic characteristics, its availability in various forms (dust, sand and whole rock), its physical and chemical characteristics, and its proximity to the JPL campus. Sourced basaltic boulders were mechanically crushed to create a sharp particle morphology, ideally suited for geotechnical tests such as rover wheel studies and deemed similar to Martian regolith morphology [51]. For further details, the interested reader is referred to the detailed description of MMS development and context in Clark et al. [77].

MMS was not available outside NASA, but since 2016 the education company The Martian Garden (started by a Kickstarter campaign) has been selling a Martian simulant to the public named MMS-1, which claims to be the same as MMS [55]. The company had no direct contact with the original developers of MMS and seems to have no specific geological expertise. It appears to be selling a highly altered cinder material (from the same general location) with abundant alteration minerals rather than the unaltered basalt that made up the original MMS [26]. While the efforts of The Martian Garden to make Mars simulants available to the general public are generally commendable, there is a real danger of professional researchers using these sub-standard simulants for high-quality research (several scientific works use MMS-1 [82, 89,93]). JSC-Mars1(A) and MMS(-1) are the major proponents of the first-generation single-source concept, which had a close relationship to analog sites for equipment testing. While the single source concept is still used for simulant development in 2020 (e.g., HIT-M-1 [78]), with evolving knowledge of Martian regolith, developers have started to use multiple sources for simulants.

In P-MRS and S-MRS, J. Fritz developed the first second-generation simulant in 2011 by mixing carefully curated minerals from various locations. The simulants were developed to calibrate the Raman spectrometer of the ESA's ExoMars mission and the simulant production process was first described by Böttger et al. [28]. In the initial paper, the reporting on simulant properties is minimal (see Table 3) and simulant properties are mentioned in various scientific publications in which the simulants are used chiefly in astrobiology, water retention and BIOMEX space experiments [83,94]. Nonetheless, the simulants follow a complex geological approach, factoring in different geological histories of Mars. They are based on observations from the OMEGA imaging spectrometer onboard the Mars Express, namely that phyllosilicate deposits do not occur in conjunction with sulfate deposits [95] and therefore simulate late basic conditions for the Phyllosilicate Mars Regolith Simulant (P-MRS) and early acidic conditions for the Sulfatic Mars Regolith Simulant (S-MRS) [28]. Despite being a sound concept, due to its low profile and limited availability, the simulant was exclusively used by researchers associated with DLR in Berlin. Furthermore, its name was not fixed and some publications use P/S-MRA for the analog instead of MRS [96,97].

Recently, two new simulants employing a similar second-generation concept were developed to improve the single source simulant properties of MMS(-1). They are JSC-RN (Johnson Space Center Rocknest) and MMS-2 (Enhanced Mars Regolith Simulant). JSC-RN developed by Clark (previously Hogancamp) et al. in 2019 is based on the original MMS but employs 22 wt% additives to approximate more precisely the chemical, mineralogical, and volatile properties of martian soils with the prime focus on low temperature evolved gases <450 °C [77]. MMS-2 is the second-generation evolution of MMS-1. The original MMS-1 is adjusted with 23 wt% additives with the aim of correcting deficiencies in the chemical composition (but not changing the erroneous mineralogical composition of MMS-1 [26]) [74].

Numerous Martian regolith properties remain currently unknown, with the consequence that simulant developers stick to well-established properties that have been measured by instruments near and on Mars. For example, the one property (almost) always reported, besides the provenance of the minerals that make up the simulants, is chemical composition (see Table 4). Such a focus on chemistry (that might be less

Table 4
Oxide constituents in wt% for simulants made available to a wide group of researchers.

Compound	JSC Mars-1 [17]	JSC Mars-1A [47]	MMS [51]	MMS-1[b] [82]	MMS-2[c] [92]	JSC-RN [77]	P-MRS[d]	S-MRS[d]	MGS-1 [42]	MGS-1C [45]	MGS-1S [49]	JEZ-1 [53]
SiO_2	43.5	34.5–44	49.4	57.3	50.9	45.82	43.6	31.8	45.57	56.13	31.9	44.2
Al_2O_3	23.3	18.5–23.5	17.1	12.9	10	13.66	11.2	5.6	9.43	16.89	10.6	11.3
$FeO_{(T)}$	–	2.5–3.5	–	–	32.4	17.71	–	–	16.85	8.24	–	9.5
Fe_2O_3	15.6	9–12	10.87	9.1	n.a.	–	20.3	19.9	–	–	11.9	–
MnO	0.3	0.2–0.3	0.17	0.1	0.1	0.18	0.17	0.41	0.1	0.04	0.1	0.1
MgO	3.4	2.5–3.5	6.08	4.1	5.2	9.51	4.48	10.9	16.5	12.57	6.4	25.9
CaO	6.2	5–6	10.45	4.9	n.a.	7.97	4.67	18.4	4.03	2.02	20.0	3.5
Na_2O	2.4	2–2.5	3.28	4.2	n.a.	3.05	0.29	1.04	3.66	1.91	–	1.9
K_2O	0.6	0.5–0.6	0.48	n.a.	n.a.	0.54	1.07	0.86	0.43	0.47	0.6	0.3
TiO_2	3.8	3–4	1.09	1.1	1.1	1.06	0.45	0.98	0.3	0.21	0.3	0.2
P_2O_5	0.9	0.7–0.9	0.17	0.2	n.a.	0.16	0.56	0.42	0.37	0.35	0.9	0.6
Cr_2O_3	n.a.	n.a.	0.05	n.a.	0.1	0.06	n.a.	n.a.	0.12	0.02	0.1	0.3
SO_3	n.a.	n.a.	0.10	n.a.	n.a.	1.77	<0.1	2.7	2.63	1.16	16.6	2.1
Cl	n.a.	n.a.	n.a.	n.a.	n.a.	0.43	n.a.	n.a.	n.a.	n.a.	0.3	n.a.
LOI	n.a.[a]	n.a.	(3.39)	4.0	n.a.	(~2)	12.4	6.4	n.a.	n.a.	n.a.	n.a.
Total	100	n.a.	99.4	97.9	99.8	99.65	99.19	96.71	99.99	100.01	99.7	100

[a] LOI of JSC Mars-1 was reported with 21.8 wt% [17].
[b] On their website, the Martian Garden gives conflicting compositions: on the one hand, it reproduces the original MMS analysis but, on the other publishes an XRF analysis report from Metallurgical Eng. Services Inc [98]. with quite different compositions. Here, a third-party analysis by Caporale et al. [82] is reproduced.
[c] XRF results are reported not for oxides but base metals – it is assumed this is a mistake, values were corrected (e.g., not silicon but SiO_2 etc.).
[d] XRF results for P-MRS and S-MRS obtained from personal communication with Jörg Fritz.

relevant, for example in engineering studies) can produce misleading study results [33].

The first third-generation simulant is MGS-1 (Mars Global Simulant), developed by Cannon et al. in 2019 [26]. MGS-1 is a high-fidelity simulant based on the current scientific understanding of Mars and aims to simulate Rocknest soil at Gale crater analyzed by MSL Curiosity. The simulant uses the second-generation concept employing single, carefully selected minerals first introduced by P/S-MRS and adds a new design philosophy by fusing single minerals into solid cobbles (with a binder) to achieve a closer match in texture and particle size distribution. Furthermore, Cannon et al. include an X-ray amorphous phase as an important simulant constituent. The authors propose that by using the correct mineral constituents, most properties (volatiles release, spectral properties and others) should more closely match real Martian regolith and MGS-1 correlates favorably with Mars rover and remote sensing measurements [26]. The simulant, which has been judged to be the most accurate basaltic Mars regolith simulant [89], is made available by CLASS Exolith Lab (UCF) as well as the Colorado School of Mines (CSM) and is expected to be used widely. Exolith Lab also produces versions of the simulant enriched in hydrated clay minerals (smectite) and polyhydrated sulfate gypsum, which are called MGS-1C (MGS Clay ISRU) [45] and MGS-1S (MGS Sulfate ISRU) [49]. These simulants are based on ISRU water extraction studies in the M-WIP NASA Water ISRU study (case C and B) [85]. Both have 40 wt% added materials and MGS-1C has smectite (most likely sodium montmorillonite from Wyoming [84], even though the most common smectites on Mars are nontronite and saponite [86] and MSL data indicates a clay abundance at Gale crater from ~3 to 28 wt%, mostly smectite [99]) and MGS-1S polyhydrated sulfate gypsum. As discussed in the previous section, our knowledge of Mars is constantly evolving, which is directly reflected in simulant development. It has become clear that Mars is not homogenous and has a complex geology. The early, first-generation simulants followed a global concept such as JSC Mars-1 (and most currently developed simulants are still global, e.g., MGS-1). However, because of the heterogeneity of Mars, it is important to develop different site-specific simulants using emerging orbiter and rover data and more simulants should follow a local simulants approach. Recently a local simulant has been developed even before the instrumental rover data has been collected. With JEZ-1 (Jezero Delta Simulant), Cannon anticipates the Jezero Carter soil based on orbital remote sensing data, even before Mars 2020 has arrived [53].

3.4. Overview of rare Mars simulants

As discussed in 3.1.1 above, researchers have tended to create their individual simulants, which led to many simulants that have found limited use as they were available only to a small group of researchers. This section lists rare simulants in three tables according to the previously introduced generation concept (Table 5: First-generation simulants; Table 6: Second-generation simulants; and Table 7: Mars-like terrestrial locations/analog sites and rover testbeds).

4. ISRU regolith bonding concepts

4.1. History of ISRU material and processing concepts

Many of the ISRU material and processing concepts discussed in the current research were first introduced for the Moon during the 1960s, 1970s and 1980s when the Apollo program's ethos and knowledge prompted a vast array of studies on lunar regolith ISRU. In Table 8, an extraordinary example of such work from 1963 is reproduced. In his book 'The geology of a Lunar base,' Green proposed various applications for basalt processing on a Lunar base, introducing the concepts for cast basalt, sintered basalt and spun basalt [109]. A further example of such research is a 1972 NASA-funded concept study of lunar settlements, which detailed materials and manufacturing on the Moon with direct use of Lunar resources [16]. In this study, Dalton et al. proposed that looking at power requirements, the direct utilization of regolith and rocks is superior to the separation of elements for metals, oxides (glass, ceramics) and single elements. Also, in 1977 Phinney et al. discussed lunar resources and their use. They proposed the processing of regolith into structural metals, glasses and ceramics for power satellites, lunar settlements or industrial facilities [110]. Concepts for processing routes for metals (especially iron reduction) were elaborated in detail. Finally, a concise summary of all ISRU concepts for ceramics (including metals) was given by Happel [111]. While early laboratory works on ISRU focused exclusively on lunar simulants, the introduction of the first Martian regolith simulant JSC Mars-1 in 1998 led to a period in which researchers tended to use Lunar and Martian simulants in the same studies. This is mirrored in review literature on the topic, which either focuses on Lunar ISRU or discusses ISRU material concepts for the Moon and Mars in conjunction (except for a short review by Scheerbaum from 2000, reporting exclusively on Martian construction materials [112]). For example, recent advances in Lunar ISRU were discussed insightfully

Table 5
First-generation simulants.

Name and reference	Material origin/description	Simulation aim/based on	Remarks
Columbia river basalt - Baker et al., 2000 [44].	Tripped, crushed (and ground) high-Fe basalt from the Saddle Mountains series of the Columbia River Basalt Group.	Martian analog basalt used for experimental hydrothermal alteration aiming to reproduce Martian meteorite minerals.	- Basalt in CO_2-saturated aqueous fluids produced carbonate Minerals [44]. - Close chemistry to global Martian regolith [30].
Salten skov I - Nørnberg et al., 2009 [58].	Red-colored sediments of Salten skov in central Denmark with high amount of hematite, maghemite and goethite.	As chemical and magnetic dust analog based on Viking, Pathfinder and, MER rover missions.	- Salten s. minerals used since 2005 as bio. simulant [100]. - Chemistry very different from Martian dust.
SSC1/2 (Surrey Space Centre) - Scott and Saaj 2009/2012 [62,63].	SSC-1 is sieved dusty silica sand with 63 μm to 1.3 mm particle size and some silt. SSC-2 is a crushed garnet mineral sand between 30 and 90 μm supplied by GMA Garnet Group.	Developed by Surrey Space Centre (SSC) for hardware testing (micro rover trafficability).	- Used in ESA ExoMars Phase A Rover Study.
Fuller's Earth/Smectite clay - Gaier et al., 2010 [66].	Commercial clay mixture with montmorillonite, kaolinite, and attapulgite.	Based on simulated Martian dust storm observed by Mariner 9 spacecraft [101].	- Used for dust devil experiments to test space suits.
ES-1/2/3/4 (Engineering Soil simulants) - Brunskill et al., 2011 and Oravec et al., 2021 [69,70].	Commercially available products, supplied by Sibelco UK Ltd (source ES-4 unkown): Stjernoy nepheline syenite S7 for fine dust analog (ES-1), Red Hill 110 silica sand for fine aeolian sand analog (ES-2), Leighton Buzzard DA30 silica sand for coarse sand analog (ES-3) and compact silty sand with gravel (ES-4).	Geotechnical simulants for ExoMars rover testbed, focusing mainly on particle size distributions based on Viking, Pathfinder, MER and Phoenix missions.	- Material chosen for short delivery time to fill 70 tonnes sandbox. - Detailed characterization in Ref. [24]. - ES-2 processing not suitable for the production of multi-ton quantities [24]. - The material origin of the silty sand with gravel making up ES-4 is not published.
Source clay minerals used by Vaniman et al., 2012 [72] and El-Maarry et al., 2015 [73].	Source clays from the clay repository of the clay minerals society: Uley mine Nontronite (NAu-2), high-defect Kaolin (KGa-2), Wyoming Na-Montmorillonite (SWy-2), Texas Ca-Montmorillonite (STx-1b).	Noachian-aged terrains are closely associated with phyllosilicate occurrences and smectites in particular. Repository clays are expected to be homogenous with properties widely researched and published.	-Source clays upon the best characterized clay materials in the world, details can be found under https://www.clays.org/sourceclays_data/-Used by Vaniman et al. as ChemCam calibration targets (sintered with a flux) [72].
Quartz simulant used by Knak Jensen et al., 2014 [75].	Commercially available quartz (Merck, 1.07536).	Chosen as an analog for erosion study because of its simple chemical composition.	- Used to research wind-driven erosion producing highly reactive sites on mineral grain surfaces as a possible methane sink on Mars.
HIT-M-1 (Harbin Inst. of Tech) -Martian Simulant 1) - Zheng and Qiao 2020 [78].	Not further specified raw material from a volcano in the Jilin Province of China.	Mars average chemical composition compared to RN bulk from Achilles et al., 2017 [102].	- Developed for welding experiments with solar concentrator. - Except for XRF analysis not further specified.

by Lim et al. in 2017 [113] and extraterrestrial construction materials (in general) were reviewed extensively by Naser [114–116].

4.2. Categorizing regolith bonding concepts

In line with the judgment from of Dalton et al., that directly using regolith and rocks is to be preferred over separating elements [16] and beneficiating regolith, which is why this review focused exclusively on regolith bonding concepts (except for two examples for regolith reduction, which can be considered relevant for early ISRU) with a special focus on Mars ISRU.

We propose to break down the various regolith bonding concepts into seven categories: sintering, melting, powder pressing, powder agglomeration, aggregate bonding, chemical fusion and freezing. Using this approach, an overview graph has been developed (see Fig. 5) to list all the regolith bonding concepts found in the literature.

In the following section, each sub-section describes works that first proposed the specific bonding concept for Lunar ISRU (as solely Martian studies are seldomly available) or Martian ISRU and aims to name one at least recent Martian ISRU study for each concept in particular.

In general, recent studies were often unavailable and literature on ISRU laboratory studies tends to focus on somewhat extravagant materials processing approaches, while few studies of traditional processes long established on Earth are available. Finally, each introduced concept is briefly discussed regarding applicability for early ISRU on Mars.

4.2.1. Sintering

The essential process for producing ceramics on earth is sintering, the compacting and forming of a solid mass by heat or pressure. The first laboratory study on sintering regolith was carried out by Simonds in 1973. He investigated the formation of geological features found on the Moon by sintering Fra Mauro glass (landing site of Apollo 14), producing compacts with porosities from ~10 to 80% [117]. To test whether lunar breccias formed under lower temperatures, Simonds employed oven sintering and hot pressing. Subsequent studies employed powder pressing followed by thermal sintering of lunar regolith simulants (Allen et al. [118] or Hintze [119], who produced a great number of large tiles by sintering in a furnace at 1125 °C for thruster tests).

For the calibration of the MSL Curiosity rover laser-induced breakdown spectrometer (ChemCam), Vaniman et al. produced ceramic calibration targets aimed at simulating minerals at Gale Crater (see Fig. 6) [72]. The well-documented Nontronite (NAu-2) and Kaolinite (KGa-2) clays from the clay minerals society's source clays repository were pre-fired at 1000 °C to induce a phase change (as clay swelling in humidity would make the samples unstable on a Mars mission). Subsequently, the clays were mixed with different amounts of anhydrite for the sulfate component and olivine-phyric tholeiitic basalt for the basaltic detritus (for amounts, see Fig. 6a).

Aiming to not release sulfur from the sulfate mineral component, Vaniman et al. performed sintering at 800 °C (which required the addition of a 9 wt% lithium tetraborate flux), producing ceramics with distinctive terracotta colors for the nontronite-containing mixtures (Fig. 6b). Samples had high porosity (see Fig. 4c) but were stable enough to be carried to Mars by Curiosity as ceramic targets that provide compositions close to the soils and sedimentary materials of Gale crater.

An example of Martian regolith simulant processing with radiant furnace sintering is Grossmann, who sintered simple shapes employing Martian MGS-1 simulant powders with different particle size distributions shaped via vibrational compaction in silica molds. Powder compacts of different particle fractions were sintered at 1150 and 1200 °C for 30 min resulting in a compressive strength of ~27–77 MPa with 0.5–13.8% porosities (volume) [120].

Karl et al. introduced wet-processing of Martian regolith simulant coupled with radiant furnace sintering similar to traditional ceramic processing on Earth. In work from 2018, slip-casting of non-clay JSC Mars-1A was used to create green bodies with complex shapes [121], followed by the development of clay containing MGS-1C/8 (5 wt% smectite clay) wet-processing material system that could be shaped

Table 6
Second-generation simulants.

Name and reference	Material origin/description	Simulation aim/based on	Remarks
Six simulants for biotoxicity study used by Schuerger et al., 2012 [48].	Ground mixtures of various minerals <200 μm of various proportions with sodium sulfate, sodium perchlorate, sodium carbonate, olivine, pyroxene, magnesite, Ti-magnetite, magnesium chloride, jarosite, kieserite, hematite, halite, gypsum, ferrihydrite, ferricopiapite, brushite, calcium carbonate, basalt, anhydrite from various sources.	Simulate potentially biotoxic geochemistries: Control (unaltered basalt only), high salt (Burroughs subclass), acidic (Paso Robles class), alkaline (Viking soils weakly alkaline/ perchlorate (Phoenix), and aeolian (Laguna class) all based on contemp. missions.	- Used to test the survival of terrestrial microorganisms under Martian conditions (in Mars Simulation Chamber for equatorial Mars conditions).
JMSS-1 (Jining Martian Soil Simulant) - Zeng et al., 2015 [52].	Crushed mixtures <1 mm of Jining basalt (93%) with magnetite (3%) and hematite (2%) from Hebei (China).	Similar chemistry, mineralogy and physical properties to Martian basaltic soil, observed by Spirit and Opportunity.	- Claimed that JMSS-1 mechanical comminution process closely resembles the physical weathering processes on Mars [52].
UC Mars1 (University of Canterbury Mars Simulant) - Scott et al., 2017 [56].	Milled, washed and mixed volcanic materials obtained from Banks Peninsula (New Zealand) of jaw crushed basalt (47%), <300 μm washed basalt (37%), jaw crushed volcanic glass (7%), <300 μm washed volcanic glass (9%).	Simulates particle size, chemistry and mineralogyof regolith at the Gusev Crater near the Columbia Hills based on Spirit rover for infrastructure development studies.	- Designed to produce 10 kg to several hundred kilograms batches. - Used for magnesium-based cements [103].
Y-Mars (Yellowknife-Mars) - Stevens et al., 2018 [59].	Crushed and sieved minerals obtained commercially from Richard Tayler Minerals (UK) of albite (31.1%), saponite (30.5%), augite (13.1%), magnetite 5.3%), enstatite (4.2%), dunite (3.9%), anhydrite (3.6%), sanidine (1.7%), pyrrhotite (2.9%), selenite (1.4%).	Geochemical analog to the Sheepbed mudstone based on John Klein drill hole at Gale Crater from Mars Science Laboratory.	- Hard to obtain saponite handpicked from vesicles in basalt. - Pressed to form pellets of simulated mudstone. - Applications for astrobiological research.
KMS-1 (Korea Mars Simulant) - Kang 2018 [64].	Crushed Yeoncheon basalt (74.9%) from Hantangang River (South Korea) mixed with elements from unsp. origin with SiO_2 (11.8%), Fe_2O_3 (7.7%), MgO (5.4%) and <0.2% Al_2O_3, CaO, SO_3 (values recalculated to 100% from Ref. [64]).	Mars average value chemical composition based on Viking, Pathfinder and MER rover mission.	- Algorithm used to fit each chemical component's difference to <1% of average Mars regolith. - Available in fine sand <3 mm and fine dust <1 mm.
Neu Mars1 (Northeastern University Mars1) - Guan et al., 2019 [67].	Crushed and ball milled and sieved basalt (93%) from Chahar volcanic group in Wulanchabu (inner Mongolia, China) mixed with magnetite (4%) and hematite (3%) of unspecified origin.	Average global simulant based on Mars landing detection data, and chemical and phase composition of JSC Mars-1 and JMSS-1 soil simulants.	- Basalt powder was oven-dried to remove volatiles.- High on alkali metal oxides (Al_2O_3, Na_2O, and K_2O) and low on MgO compared with Martian soil and other soil simulants.

Table 6 (continued). Second-generation simulants.

Name and reference	Material origin/description	Simulation aim/based on	Remarks
OUCM-1/2 (Open University simulants) - Ramkissoon et al., 2019 [30].	Crushed and sieved minerals obtained from Mayko Natursteinwerke GmbH, Northern Geological SuppliesLtd., Dr. F. Krantz GmbH, Sibelco and Scangrit, UK of (OUCM-1): Fe-silicate (30%), phono-tephrite (40%), quartz (3%), dunite (8%), anorthosite (7%), wollastonite (3%), pyrite (4%), magnetite (3%), apatite (1%), gypsum (1%).	Simulates global Mars chemistry (with focus on Fe^{2+} conc.) and particle size based on Rocknest region analyzed by Curiosity.	- All OU simulants in five particle size fractions (>900 μm, 900–400 μm, 400-300 μm, 300–280 μm and <280 μm). - All OU simulants used to study pot. habitability of Martian environments. - OUCM-2 with modified Fe^{2+} concentration.
OUEB-1/2 (Open University Early Basaltic) - Ramkissoon et al., 2019 [30].	Crushed and sieved minerals of (OUEB-1): Fe-silicate (30%), phono-tephrite (10%), quartz (14%), dunite (19%), anorthosite (12%), wollastonite (12%), magnetite (2%), apatite (1%).	Simulates regional Mars chemistry (with focus on Fe^{2+} conc.) based on Zagami shergottite meteorite.	- OUEB-2 with modified Fe^{2+} concentration.
OUHR-1/2 (Open University Hematite-Rich) - Ramkissoon et al., 2019 [30].	Crushed and sieved minerals of (OUHR-1): Fe-silicate (19%), phono-tephrite (27%), quartz (3%), dunite (11%), anorthosite (6%), wollastonite (3%), pyrite (6%), magnetite (4%), apatite (1%), hematite (20%).	Simulates regional Mars chemistry (with focus on Fe^{2+} conc.) of regolith at Hematite Slope at Meridiani Planum analyzed by Opportunity.	- OUHR-2 with modified Fe^{2+} concentration.
OUSR-1/2 (Open University Sulfur-Rich) - Ramkissoon et al., 2019 [30].	Combined minerals of (OUSR-1): Fe-silicate (10%), phono-tephrite (27%), dunite (8%), pyrite (40%), magnetite (3%), apatite (7%), gypsum (5%).	Simulates regional chemistry (with focus on Fe^{2+} conc.) of Paso Robles composition at Columbia Hills analyzed by Spirit.	- OUSR-2 with modified Fe^{2+} concentration. - Pyrite as altern. for non-available Fe-sulfates used. - Fe^{2+} conc. not equiv. to those believed on Mars.

using all typical ceramics processing routes (slip casting, hand forming, material extrusion, binder jetting additive manufacturing, as well as dry-pressing) [22]. The slip-cast JSC Mars-1A green bodies were sintered at 1000 °C and 1130 °C (with holding times of 10 min and 10 h), giving porous ceramics similar to terracotta with a Weibull flexural strength (ring test) of 15–51 MPa [121], with the MGS-1C/8 sintered in terrestrial and simulated Martian atmosphere 1130–1160 °C (with various holding times) resulting in relatively dense ceramics (see Fig. 7) with Weibull flexural strength of with 57.5/53.3 MPa in terrestrial/simulated Martian atmosphere [22]. Wet-processing - the most used shaping method for ceramic materials on Earth - has several advantages over dry processing (higher packing density of green bodies, no/fewer additives needed, complex shapes possible, convenient feedstock handling), making it a valuable addition to the ISRU portfolio for Mars (the merits of radiant furnace sintering are discussed in conjunction with microwave sintering in the passage below).

Another method of inducing heat for sintering is the use of microwaves for materials that couple with this radiation. Based on the observation that lunar regolith contains ilmenite ($FeTiO_3$), which shows high microwave absorption, Meek et al. studied microwave sintering of lunar regolith simulant [122]. With the goal of producing fused ceramics materials, reactant grade chemicals were fritted, milled and pressed into pellets. Microwave radiation at 25 GHz was used for microwave sintering, producing samples of various densities with a compressive

Table 7
Mars-like terrestrial locations/analog sites and rover testbeds.

Name and reference	Material origin/description	Simulation aim/based on	Remarks
Chilean Atacama desert (Yungay) Mars analog soil - Navarro-Gonzalez et al., 2003 [43].	Soil samples collected from various locations in the Atacama Desert in Northern Chile (at the precipitations gradient in a north-to-south transect centered on ~70°W between 24°S and 28°S [43]).	Simulates Mars soils investigated by the Viking Biology Experiment, employed in organics analysis.	- Atacama Desert has been widely used as an organic Mars soil analog. - No specific location fixed (various general locations used by different groups). - Used for GC-MS analysis [104, 105].
Rio Tinto River Basin - Fernández-Remolar et al., 2003 [46].	Samples collected at various locations in the northern domain of Rio Tinto River Basin (Huelva/Spain) of ferric iron-enriched sediments dominated by sulfate and oxyhydroxide associations.	Bulk Mars analog for acid-sulfate chemistry based on aqueous origin of jarosite and hematite found via Mössbauer meas. from Opportunity [106].	- Allows engineers to fine-tune mineralogy-based rover instruments [25]. - Poor match for Martian physical or mechanical properties.
Navajo hematite concretions in Utah - Chan et al., 2004 [50].	Soil samples analyzed from Jurassic Navajo Sandstone of southern Utah.	Model for hematite-rich spherical balls from Opportunity at Meridiani Planum.	- To study history of fluid flow in the hematite region of Mars. - Abundance of quartz (no spectral matches on Mars).
Acid–saline lakes of Western Australia - Benison and Bowen 2006 [54].	Soil samples from Yilgarn Craton of Western Australia Lake Aerodrome, Lake Cowan basin Bandee Lakes.	Terrestrial analog for the Burns formation acid saline systems analyzed by MER.	- Claimed to be strikingly similar in mineralogy, sedimentary structures, and diagenetic feature [50].
Moon Plain area of Southern Australia - Clarke et al., 2006 [57].	Regolith of the Moon Plain area outside Cooper Pedy (South Australia) rich in magnesium sulfates (mainly epsomite), gypsum and clay.	Proposed Mars analog site for water ISRU plant based on hydrated calcium and magnesium sulfates found by Opportunity at Terra Meridiani.	- Regolith at site proposed to contain epsomite, gypsum, and smectite clays in abundances above 10%, each [57].
Mars PJ (Peruvian Mars Analog) - Peeters et al., 2009 [60] and Valdivia-Silva et al., 2011 [61].	Soil samples collected from Arequipa (16°S41-44′ W72°01–02′) and the Pampas de La Joya desert (between 16°S and 17°S latitude).	Chemical and organic Martian hyperarid analog with sulfate mineralogy and organic content with extreme salinity based on rover and orbiter missions.	- Used mainly for astrobiological studies - Used for potatoes in high salinity environments [107]. - Mars PJ: https://pampasdelajoya.wixsite.com/marspj.
Dry Valleys of Antarctica - Tamppari et al., 2012 [65].	Soil samples excavated in McMurdo Dry Valleys (Taylor/University) in Antarctica.	Organic host analog/climate analog sites used for Phoenix Lander testing and soil analyzed.	- Compared to Martian meteorite and simulant of Pheonix soil [108].
Great Salt Lake, analog for martian hypersaline aqu. Sys. - Perl and Baxter 2020 [68].	Hypersaline north arm of the Great Salt Lake (GSL) in Utah with evaporitic environment, generated by halite and gypsum precipitation events.	Analog for ancient Martian salt lakes and evaporitic systemsAnticipated to be studied in Jezero Crater by Mars 2020 rover Perseverance.	- Work on biosignature preservation in GSL could inform missions on Mars.
JPL Lab 82/107 (Jet Propulsion Laboratory) sand boxes - Perko et al., 2006 [71].	Washed ruby garnet mix (Lab 82, and washed silica sand (Lab 107), both dust free;	Indoor sand box test facilities at JPL during the time of the 2003 Mars Exploration Rover (MER) mission to simulate soil mechanics for rover tests and other equipment for Mars exploration.	- Origin of materials not further specified.

Table 7 (continued). Mars-like terrestrial locations/analog sites and rover testbeds.

JPL MER Yard at building 317 - Perko et al., 2006 [71].	Crushed volcanic rock.	Mars Exploration Rover (MER) Spirit and Opportunity landing sites.	- Origin of materials not further specified. - Silt content 5. %
JPL Mars Yard - Perko et al., 2006 [71].	Granite brick dust (decomposed) and cinders with washed sand (in 2006 [71].), in the early 2000s–25 tons of MMS sand simulant were mixed into the previous materials [70].	Mars Yard is a simulated Martian landscape developed by the Mars Technology Program and used by to test different prototypes for example Mars 2020.	- Large obstacles used for MER simulants - Silt content 2. % - Soil is stored in unprotected outdoor area and constantly changing.
Astrium Mars Yard in Stevenage (UK) - Gouache et al., 2011 [24].	Washed dry quartz sand (dust-free).	Used for early ExoMars rover traction testing at the Astrium Mars Yard in Stevenage (UK).	- Origin of materials not further specified. - Later materials used for ExoMars were SSC1/2 and ES-1/2/3.
M90 (Jet Propulsion Laboratory) - Oravec et al., 2021 [70].	A fine grained, poorly graded, sand supplied by Soil Direct, which was kiln dried.	Used for Mars 2020 wheel studies and testing especially focusing on traction capabilities for sand dunes and ripples.	- Specific sand used for M90 us unkown (the Soil Direct website lists different sands). - Oravec et al. give M90 the highest fidelity ranking for surface mobility studies [70].

strength of 5–25 MPa [122]. Elaborating on this approach, Taylor and Meek fused 80 g of real lunar soil from Apollo 17 [123], revealing that results from the microwave sintering of simulants were misleading, as nanophase-sized Fe^0 grains set within silicate glass were claimed to have absorbed high amounts of energy (a topic that is still controversially discussed). Taylor (with others) discussed problems of applicability for lunar simulants in great detail [38–40].

The use of heat from an external source for radiant furnace sintering (e.g., fire or heating element) is the predominant sintering approach on Earth. While ISRU proponents might find the idea of firing ceramic kilns for several days unnerving (and therefore be excited about such a 'fast' process as microwave sintering), this long process is a quintessential requirement for sintering non-technical powders (i.e., regolith). Firstly, during ramp-up, the gas release needs to be rigorously controlled to ensure parts do not explode during fast heating and that gases are not trapped inside the body by closed outside pores (bloating). Secondly,

Table 8
Exemplary applications of processed basalt on a Lunar base proposed in 1963 by Green [109].

Cast basalt	Sintered basalt	Spun basalt (fibers)
Furnace material for water-extraction operations	Nozzles	Cloth and bedding
Crusher jaws	Tubing	Resilient shock-absorbing pads
Pipes and conduits	Wire-drawing dies	Acoustic insulation
Conveyor material (pneumatic, hydraulic, sliding)	Ball bearings	Thermal insulation
Linings for ball, tube or pug mills and for flue ducts, ventilators, cyclers, drains, mixers, tanks, electrolyzers, mineral dressing equipment	Wheels	Filler in sulfur cement
Tiles and bricks	Low-torque fasteners	Fine springs
Sidings	Studs	Packing material
Nose cones	Furniture and tableware	Strainers or filters for industrial or agricultural use
Track rails	Low-load axles	
Ties	Scientific equipment, frames and yokes	
Pylons	Light tools	
Heavy-duty containers for "garden and orchard" use	Light duty containers and flasks for laboratory use	
Radar dish frames	Pump housings	
Mirror bases		
Thermal rods		

high-performance ceramics will require dense sintering, which is an intricate and sensitive process (see Karl et al. [22]) best controlled over longer times. Thirdly, ceramic production often necessitates a slow cool-down to prevent dunting (cracking from rapid cool-down) due to thermal stresses induced from phase transformations during sintering (e.g., cristobalite and quartz inversions). While microwave sintering might be feasible for highly purified technical ceramics and porcelains, process control issues for non-hybrid microwave ovens (microwave coupling regions cannot be controlled [124]) and rapid processing times are not well suited to for non-beneficiated/unpurified Martian regolith materials.

Hot pressing used by Simonds (discussed earlier) falls within alternative sintering approaches that have recently received attention under the term cold sintering [125]. Such cold sintering has been applied by Chow et al., who were able to achieve high strength values using quasi-static compaction of JSC Mars-1A at increased pressures (360–800 MPa) or impact compaction with various boundaries resulting in parts with flexural strengths in the range of sintered ceramics from 23 to 45 MPa [126]. Chow et al. further showed direct compression of pre-dried JSC Mars-1A simulant using similar compaction procedures. The researchers theorize that compression induces a phase transformation of nanoparticulate iron oxide phases (npOx) into goethite or magnetite, acting as a binder phase. Powder compacts produced from JSC Mars-1A had ~30 MPa flexural strength for quasi-static and ~50 MPa for dynamic compaction, similar to those of solid rocks. In general, dynamic compaction of powders leading to cold plastic flow is categorized as a pressure-assisted sintering technique. While natural shock sintering is typically observed in rock formation, achieving such high pressures industrially is challenging [125] and the ISRU feasibility of the method proposed by Chow et al. for habitat building may be questionable.

4.2.2. *Melting*

In 1972 Da et al. elaborated on the direct melting of regolith for cast basalt (see Fig. 8) previously introduced by Green [109]: A melt of regolith is produced, poured into forms and cooled slowly with the material crystallizing instead of vitrifying [16]. On Earth, such cast basalt has various applications in thermal power stations for the

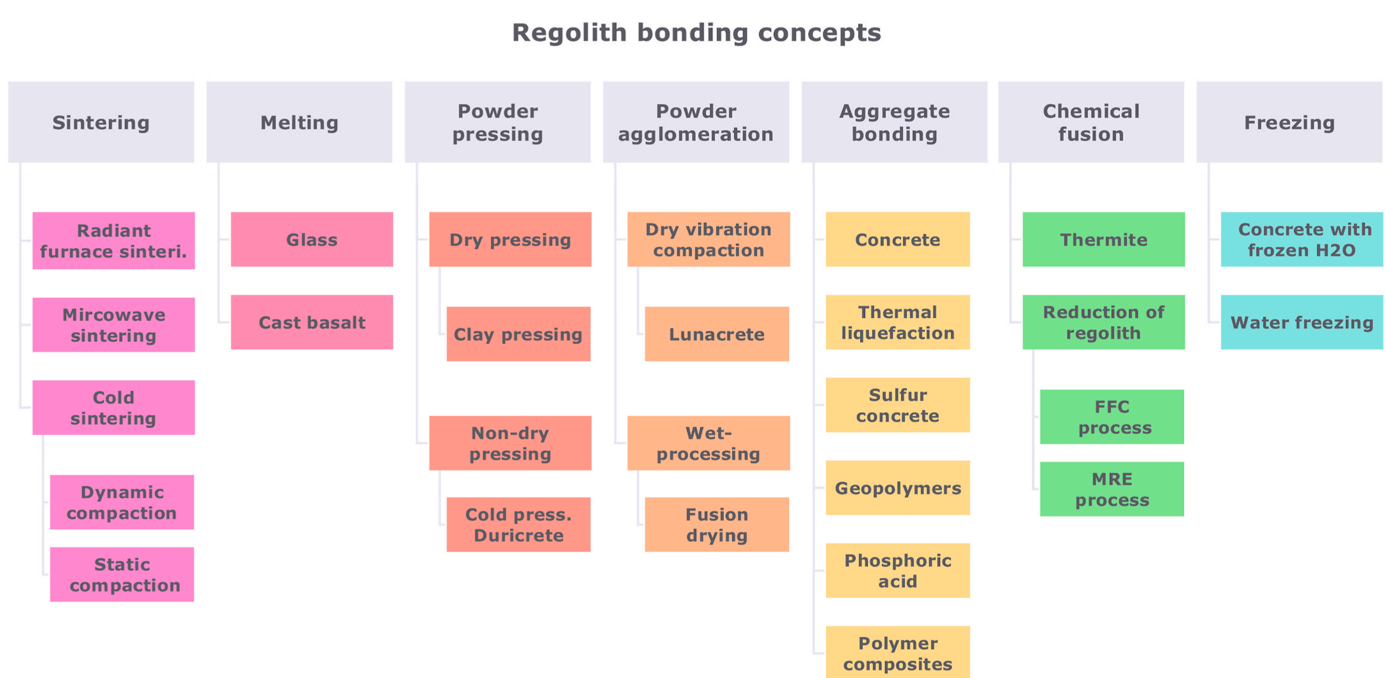

Fig. 5. Overview of proposed regolith bonding concepts for early ISRU.

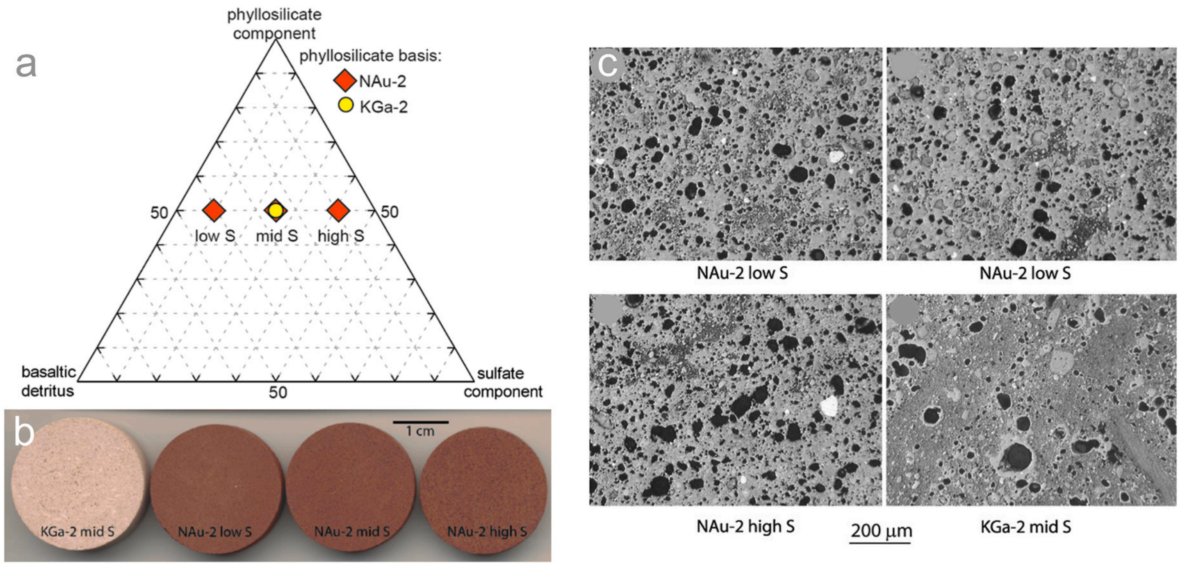

Fig. 6. (a) Ternary diagram with as-mixed weight proportions of basalt, anhydrite and processed clay minerals in the ceramic targets. (b) Discs of ceramics from mixtures of pre-fired source clays (1000 °C) with anhydrite, basalt and 9 wt% $Li_2B_4O_7$ flux sintered at 800 °C. (c) Micrographs of polished sections of these ChemCam ceramic calibration targets carried to Mars by Curiosity. Images open access permission (CC BY) from Vaniman et al. [72].

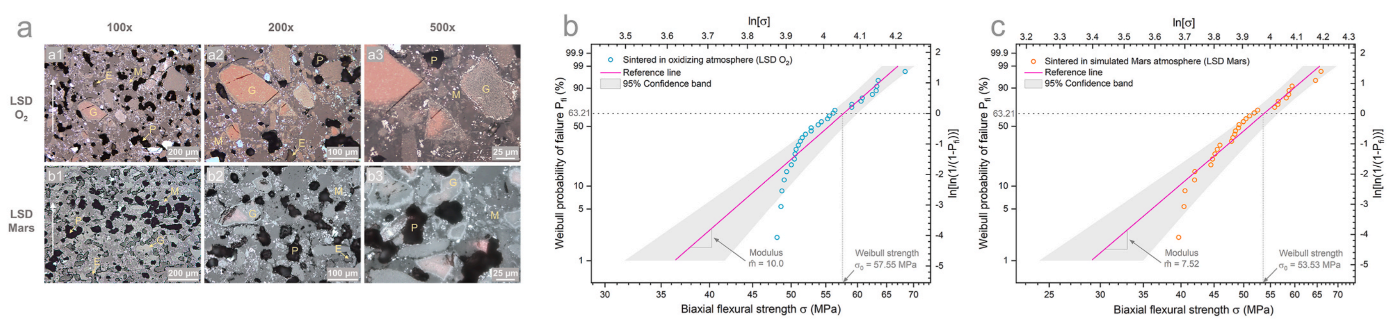

Fig. 7. (a) Optical micrographs of polished crosssections of ceramics sintered in oxidizing atmosphere (LSD O_2) and simulated Mars atmosphere (LSD Mars) from green bodies generated by layerwise slurry deposition of MGS-1C/8 slurry coupled with binder jetting. (a and b) Weibull fracture probability plots of such ceramics with (a) LSD O_2 and (b) LSD Mars. Images open access permission (CC BY) from Karl et al. [22].

manufacture of hoppers, bends, pipelines, trenches and coal piping. Melting of regolith could also be used to draw (basalt) fibers [16]. Blacic suggested that lunar glasses (for example, in the form of fibers) would possess very high tensile strength (compared to similar materials on Earth) due to the hard vacuum conditions on the Moon, where no hydrolysis of Si–O bonds would occur [127].

Melting experiments with JSC Mars-1 were undertaken by Carpenter et al. in a conventional oven under argon purge and in a microwave oven. They produced quenched basalt glass beads, noting dispersed metallic iron particles within the melt body and settled or nucleated FeP spherules [128]. Using JSC-1 lunar simulant and a self-made Mars simulant (aiming for the chemical composition of JSC Mars-1), Ray et al. developed glass magnets by melting at 1500 °C and quenching on a steel plate or into a steel mold [129]. The researchers obtained opaque glasses that were almost black, which they attributed to the iron oxides in the samples. Glass samples were soft magnets and displayed ferromagnetic behavior [130]. In further work, the group pulled meter-long JSC-1 glass fibers from melts, which they proposed to use for composite materials and structural applications [131]. Recently, Schleppi et al. produced mirrors from glasses made by microwave heating of lunar simulants and coating with aluminum or silver, which reflected 30%–85% of incident solar light (uncoated samples reflected <7%) [132]. The use of melting for glass or glass-ceramics is a realistic processing option for early ISRU on Mars that could be used to produce glass fibers for insulation and as aggregate for other bonding approaches discussed here.

4.2.3. *Powder pressing*

While the use of loose regolith is being considered to shield habitats from radiation, meteoroid impact and launch blast debris, further stability could be gained by compacting regolith into slopes with very high angles (up to vertical for low load levels) [111] and compaction by powder pressing is a typical forming route for oxidic powders widely used on Earth. Boyd et al., in 1989 proposed a similar approach to dry compaction using cold pressing, naming it duricrete. The group employed self-made simulants (12% $MgSO_4$, 1% NaCl, 2% Fe_2O_3, and 85% bentonite clay or Pennsylvania nontronite) and different fiber additives (nylon mesh, rayon cloth, kevlar fiber or glass wool) plus water or sulfur (sulfur with heating), obtaining a compressive strength of 1.8–3.97 MPa [133]. Similarly, in 1992 Ishikawa et al. put forward smectite clay (which can be found on Mars) as raw material for dry and non-dry pressing (see Fig. 9) [134].

The group cold pressed dry and non-dry silica sand with different amounts of bentonite (see Table 9). Pressed bricks showed compressive strength ranging from 0.87 to 7.39 MPa depending on material mixtures and water absorbed in the bentonite [134].

A similar material system of MGS-1 and 5 wt% montmorillonite (MGS-1C/8) was used of late by Karl et al. to press green bodies with a compressive strength of 1.64 ± 0.08 MPa (the somewhat lower

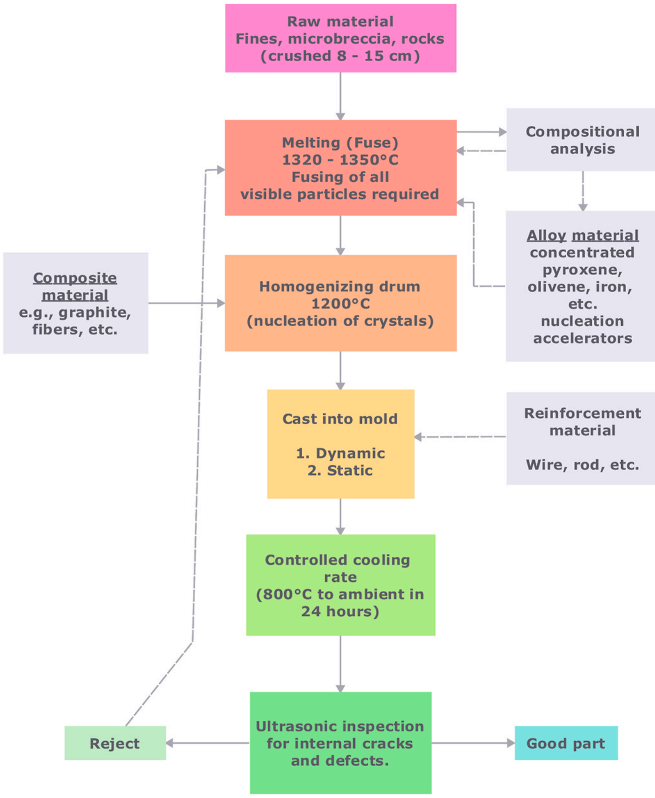

Fig. 8. Flow diagram of basalt casting process. Redrawn from Dalton et al. [16].

compressive strength compared to Ishikawa is likely to stem from the low smectite clay content) [84]. Recently, Chow et al. used high pressures to form powder compacts of montmorillonite (see Fig. 10) using what they described as direct formation (work by the same group using higher pressures with JSC Mars-1 has been discussed in the section on cold sintering) [135].

Pellets made from smectites (montmorillonite), dried at temperatures from 90 to 600 °C for 10 h, were quasi-statically compacted with rigid lateral boundary in a rigid steel dye with 150 MPa, which gave parts with an average flexural strength of 2.29–8.93 MPa (higher water content resulted in higher flexural strength). Samples produced using the free boundary and flexible tube boundary conditions lead to even higher flexural strength (see Fig. 10c).

Pressed/rammed clay earth has been and is widely used on Earth to build large structures (which is illustrated by an estimation from 1994 of a third of the world's population living in houses built of earth [136]) and the clay material system is re-gaining interest because of climate/energy issue associated with concrete. As they require only minimal processing, powder compacts with or without clay from pressing (and powder agglomeration, see 4.2.4) can be expected to play a vital role in early ISRU approaches to building infrastructure on Mars.

4.2.4. Powder agglomeration

Besides the compaction of powder from pressure, an often-observed phenomenon is powder agglomeration leading to powder compacts from vibration, moisture or when powder colloids are dried. Various authors have proposed that agglomeration phenomena could be used to compact/fuse regolith. In 1985, Beyer used a version of dry compaction based on a process from the refractory industry [137]. Named Lunarcrete, dry lunar regolith would be compacted using vibration in a mold. Depending on regolith properties, the compact could also be fixated using a low-temperature binder or post sintered (as done by Grossmann for MGS-1 [120]).

A different approach to forming powder compacts (especially from materials containing nanoparticle-sized powders) is colloidal wet-processing, followed by the fusion drying concept. The simplicity and universal appeal of fusion drying can be seen from Karl et al. (2021), who dispersed silica sand and feldspar (a simple lunar regolith simulant) in deionized water and water with a pH buffer for 3 days [138]. Water-reduced pastes were molded into cylindrical shapes, which after drying, had a compressive strength of 0.23–0.7 MPa. Compressive strength can be expected to increase significantly for feedstock materials with smaller particles and stronger leaching behavior such as lunar

Fig. 9. (a) Bentonite clay with silica sand were cold-pressed in different states (b), producing powder compacts (c). Images reprinted by permission from Springer Nature CCC: V. Badescu (Ed.), Mars (2009) 543–50, Ishikawa [134] copyright 2009.

Table 9
Properties of cold pressed and cured (dry and non-dry) silica sand and bentonite. Table reprinted by permission from Springer Nature CCC: V. Badescu (Ed.), Mars (2009) 543–50, Ishikawa [134], copyright 2009.

Regolith mixture before pressing			Curing condition	Strength results		
Bentonite content (%)	Sand (silica) content (%)	Water content (wt% of bentonite)		Density (g/cm^3)	Water content (%)	Compressive strength (MPa)
50	50	20	dry	1.953	13.4	5.67
			non-dry	1.896	13.4	1.45
70	30	20	dry	1.963	19.6	7.39
			non-dry	1.992	19.6	2.00
30	70	20	dry	1.784	7.5	1.33
			non-dry	1.810	7.5	0.87

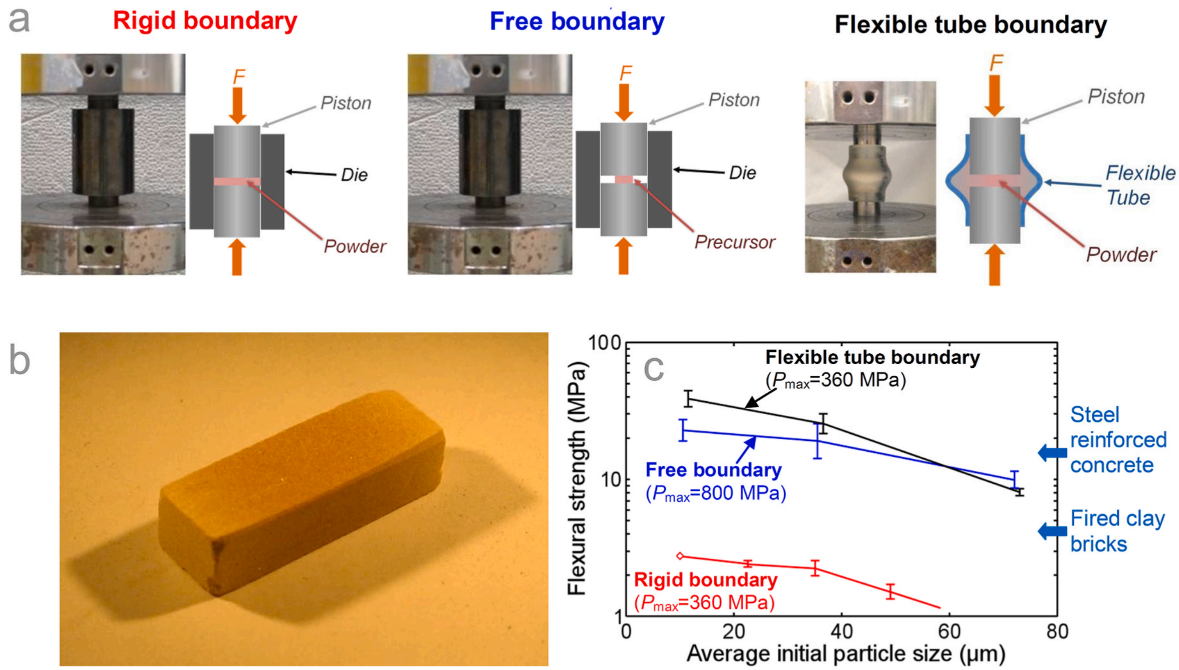

Fig. 10. (a) Direct formation (high-pressure pressing) of montmorillonite under different boundary conditions, (b) sample cut (middle section) from a pressed pellet and (c) mechanical properties of produced parts. Images reprinted from Advances in Space Research 60 (2017) 1443–1452, Chow et al. [135], copyright 2017 with permission from Elsevier.

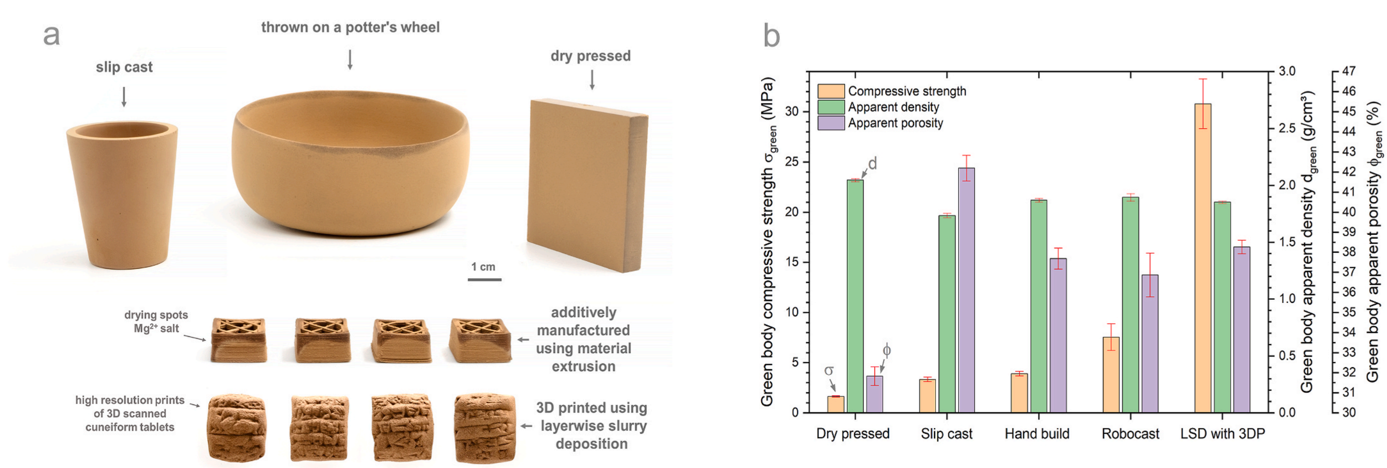

Fig. 11. (a) Various adobe structures generated through wet-processing (and a dry pressing reference) made of the 5 wt% smectite Martian simulant MGS-1C/8, (b) green body compressive strength and apparent density/porosity for different shaping approaches. Images reprinted from Acta Astronautica 174 (2020) 241–253, Karl et al. [84], copyright 2020 with permission from Elsevier.

regolith [139] or materials that turn into nanoparticles when dispersed in water like clay minerals found on Mars (and Asteroids). Such wet-processing of clays (one of the earliest human inventions originating before the Neolithic period) can be expected to yield structures with high compressive strength after (fusion) drying as evidenced by houses of dried clay bricks that reach 30 m in height, for example, in the city of Shibam in Yemen. Along those lines, Karl et al. (2020a) could show the versatility of clay ISRU wet-processing using tempered smectite clays (MGS-1/8C) which could be adapted to fit all typical ceramic shaping approaches (see Fig. 11) [84].

They formed green bodies with varying complexity, cups (slip casting), bowls (throwing), test cubes (material extrusion/robocasting) and cuneiform tablets (3D printed using layerwise slurry deposition) with compressive strength of fusion dried green bodies showing typical values similar to unfired clay bricks employed in numerous cultures with up to 7.5 MPa. Furthermore, 3D printed LSD green bodies with 5 wt% polymeric binder (that were water-resistant) had compressive strengths as high as 30.8 ± 2.5 MPa, similar to general purpose concrete. As already discussed in the powder pressing section (see 3.2.3), powder compacts (often from clay earth) are widely used on Earth for infrastructure. Wet-processing and shaping of clay materials could have similar importance for early ISRU, as it had in human history on Earth (for an overview of clay shaping approaches on Earth and their requirements for ISRU see Table 10).

Strong points for further investigation of this approach are the possibility that no materials would have to be shipped to Mars when operating in regions with clay deposits and the broad application flexibility with fusion dried green bodies either used directly as adobe structures or subsequently sintered to generate high strength ceramics (see 4.2.1).

Table 10
Examples for the use of different clay ISRU shaping technologies on Earth and assessment of requirements for green body ISRU on Mars. Table reprinted from Acta Astronautica 174 (2020) 241–253, Karl et al. [84], copyright 2020 with permission from Elsevier.

Shaping technology[a]	Use on Earth[b]	Mass of equipment required[c]	Other materials needed[c,d]	Total energy required for process[c,e]
Dry pressing	Simple shaped ceramic parts: Tiles, fireclay bricks, structural clay, porcelain products	high	none	high
Slip casting	Complex shaped part (with fine details): Sanitary ware, tableware, and porcelain.	low	ISRU gypsum for molds	low
Hand deformation of clay bodies	Throwing of pottery, press molding of mud bricks/adobe bricks.	low	none	low
Material extrusion	Forming of parts with one cross-section (and unlimited length): Clay brick, tile, vitrified clay pipe (sewer pipes), porcelain insulators	medium	none	medium
Material extrusion (robocasting)	Vases, artistic objects, clay walls/houses.	low	none	medium
Tape casting/doctor blade processing	Production of thin ceramic plates: Thin porcelain tiles or layerwise slurry deposition (high-density small objects with good resolution)	high	binder system for LSD[f]	very high

[a] Main clay shaping categories were used.
[b] Commonly used on Earth to shape what kind of clay-based green bodies.
[c] Assessed for Mars ISRU on a five-point scale: none, low, medium, high, very high.
[d] Additional ISRU resources needed (assuming MGS-1C/8 without dispersant is used).
[e] Including energy needed for the preparation of feedstock (sorting, milling, etc.).
[f] Inorganic ISRU binders could be developed or polymeric binder ISRU produced (needed ~ 5 wt%).

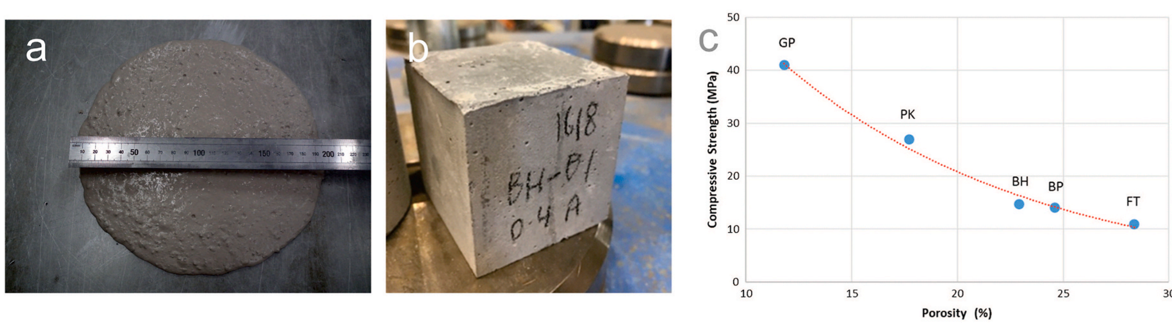

Fig. 12. (a) Self-compacting fresh MgO-silica mortar, (b) hardened mortar cube samples and (c) compressive strength versus porosity of twenty-eight day cured mortar with four different New Zealand Mars simulants (BH-Black Head, PK-Pukekawa, BP-Banks Peninsula, FT-Flat Top and GP cement control). Images with permission from ASCE Scott et al. [103].

4.2.5. Aggregate bonding

The bonding of regolith aggregates using various binding agents (such as cement) has been extensively researched. Concrete is an essential building material on Earth and has been widely explored for ISRU (a detailed summary can be found in Ref. [114]). Small quantities of actual lunar regolith from Apollo 16 have been used as aggregate by Lin et al. for concrete with a calcium aluminate cement mortar produced in 1988 [140]. Test cubes from this concrete had a compressive strength of 75.6 MPa and a Poisson's ratio of 0.39. McKay and Allen propose the use of concrete for a Mars habitat. They additionally argue that the material is much better suited for Mars than for the Moon because Mars is a better source of concrete raw materials with aggregate, cement components and water available [141].

Recently, Scott et al. used four Mars regolith simulants from New Zealand as aggregates for magnesium-based cement (see Fig. 12). The group cast 5 cm cubes using a cement of MgO and silica (each ~25–27.2 wt%) with superplasticizers (2–4%) that had compressive strength from ~12.5–35 MPa after 90 days [103]. Concrete is currently the most-used building material for industrialized societies on Earth. However, concrete production and processing are challenging, requiring specific raw materials and high amounts of energy. Concrete might not be the first choice for early ISRU on Mars.

A combination of aggregate bonding and sintering was proposed by Desai and Girdner in 1992 [142]. Named thermal liquefaction, the concept is based on the partial sintering/melting of a fiber binder. Fibers of aluminum, carbon steel and stainless steel were fused with Arizona Lunar Simulant (ALS), creating an intermediate ceramic composite with a flexural strength of 8.6–28.9 MPa. As this process uses metal fibers, early ISRU applicability for Mars is in question.

Sulfur concrete uses heat to melt sulfur, a process followed by cooling to produce a composite stable under specific conditions (see Fig. 13).

Grugel used lunar regolith simulants for sulfur concrete and reported that sulfur sublimation rates were rapid during lunar temperature highs combined with the hard vacuum conditions, representing challenges for the production of sulfur concrete on the Moon [143].

Wan et al. drew on Mars as a 'sulfur-rich planet' and mixed different fractions of JSC Mars-1A with various percentages of sulfur above 120 °C, which were cast into simple shapes [144]. After casting, sulfur solidifies as it crystallizes into monoclinic sulfur, which transforms into orthorhombic sulfur upon further cooling. Mars surface conditions in Fig. 13 indicate sulfur would be in the rhombic state at the construction site and the pressure above the solid-vapor line (which is important to prevent disintegration). Parts from different sized aggregates with 40–60 wt% sulfur showed a compression strength of ~5–60 MPa with a strong dependence on the particle size distribution of the aggregates (see Fig. 14) [144].

The sulfur concrete concept (later named Marscrete [145]) could be used as a reliable construction material with good acid and salt resistance. In general, sulfur is a common element on Mars, proven by rovers, landers, remote sensing observations and Martian meteorites [146], but extraction feasibility (for example, from gypsum or pyrite minerals) would determine real ISRU applicability for sulfur concrete.

Yet another aggregate bonding concept was introduced by Alexiadis

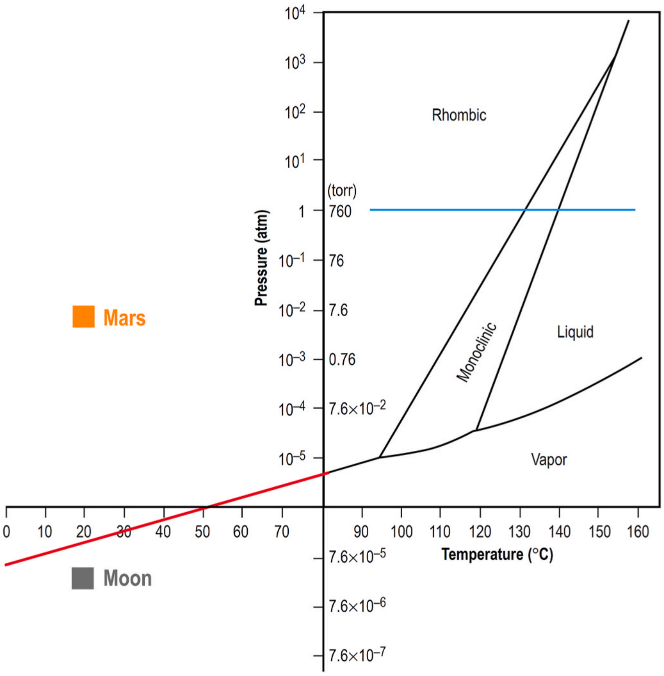

Fig. 13. Sulfur phase diagram with labeled environmental conditions on the Moon and Mars. Sulfur sublimation rates on the Moon can be high but are expected to be low on Mars. Image courtesy of NASA [143].

et al., who explored the production of geopolymers from JSC Mars-1A [147]. Geopolymers are a class of cementitious materials that gain their structural strength from a polymeric reaction of an aluminosilicate precursor mixed with a liquid alkali or alkali-silicate activator solution. In theory, any material with high fractions of amorphous silica and alumina (such as regolith) could geopolymerize. Alexiadis et al. mixed JSC-1A and JSC Mars-1A with various amounts of NaOH and K-silicate (K_2SiO_3), obtaining a viscous fluid that was poured into silicone stamps and dried at 80 °C for 3 h. JSC Mars-1A samples cured at room temperature for 28 days had a compressive strength of 0.7–2.5 MPa (2–18.4 MPa for JSC-1A). Montes et al. evaluated geopolymers from JSC-1A (Lunamer) as a radiation shield. They found that a lunar base made of Lunamer would be sufficient for a prolonged human lunar mission, as the absorbed dose was in the same order as the annual whole-body radiation worker limit (5 cSv, 5 rem) [148]. Geopolymers hinge on the activation of regolith using alkali or alkali-silicate activators. Once ISRU production of activator materials has been demonstrated for Mars, geopolymers could be used independently or in tandem with other processing approaches (e.g., fusion drying with clay ISRU).

A further method for fusing aggregate relies on phosphoric acid, a concept introduced by Buchner et al. [128]. Most metals form phosphates; phosphates with multivalent cations are rock formers (e.g., $Ca_3(PO_4)_2$, $AlPO_4$, or $FePO_4$). Thus, Buchner et al. expect phosphate binder to apply to a wide range of substrates present in Martian regolith. The group used JSC Mars-1A with phosphoric acid for dry pressing and material extrusion, obtaining parts with a compressive strength of ~20 MPa. A more detailed discussion of this approach can be found in section 5.1.1. The authors propose that at least 33 wt% of phosphates would have to be shipped, making the concept quite cost-intensive.

Recently, Shiwei et al. proposed a bioinspired regolith composite employing the biopolymer chitosan to fuse MGS-1 (see Fig. 15) [149]. The group dissolved chitosan (3% w/w) in a 1%(v/v) aqueous acetic acid solution and mixed it with different ratios of MGS-1 (dry w/w of 1:25, 1:50, 1:75, 1:100, 1:125) followed by drying/curing either in an oven for 24 h at 60 °C for cast samples or heating by a hot air gun for materials extrusion. While the overall compressive strength from ~2.6–3.6 MPa was only a fraction of most other aggregate bonding concepts discussed here (which typically use higher binder fractions), the materials showed a high flexural strength to compressive strength ratio (flex strength from 1.25 to 1.74 MPa) for a material employing aggregate bonding, indicating the biopolymer's influence.

Finally, Sen et al. proposed employing an organic binder to fuse aggregate using the synthesis of organic polymers from the Martian atmosphere and employing these to fuse regolith for radiation shields. 20–40 wt% of polyethylene (PE) was mixed with JSC Mars-1 and hot

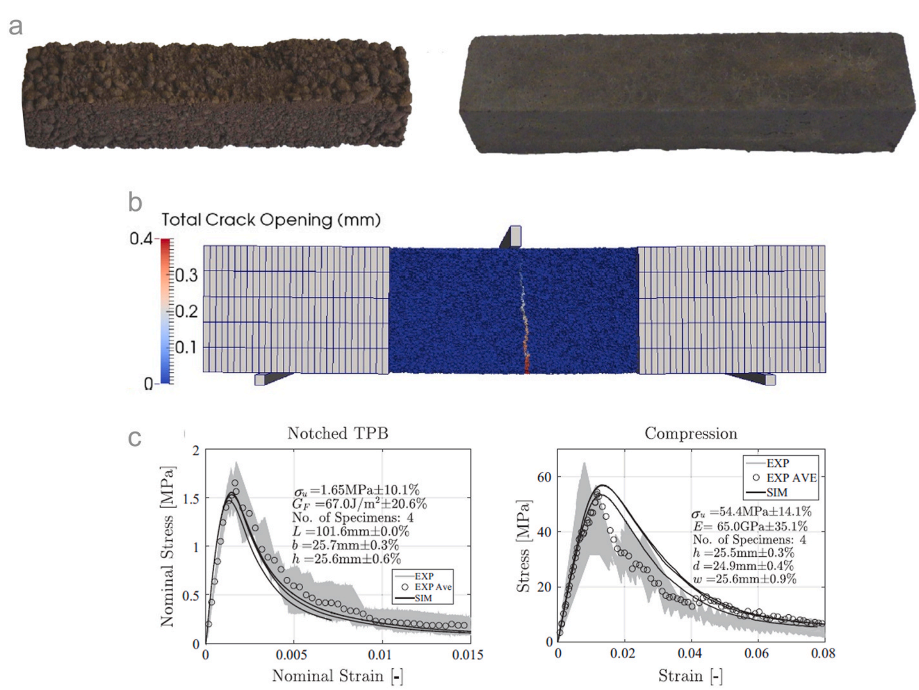

Fig. 14. (a) Beams from Martian sulfur concrete for bending test. The beam on the left uses a max. 5 mm aggregate and the one on the right a max. 1 mm aggregate. (b) Simulation of unnotched TPB test setup and (c) left side experimental results and simulations, right side unconfined compression tests. Images reprinted from Advances in Construction and Building Materials 120 (2016) 222–231, Wan et al. [144], copyright 2016 with permission from Elsevier.

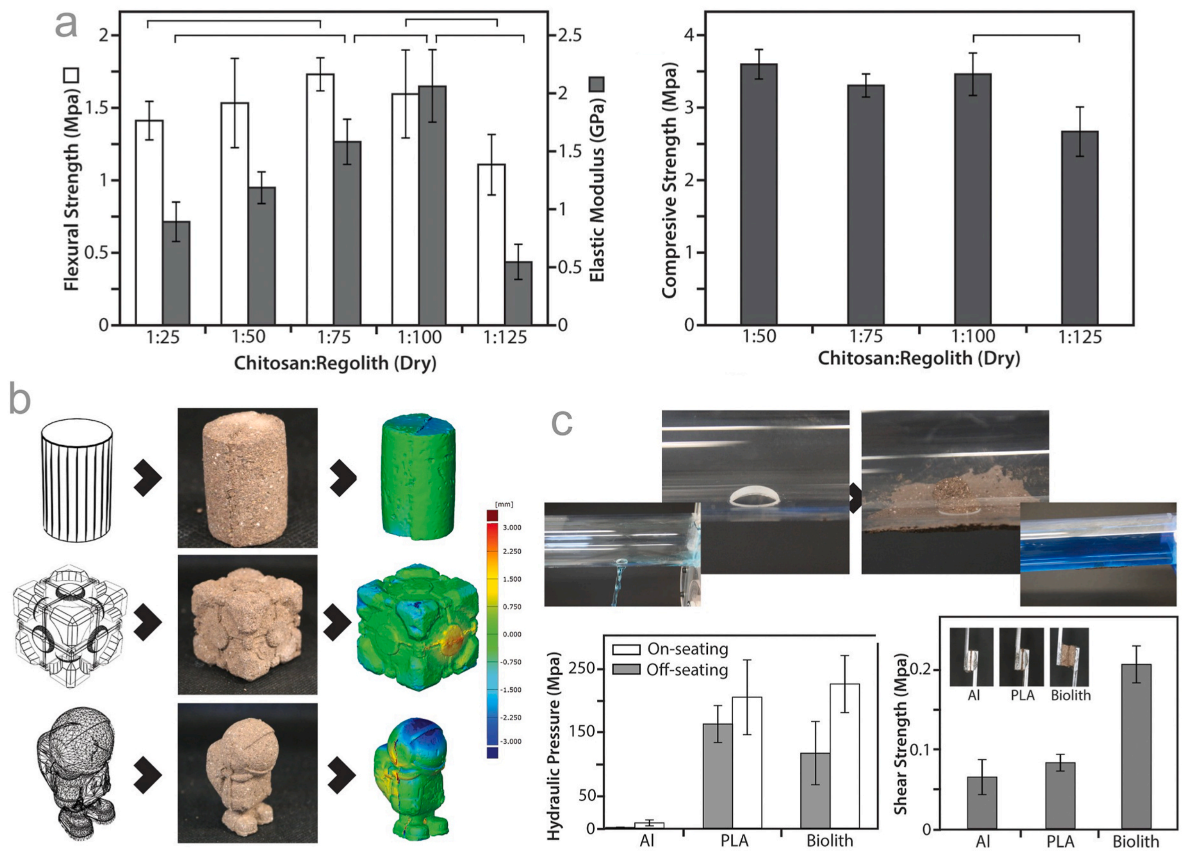

Fig. 15. (a) Flexural strength/elastic modulus and (b) compressive strength of biolith with varying chitosan to regolith ratios, (c) samples cast using biolith in silicone molds and (c) biolith used as a mechanical sealer to stop leakage from a drilled hole with hydraulic pressure/shear strength of such seals using biolith applied onto aluminum or PLA surfaces. Images with open access permission (CC BY)from Shiwei et al. [149].

pressed at 140 °C with 240 MPa, giving polymer composites with a flex strength of 38–47 MPa [150]. While radiation shielding properties for PE are promising, it seems doubtful that ISRU polymer production would be energetically feasible. Also, water might be a better choice for radiation shielding.

4.2.6. *Chemical fusion and reduction of metal oxides*

Metallic powders can be used as fuel for an exothermic reduction-oxidation (redox) of metal oxides or thermite reactions, which have welding applications. Faierson et al. explored thermite reactions for lunar simulants using metallic aluminum powder as an oxidizer [151]. A mixture of 67 wt% JSC-1A with 33 wt% aluminum was poured into crucibles and the thermite reaction was initiated via electric current over a NiCr wire. This geothermite reaction was used to produce a special voissoir element geometry with a compressive strength of ~10–18 MPa [151]. Corrias et al. elaborated on this technique by using JSC-1A, JSC Mars-1A and MMS simulants for a thermite process called Self-propagating High-temperature Synthesis (SHS) [152]. While the Lunar simulant was mixed with various amounts of $FeTiO_3$ and metallic aluminum, Mars simulants were mixed with 38 wt% Fe_2O_3 and 16 wt% aluminum. Pressed pellets of the mixtures were reacted in a special SHS reaction chamber under vacuum. Only the compressive strength of samples with JCS-1A is reported, which was 25.8–27.2 MPa for the best samples. However, as this process requires a significant amount of metallic aluminum, early ISRU is in doubt.

Various efforts have been made to use the reduction of regolith to produce O_2 and metals in one process (see Fig. 16). Lomax et al. have investigated the FFC-Cambridge process for the electro-deoxidation of lunar regolith producing oxygen and metals/alloys [153].

In this electrochemical process, metal oxides are cathodically reduced in molten salts to metals/alloys. The electro-deoxidation of JSC-2A lunar regolith simulant by an oxygen-evolving SnO_2 anode in a bath

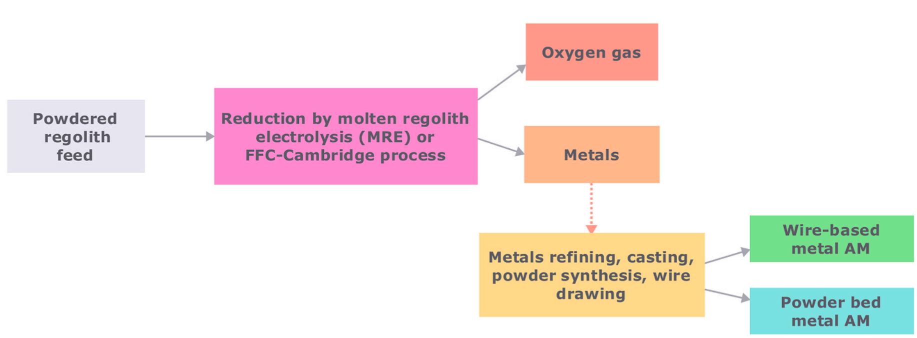

Fig. 16. Proposed process flow for the reduction of regolith producing O_2 and base metals, towards ‘metal’ AM by the MRE and FFC approaches.

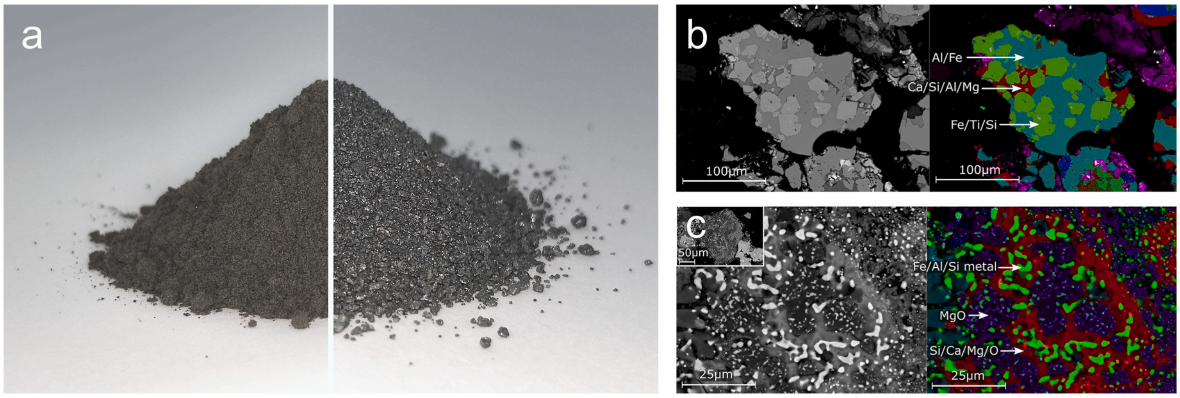

Fig. 17. (a) Lunar simulant (JSC-2A lunar) FCC electrolysis reduction process input (left) and metallic output (right). (b) Reduced regolith grains showing phase separation in three common phase groupings and (c) BSE and phase map images of a partially reduced olivine-rich grain (overview image top-left corner). Image (a) with kind permission of Bethany Lomax and (b–c) reprinted from Planetary and Space Science (2019) 104748, Lomax et al. [153], copyright 2019 with permission from Elsevier.

of molten $CaCl_2$ salt at ~950 °C produced alloys that were essentially metallic with 96% of the total oxygen removed. In addition to the Al/Fe, Fe/Si and Ca/Si/Al alloys that dominated the product (see Fig. 17), this process would have a potential oxygen yield of 40–45 wt% for every kg of regolith excavated.

Schreiner detailed the history of ISRU regolith reduction, focusing chiefly on oxygen production [154]. He designed a molten regolith electrolysis (MRE) reactor based on the direct electrolysis of molten regolith to reduce its oxide constituents to produce metals and oxygen.

Oxygen reduction from regolith produces metallic alloys that contain high percentages of silicon; pure silicon is a tetravalent metalloid that is brittle and crystalline. While such Si-alloys could be called 'metallic', in the sense that they are not oxidic, they have a brittle nature and do not possess the enhanced ductility associated with engineering metals for

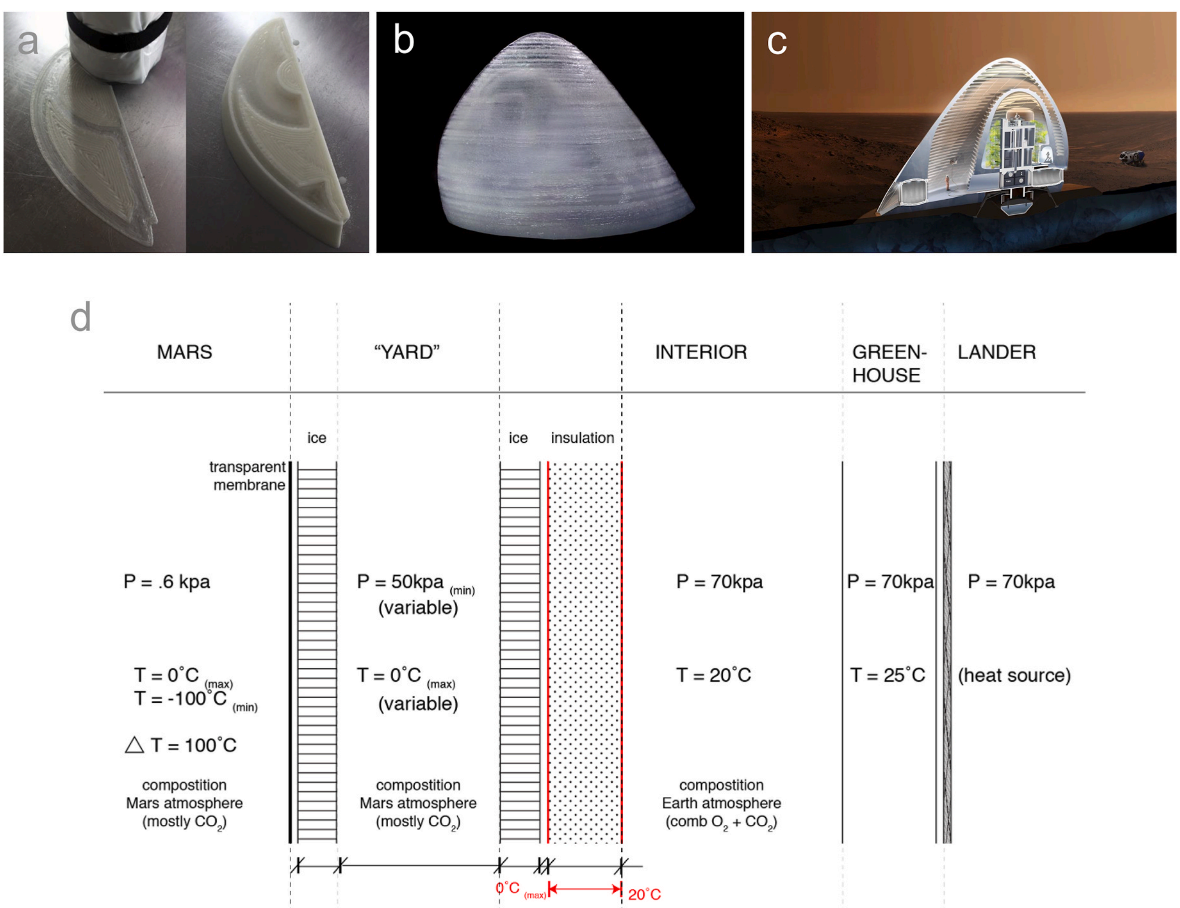

Fig. 18. (a) Rapid freeze prototyping of water ice and brine support structure and (b) final Ice House geometry after melting brine support structures. (c) Rending of cross-sectional Mars Ice House architecture concept, revealing double-wall condition, vertical garden and interstitial yard. (d) Proposed concept for wall sections of the Mars Ice House with layered composition and variable pressure and temperature in each zone. Images reprinted with kind permission by SEArch and Clouds AO from Morris et al. [158].

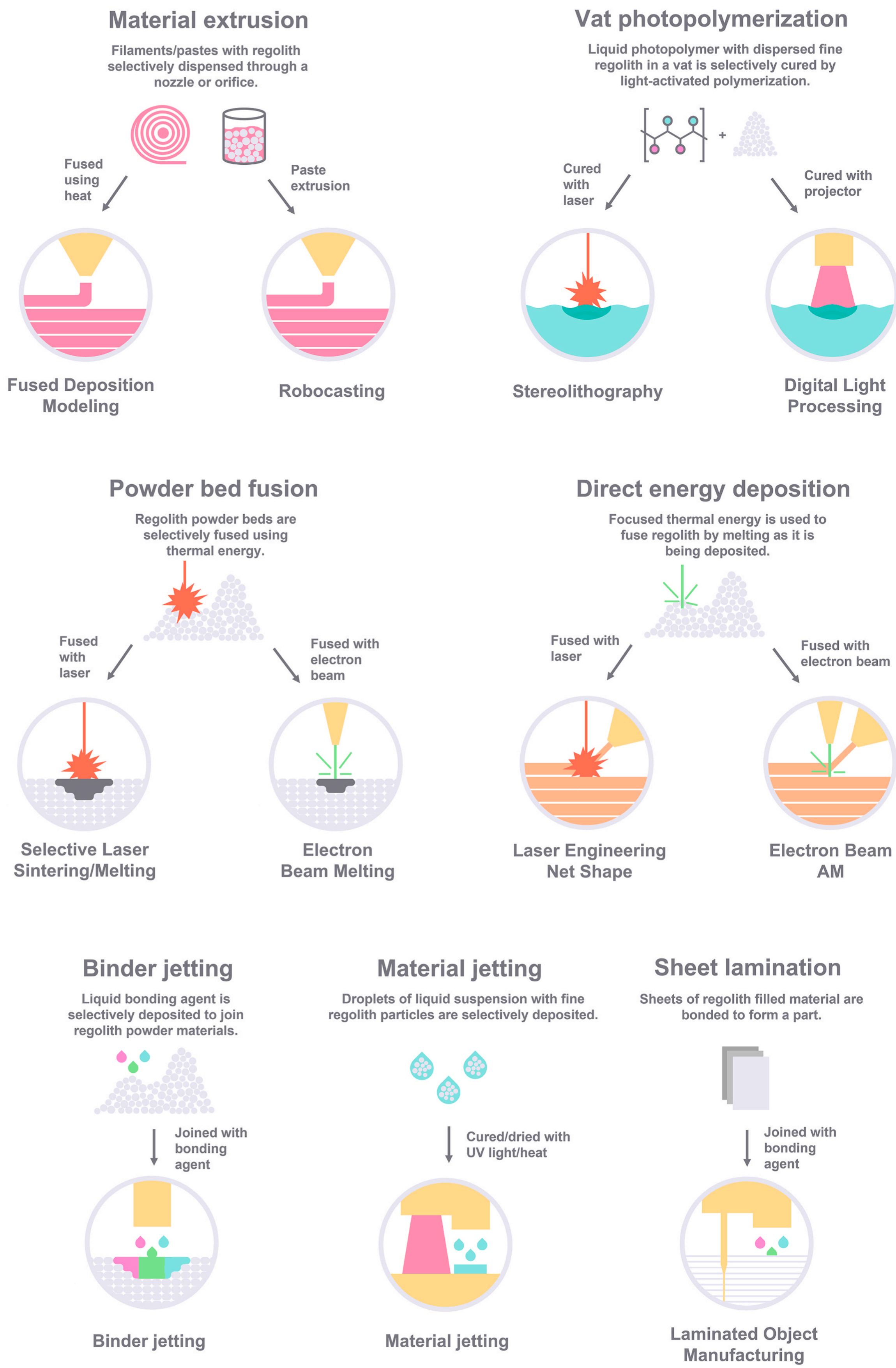

Fig. 19. Overview of AM concepts for regolith processing according to ISO/ASTM 52900.

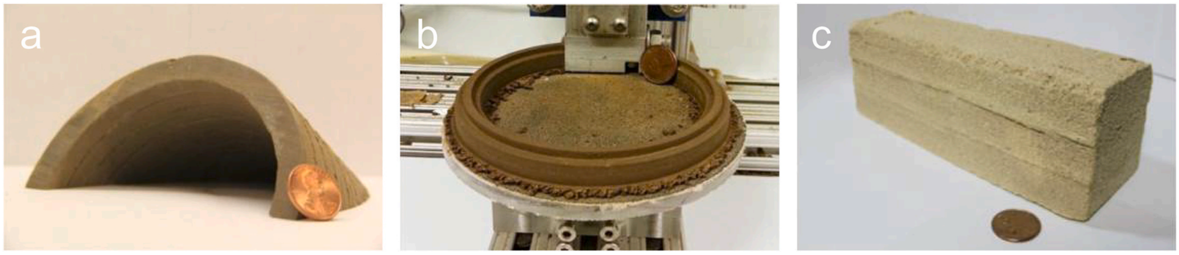

Fig. 20. Contour crafting of (unspecified) Martian regolith simulant with sulfur, producing (a) Martian regolith dome, (b) extruded sample with a smooth surface and (c) sample with large layers. Images reprinted with permission from Rapid Prototyping Journal 22 (2016) 848–856, Khoshnevis et al. [170], copyright Emerald Publishing Limited all rights reserved.

technical parts. In essence, regolith reduction can be viewed as a smelting process yielding alloys that are brittle and would need to be processed similarly to technical ceramics/along powder metallurgical routes. This explains why the reduction of regolith has been included in this review. While the concept to produce two essential necessities at the same time seems appealing for Mars ISRU, O_2 production from the atmosphere (MOXIE) or by water-splitting can be expected to be cheaper in energy terms. Furthermore, regolith reduction using silicate-based materials does not produce ductile metals and can rather be viewed as a route towards technical ceramics. Because of their complex and costly production, technical ceramics have very limited application reach, which would be especially true for early ISRU on Mars.

The misconception that metallic alloys would possess ductility forms the basis of a study by Grossmann et al., who proposed the use of metal alloys from MRE reactions as feedstocks for wires (which would later be processed using AM) [155]. The group mixed ferrosilicon (a primary metallic alloy produced during the reduction of metal oxides from MRE) with chemical-grade Fe at different amounts of Si (3, 6, 9, and 12 wt% Si) and melted the mixture in an arc melt furnace. The flexural strength of cut bars was ~12–58 MPa (for reference, pure Fe was 134 MPa). Grossmann et al. concluded that the samples with the lowest amount of Si (3 wt%) had enough ductility to be used in the form of wires for AM. However, the concept may in practice be unfeasible as ferrosilicon alloys from regolith reduction are expected to possess much higher Si ratios.

4.2.7. Freezing

Multiple observations have confirmed the presence of water on Mars, for example, at the NASA Phoenix Mars Lander landing site, where a hard substrate of ice was uncovered during landing [156]. While such water can be a critical ISRU resource, the presence of subsurface ice on Mars highlights the fact that weather conditions are an essential consideration for surface operations and production concepts on extraterrestrial bodies. For the Moon, in 1992 Ishikawa et al. proposed using freezing by spraying water or cement paste inside a cold chamber or onto the surface of a cold metallic board producing powdered ice [157]. Cement, aggregate, and powdered ice would be mixed under low temperature and vacuum. The concrete mix is then covered with an airtight material and is thawed using energy applied from the outside (for example, from microwaves) while being compacted with applied vibration and pressure. After a predetermined curing period, the concrete would be used as a structural material. In essence, freezing is used as an intermediate stage and the previous evaluation of concrete ISRU on Mars can also be applied to this concept.

The direct use of ice as a structural material for Mars ISRU habitat building was proposed by Morris et al. in 2015 [158]. Their Mars Ice House depicted in Fig. 18 (developed during NASA's 3D-Printed Habitat Competition) is a detailed design concept based on a lander that uses subsurface ice to construct a hull made of solid H_2O (H_2O is favorable for its excellent radiation protection and light transmittance).

Small robotic movers would build ice walls (and later climb them) by depositing water, which would subsequently freeze. Support structures for this AM method are proposed to be constructed using brine water (which has a lower melting point than pure ice). Looking at terrestrial precedents, ice houses on Earth benefited from the addition of fibers such as wood pulp to reinforce the ice shell. On Mars, fibers drawn from regolith melts could be used as reinforcements for the solid ice, which Morris et al. claim would increase the tensile strength of ice from ~2 to 3 MPa by order of three [158] (compressive strength for ice from 0 to 10 °C in terrestrial atmospheric conditions can be expected to range from 5 to 20 MPa [159]).

The very promising, detailed approach of the Ice House concept has attracted much publicity. The use of ice as radiation shielding and as a structural material is an appealing concept. More work is needed to evaluate the stability of ice at Martian surface conditions and to determine in detail which additional measures would be necessary to stabilize ice for long periods.

5. Additive manufacturing in ISRU

Robotic manufacturing has been proposed for space missions from the 1970s onwards as a way of facilitating the production of planetary surface structures before the arrival of human astronauts. One of the suggestions was to use robots for masonry (an idea still of interest today [19]) to remotely build habitats by laying bricks, similar to human masonry on earth. In a sense, a modern embodiment of robotic masons (that put down brick after brick) are the AM technologies that use layer by layer manufacturing. Initial advances for AM in ISRU were made by some specialists (e.g., Khoshnevis and co-workers [160]), but only after '3D printing' became a mass phenomenon did a larger number of researchers join the field. The topic has attracted considerable media coverage since NASA's three-stage Mars Centennial 3D-Printed Habitat Challenge that started in 2015 and prompted a greater number of researchers to join the field of AM ISRU. Here, no general introduction to AM is given. The interested reader is referred to one of the numerous textbooks on AM in general [161–163] and specifically to the excellent ISO norms defining the seven different AM categories [164,165]. Rather, an overview image of AM concepts in general is provided in Fig. 19.

5.1. Material extrusion

Material extrusion is judged to be a prime technology for building infrastructure on extraterrestrial bodies due to its good scalability, ease of use, broad material processing spectrum and suitability for vacuum and low gravity environments [166]. Various studies have explored material extrusion in ISRU, including works by NASA and ESA. For example, most submissions of NASA's centennial challenge to 3D print a habitat on Mars used material extrusion.

In 1998 Khoshnevis introduced contour crafting. This material extrusion technique can be described as robocasting with trowels that flatten extruded material to attain a smooth and accurate surface finish [160]. The technologies established large, square orifices, making it possible to extrude slurries with large particles, as well as a hybrid nozzle, to build hollow walls [167]. While terrestrial applications of contour crafting use mainly cementitious materials, the technology can

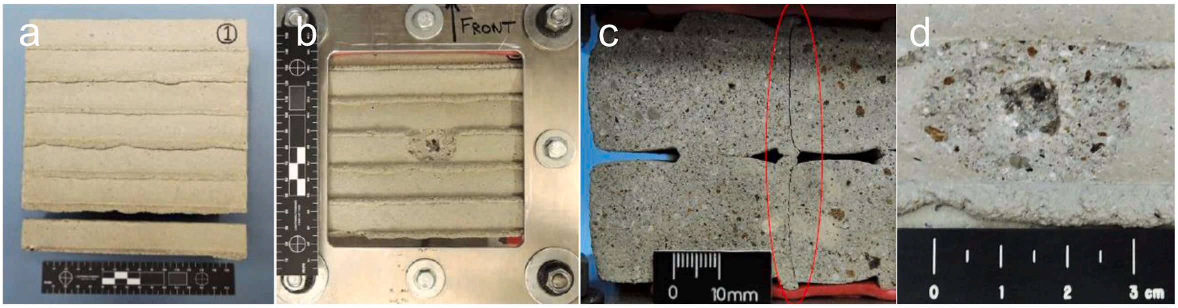

Fig. 21. (a) AM sample from JSC Mars-1A mixed with Portland cement (stucco admixture with water) showed weak layer adhesion between a dry mortar layer and a wet mortar layer added on consecutive days (sample broke during shipping). (b–d) Hypervelocity impact testing of such printed structures. Images courtesy of NASA [171].

Table 11
Average compression test results for simulant and ordinary Portland cement (OPC) mortars. Table reprinted with permission of ASCE from Edmunson et al. [169].

Size Fraction (μm)	JSC Mars-1A (MPa)		JSC-1A (MPa)	
	7-Day	28-Day	7-Day	28-Day
4000–5000	20.3	32.2	–	–
2000–3999	21.1	35.5	–	–
1000–1999	22.1	32.6	–	–
500–999	21.3	33.5	20.5	28.2
250–499	21.9	35.6	24.7	34.2
125–249	25.6	31.9	21.1	26.2
63–124	27.6	34.3	27.8	37.1
<63	23.9	30.0	29.4	37.1
Unsieved	22.8	24.4	27.8	36.1

be adjusted to extrude molten regolith or sulfur concrete for Lunar/-Martian infrastructure and habitat construction [168]. The Khoshnevis group has investigated such sulfur concrete contour crafting with unspecified Martian regolith simulant [169] and 30–35 wt% sulfur by heating the extrusion feedstock to ~150 °C [170].

Heating is necessary as molten sulfur significantly reduces viscosity during extrusion, which is essential to produce parts with low porosity. One significant advantage over calcium-based concrete is that sulfur concrete cures in less than 10 min, reaching its highest compressive strength after 24 h (see Fig. 20).

Because of the material extrusion's highly promising potential, NASA has overseen large-scale efforts to use material extrusion on the surface of planetary bodies in the framework of different additive construction with mobile emplacement (ACME) projects mainly using aggregate bonding. Such systems include a gravity-fed dry feedstock delivery system with a heated nozzle to extrude polymers mixed with basalt simulant and a gantry mobility system that moves an extruder connected to a mixer with a pump for concrete (see Fig. 21) [169].

During material development for the gantry mobility system, Edmunson et al. tested the influence of simulant aggerate particle size (for JSC Mars-1A and JSC-1A) fused using ordinary Portland cement (OPC) mortars on the compression strength of cubes (see Table 11). While large samples produced using material extrusion in an ambient terrestrial atmosphere were promising, layer adhesion between dry mortar layers and wet mortar layers was weak compared with the layer adhesion of two wet layers (see Fig. 21a), which came to light during shipping to perform hypervelocity impact tests on the materials (Fig. 21b–d).

In the framework of the 3D-Printed Habitat Competition, Hojati et al. extruded OPC, sorel cement (a magnesium oxychloride cement) and metakaolin based geopolymer binder with basalt aggregate (and low amounts of carbon fibers), producing medium scale cylinders with a compressive strength of 15.1 MPa for OPC and 2.2–4.4 MPa for the metakaolin geopolymer system (sorel cement strength not reported) [172]. A further interesting approach was taken by Pilehvar et al., who investigated the utilization of urine as an accessible superplasticizer for the material extrusion of lunar geopolymer mixtures [173]. A geopolymer paste of DNA-1 lunar regolith simulant with an alkaline solution of sodium hydroxide and urea showed good extrusion processability. Samples cast from this paste were cured at 80 °C for 6 h and freeze-thaw cycled. The initial compressive strength was 13 MPa and ~15 MPa after 8 freeze-thaw cycles. Another approach was taken by Jakus et al., who extruded regolith polymer composites of a complex resorbable biopolymer (PLGA) filled with JSC-1A and JSC Mars-1A in toxic DCM generating samples with elasticity [174]. While the

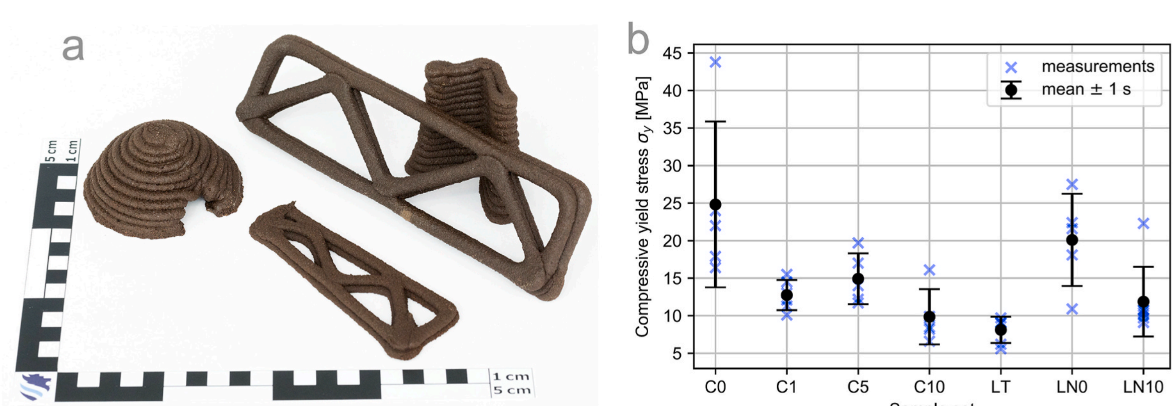

Fig. 22. (a) Structures printed using a phosphoric acid binder with JSC Mars-1A and (d) compressive strength after temperature cycling experiments of such materials (C0–C10: number of thermal cycles, LT: long-time heated, LN0 and LN10: liquid nitrogen immersion after 0 and 10 cycles, respectively). Images reprinted from Acta Astronautica 143 (2018) 272–284, Buchner et al. [175], copyright 2018 with permission from Elsevier.

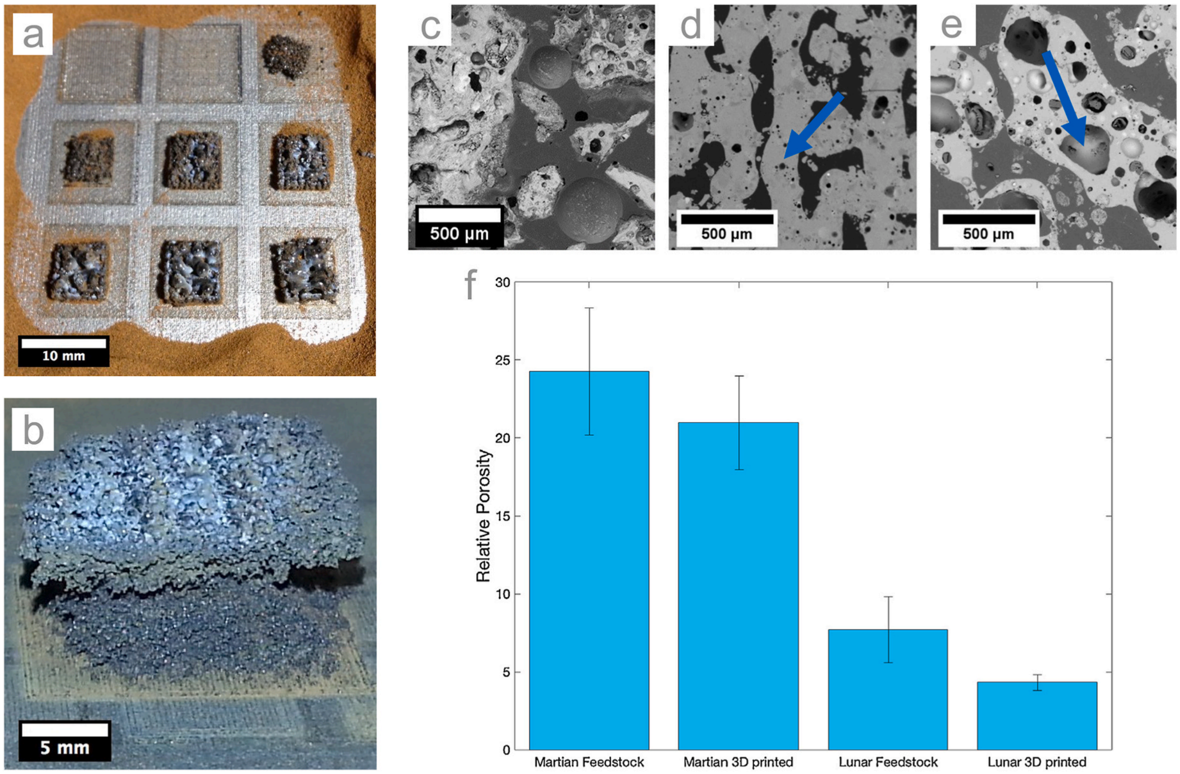

Fig. 23. (a–b) Samples built by PBF from JSC Mars-1A with poor consolidation due to the simulant's high volatile content. (c–d) SEM micrographs cross-sections of pre-processed Martian regolith, (e) laser fused JCS Mars-1A crosssection and (f) relative porosities of JCS Mars-1A and JSC-1A before and after PBF. Images reprinted from Goulas et al. [180] with permission of SAGE Publications.

production of elastic parts seems interesting, their choice of polymer and solvent is judged inappropriate for ISRU applications.

Buchner et al. proposed material extrusion using a phosphoric acid binder. A paste of 6 parts concentrated phosphoric acid (85 wt%), 2 parts water and 10 parts JSC Mars-1A by weight was extruded in layers to produce simple parts (see Fig. 22). After curing, samples from material extrusion showed a compressive strength of ~20 MPa. Thermal cycling to simulate Martian environmental conditions reduced the yield stress to 10 MP, while immersion in liquid nitrogen did not seem to affect the yield stress significantly.

Karl et al. (2020a) used material extrusion of MGS-1C/8 clay feedstocks (taking advantage of clay plasticity when mixed with water) to produce adobe structures that showed a compressive strength of 7.55 ± 1.33 MPa (see Fig. 11) [84]. As this approach could be additive-free (when done using exclusively Martian clay minerals) and requires minimal feedstock preparation (except for mineral collection, tempering and possibly aging), clay wet-processing followed by fusion drying could be of great benefit to early ISRU (as discussed in 4.2.4).

Finally, the deposition of liquid water in freezing conditions for the Mars Ice House submission in NASA's 3D printing challenge loosely falls into the material extrusion category. The technology is based on extensive work for rapid freeze prototyping (later named freeze-form extrusion) by Leu and co-workers, starting around 2000 [176,177]. Morris et al. have given an insightful and detailed account of how the deposition of ice could be used for Martian habitat construction [158], arguing that transparency, radiation shielding capacity, non-toxicity and wide availability would make it ideally suited as an ISRU building material.

5.2. Powder bed fusion

The selective fusion of powder beds (PBF) using thermal energy is a widely used terrestrial AM technology. In theory, PBF processes are promising for ISRU as they solely require regolith and energy without any further additives. However, ceramics and glass production from regolith with very fast heating rates can induce thermal stresses, resulting in cracks and typically lead to non-favorable microstructure in AM parts.

Several researchers have explored the fusion of regolith simulants using lasers and concentrated solar energy. Fateri and Khosravi used a 100 W fiber laser to fuse simple objects from (not further specified) sand [178]. Fateri went on to fuse JSC-1A simulant into black glassy parts in various geometries [179]. However, no mechanical properties were reported and microscopy images reveal intensive crack formation in the single laser lines. Similarly, Goulas et al. fused JSC-1A and JSC Mars-1A using a ytterbium-doped fiber laser (λ = 1.06 µm) with a maximum power output of 50 W, producing lattice structures (see Fig. 23) [180].

The group outlined several processing difficulties, such as low powder bed packing due to non-round particle morphology and high internal porosity of starting simulants. This contributed to poor interlaminar and planar consolidation and high open and closed porosities with ~4% and ~21% relative porosity for JSC-1A and JSC Mars-1A, respectively. Only mechanical strength for JSC-1A was reported with compressive strength ranging from 0.3 to 4.25 MPa [181]. Recently, Caprio et al. used powder bed fusion for the lunar highlands regolith simulant NU-LHT-2M producing parts with high porosities of 37–65% but a reasonable compressive strength of 31.4 MPa and microhardness in excess of 680 HV [182].

Hintze et al. introduced the use of concentrated solar energy for melting/sintering. In 2008 they focused solar light on a bed of JSC-1, quickly melting the simulant in the focal spot [183]. The group proposed using solar energy to cure polymer binders (sprayed onto regolith) and using the solar concentrator technology to build landing pads. To study the sintering of the top regolith layer, they built the Large Area Surface Sintering System (LASSS), a rover equipped with $MoSi_2$ resistive heating elements operated at 1000 W [119]. In a field test at Mauna Kea

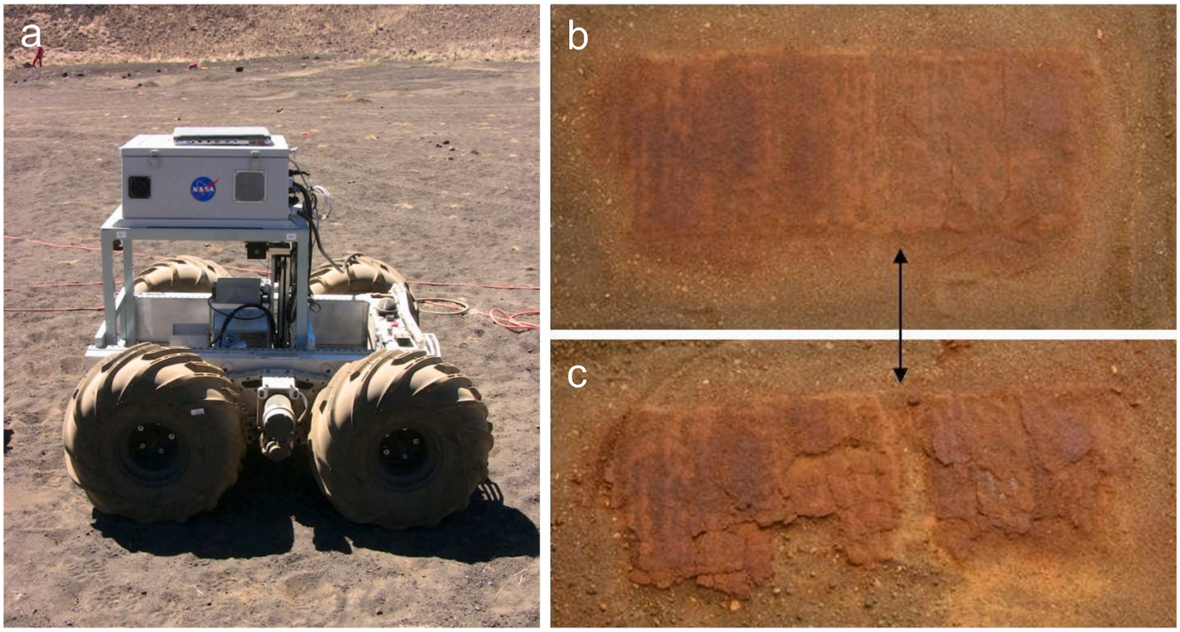

Fig. 24. (a) LASSS during a field test at Mauna Kea mounted on a rover. (b) Area sintered by LASSS and (c) the same area after thruster firing test. Images courtesy of NASA [119].

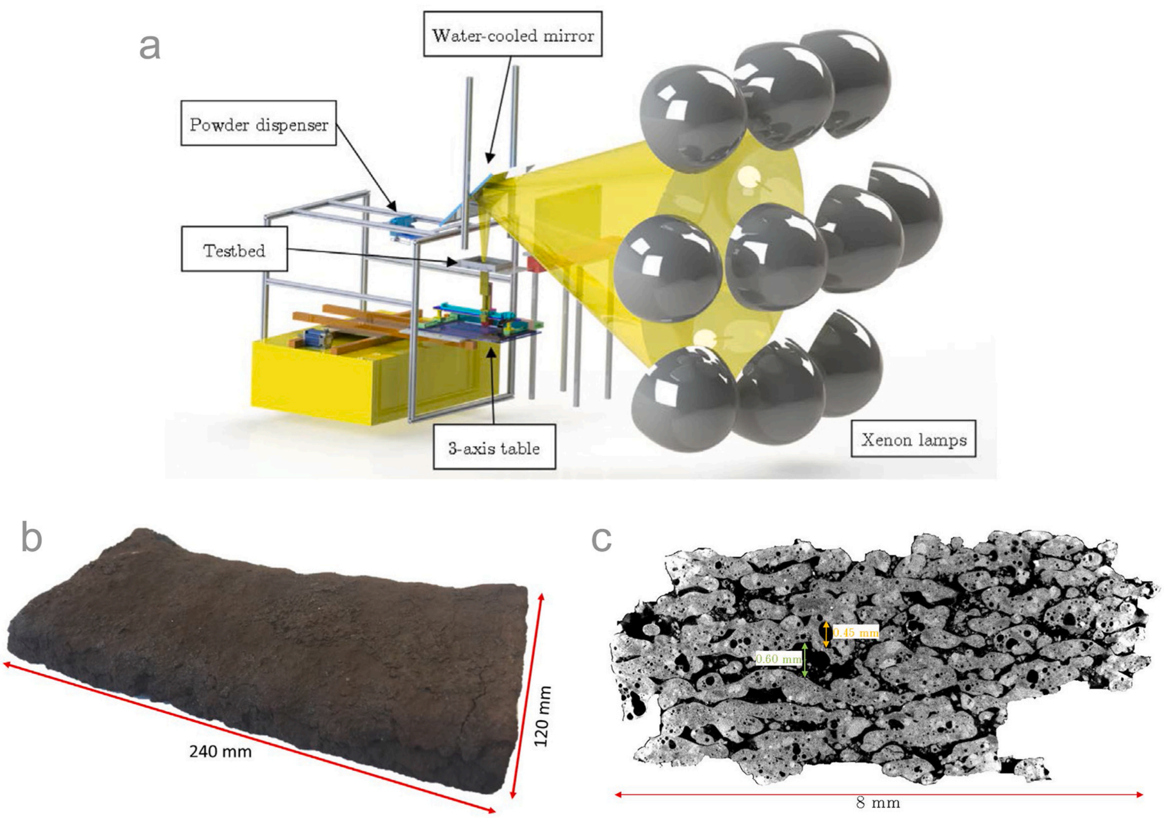

Fig. 25. (a) Rendering of powder-bed fusion solar simulator setup with Xenon lamps from the Xenon High-Flux Solar Simulator. (b) Brick made in the setup from JSC-2A lunar simulant and (c) tomography cross-section of brick samples with large open and closed pores. Images reprinted with open access permission (CC-BY-NC-ND) from Meurisse et al. [186].

(Hawaii), LASSS could fuse the top layer of tephra (see Fig. 24) while encountering some efficiency losses due to environmental conditions (wind, increased thermal conduction from wet ground and uneven surface), making homogenous sintering difficult [119]. The field test included the firing of rocket thrusters, with much of the sintered area surviving the exhaust although with some damage (see Fig. 24c). Further studies of the optical absorption properties of different lunar simulants (FJS-1, JSC-1A, NU-LHT-2M, and OB1) and their sintering

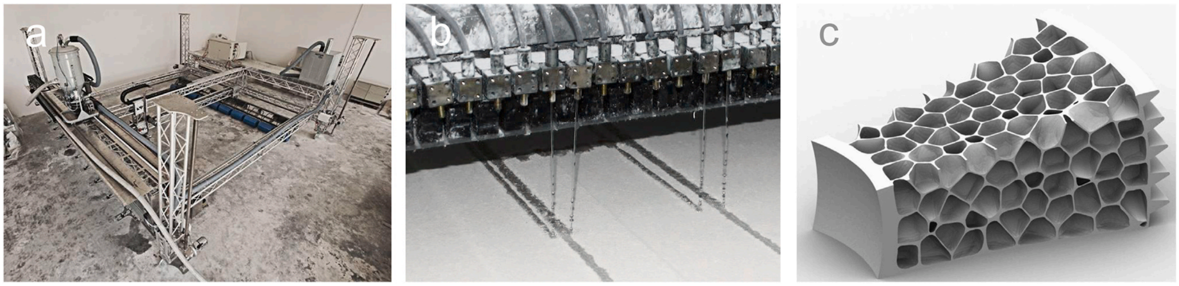

Fig. 26. (a) Complete D-shape binder jetting setup with (b) detail of the printing process with binder deposited on sand and (c) rendering of an exemplar structural element. Images reprinted from Acta Astronautica 93 (2014) 430–450, Cesaretti et al. [187], copyright 2014 with permission from Elsevier.

behavior revealed that regardless of composition, the glassy phases are the first to melt, making them an essential component in simulants used for sintering experiments [184]. Other experiments with solar concentrators and simulants were performed by Fischer, who used a Fresnel lens to pyrolyze lunar regolith simulant MLS-1. He found a vaporization temperature under slightly reduced pressure of 1800 K coupled with SiO, O, O_2 Fe and Mg gas release [185]. Zheng and Qiao used a solar concentrator to weld metal joints (Fe and Ti) with custom-made lunar and Mars simulants (HIT-L/M − 1) [78]. They produced brittle welding joints with an ultimate tensile strength for lunar/Mars regolith simulants of 2.94/1.66 MPa for Iron parts and 4.95/2.59 MPa for Titanium parts.

AM with solar concentrators was introduced by Meurisse et al., using solar 3D printing of JSC-1A and JSC-2A lunar regolith simulant (see Fig. 25) [186].

The group explored the use of concentrated sunlight and focused Xenon light as they fused simulant powders layer-by-layer. Processing was challenging due to inhomogeneously sintered sections in the powder bed and end parts had high porosity levels and weak layer-to-layer bonding. However, for compression tests, brick-shaped parts could be manufactured and the study was the first to report on mechanical strength for powder-bed sintered regolith, revealing a compressive strength of 2.31 MPa. The low strength is consistent with high porosity values of powder bed fused regolith in general and was later elaborated on by this group, giving a flexural strength of 0.23–0.55 MPa, dependent on build direction (perpendicularly or parallel to layers built) [19].

A key challenge for the ISRU use of dry powder bed technologies is not layer fusion (on which research has focused thus far) but layer deposition under extraterrestrial conditions. An extreme example would be lunar PBF: First, the direct use of regolith as feedstock is judged problematic, as lunar regolith grains have a non-round morphology (very sharp corners due to the specific space weathering phenomena), which drastically reduces powder flowability and powder-bed packing. A second challenge would be the lower gravity, as gravity is the critical force to facilitate powder flow, illustrated by the fact that lunar dust/slow-settling particles are a key challenge for Moon missions [40].

5.3. Binder jetting

Another powder bed process explored for ISRU is binder jetting. In this technique, a liquid bonding agent is selectively deposited to join powder materials. In cooperation with ESA, Cesaretti et al. put forward binder jetting with a magnesium salt binder to produce Sorel cement with lunar regolith simulant aggregates using the D-shape technology for large structures (see Fig. 26) [187].

On Earth, Sorel cement is often combined with different fillers (especially wood) and used in floor tiles, industrial floors and wall insulation panels. While being incompatible with steel reinforcement (low alkalinity and chloride ions facilitate steel corrosion) [188], the material's low alkalinity supports glass fiber reinforcement. For the much-cited study, Cesaretti et al. specifically developed a lunar regolith simulant DNA-1 (aiming to reproduce JSC-1A) of volcanic material collected close to Bolsena Lake in Italy that was milled and mixed with 5 wt% MgO to increase reactivity. These powders were spread layer by layer in a large bed and fused using an ink made of a saturated salt solution with 77 wt% water and 23 wt% of predominantly $MgCl_2$, as well as smaller amounts of $MgSO_4$, KCl, NaCl.

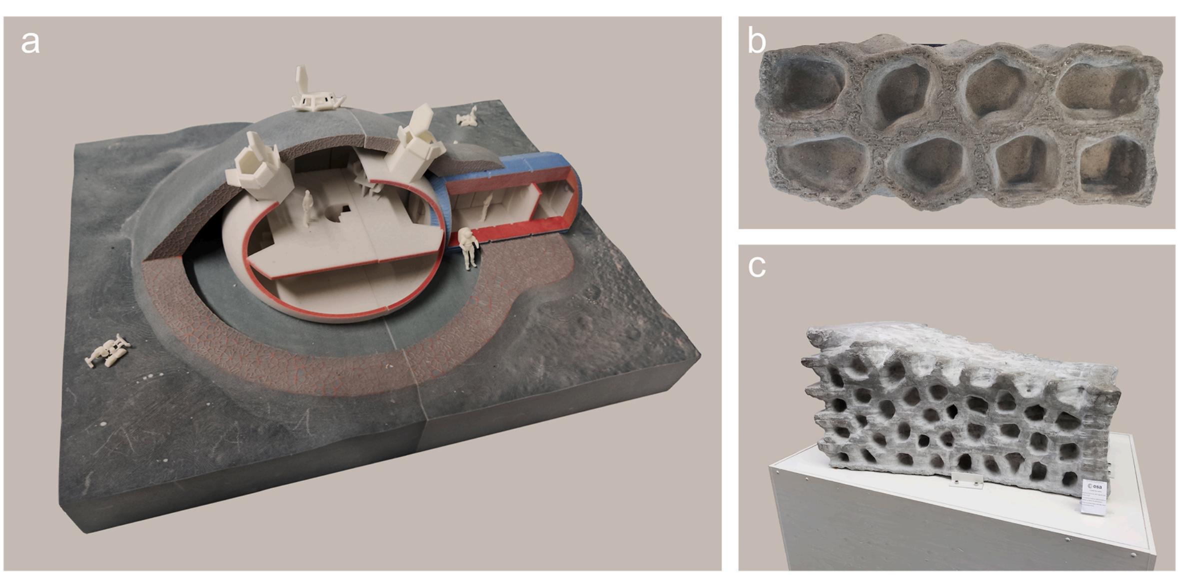

Fig. 27. (a) 3D printed scale model of ESA's lunar base concept. (b and c) Technological demonstrators of structural wall elements produced using D-shape binder jetting technology [187] at the ESTEC foyer in Noordwijk.

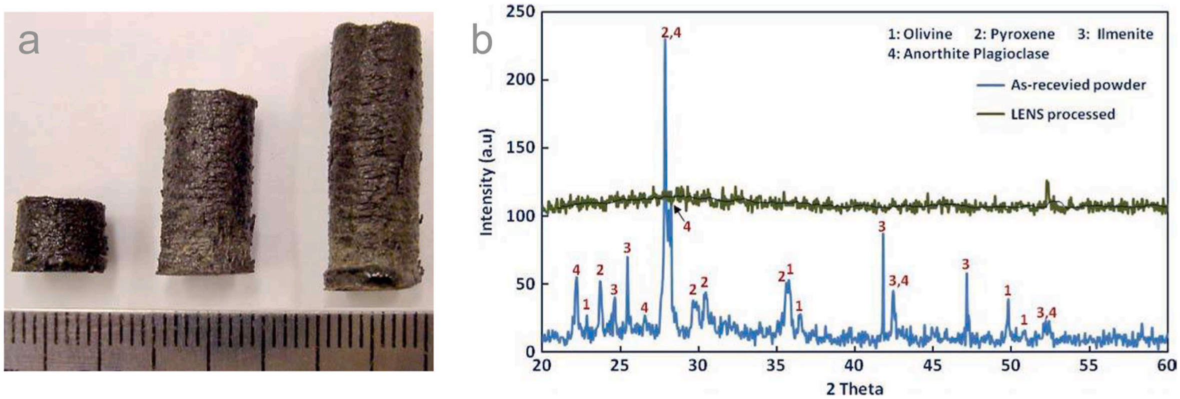

Fig. 28. (a) Samples from directed energy deposition (DED) of JSC-1AC by LENS and (b) XRD patterns of crystalline JSC-1AC feedstock and amorphous LENS processed samples. Images reprinted with permission from Chemical reviews 116 (2016) 4170–4204, Balla et al. [189], copyright Emerald Publishing Limited all rights reserved.

Parts of considerable size with geometries specially designed for a lunar architecture (see Fig. 27) were produced and these had a compressive strength of 20.35 MPa, which is comparable to general-purpose concrete that typically has >20 MPa after 28 days. Furthermore, jetting binder on regolith simulant in a vacuum chamber revealed that fusing of parts in a lunar atmosphere would be feasible. The group also gave a preliminary evaluation of transportation requirements to build a complete habitat on the Moon, estimating the need to ship 8 tonnes of dry salt as a binder, the printing equipment and an inflatable inner core at a price of 1600 M€.

As a powder bed process, binder jetting faces the same issues for powder deposition discussed earlier for PBF. One approach to overcoming such issues is to use layer-wise slurry deposition (LSD) for powder deposition, a wet-processing approach based on the deposition of colloids. Karl et al. (2020a) used LSD with binder jetting to deposit MGS-1C/8 slurries and generate complex parts (that had a ~5 wt% polymeric binder component) that showed compressive of 30.8 ± 2.47 MPa without further processing (see Fig. 11) [84]. While the LSD approach was developed to generate high-density sintered ceramics (and current setups are small in size), a similarly large area deposition of ISRU binder (which could be made from liquid Martian brines) using a deposition setup with large nozzles (comparable to the D-shape technology) could be a useful addition to the AM portfolio of early IRSU on Mars.

5.4. Directed energy deposition, selective separation sintering and vat photopolymerization

Several studies of other AM technologies have been performed that might have niche applications in ISRU AM. The use of focused thermal energy to fuse materials (powders and filaments) as they are deposited is called directed energy deposition. In 2012 Balla et al. demonstrated direct laser fabrication of JSC-1AC lunar simulant (see Fig. 28) using a process called Laser Engineering Net Shaping (LENS) [189].

Simulant powders were fed at ~12 g/min into a 50 W Nd-YAG laser beam moving at a scan speed of 20 mm/s. The group could manufacture dense vitrified parts without any macroscopic defects that had a hardness of ~500 Hv compared to soda-lime glass with 545 Hv (no other mechanical properties reported). In its use of laser energy, this AM approach is similar to PBF and faces similar issues with fast heating rates for oxidic regolith material. Furthermore, the low flowability of regolith can be expected to hinder the applicability of this technology for early ISRU.

Khoshnevis et al. put forward another AM technology for planetary construction called selective separation sintering (SSS) [190]. SSS combines the deposition of layers of a base powder with a special separator powder that is selectively dispersed in each layer using a needle with a piezo vibrator (see Fig. 29).

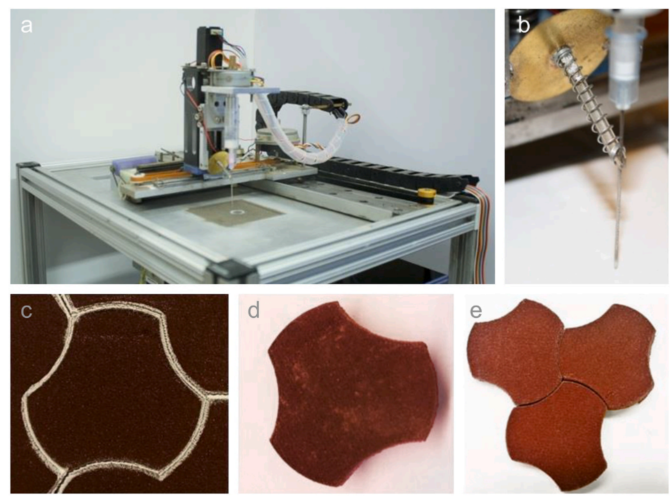

Fig. 29. (a) Powder bed selective separation sintering machine with (b) close-up of dry powder delivery system for inhibitor powder. (c–e) Sintered ceramics from JSC-1A lunar simulant with (c) directly after sintering, (d) after separation and (e) the interlocking brick pattern. Images from Khoshnevis et al. [190] with permission from AIAA.

After layer deposition is finished, the powder-bed as a whole is heated in a furnace with the base powder sintering while the separator powder does not sinter. The process can be used for ceramics and metals. In a preliminary study, JSC-1A was deposited as a base powder and alumina as separator powder. After sintering at 900–1130 °C for 30–60 min, the simple tile geometries with interlocking design could be separated promptly, as the alumina powder had not sintered (no mechanical properties reported). In a sense, the technology inverts the fusion principle of standard powder-bed AM technologies and could be well suited to produce simple flat geometries with good efficiency.

For vat photopolymerization, a liquid photopolymer in a vat is selectively cured by light-activated polymerization. In cooperation with ESA, the Austrian company Lithoz employed vat photopolymerization using EAC-1A lunar regolith simulant to produce small ceramic parts with print precision (see Fig. 30) [191].

Using Lithoz's LCM technology, Altun et al. dispersed low weight percentages of EAC-1A (ground and sieved) in photocurable resin and selectively cured via a projector from the bottom [192]. After debinding, the green parts had a relative density of 67.9%, which was reduced to 55.9% after sintering at 1000 °C resulting in an ultimate compressive strength of 5.4 ± 0.3 MPa. Further work on vat photopolymerization was

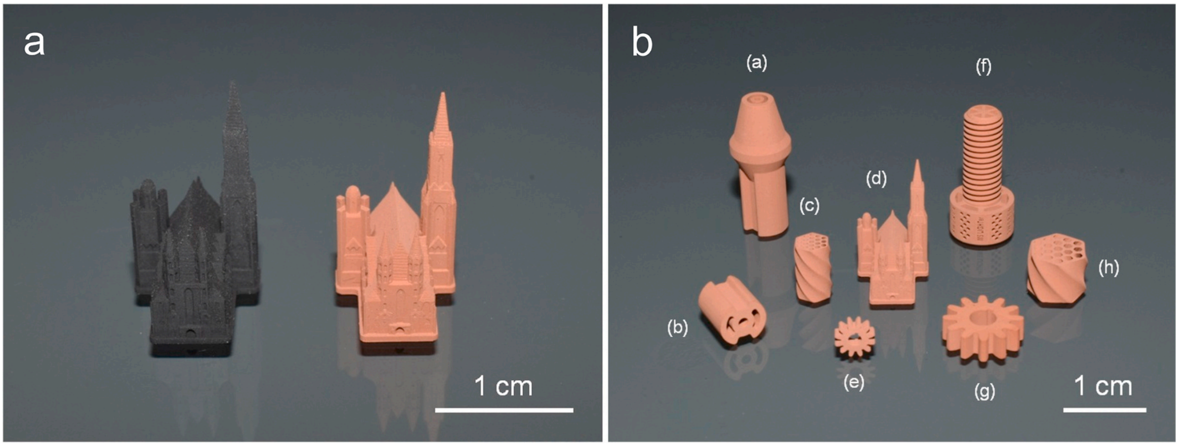

Fig. 30. Ceramic parts made from EAC-1A lunar regolith simulant by Lithoz (and ESA) using vat photopolymerization followed by debinding and sintering. (a) St. Stephen's Cathedral as-printed part (right) and part debinded and sintered at 1000 °C (left); (b) various demonstrator parts with high complexity from the same process. Images with open access permission (CC-BY) from Altun et al. [192].

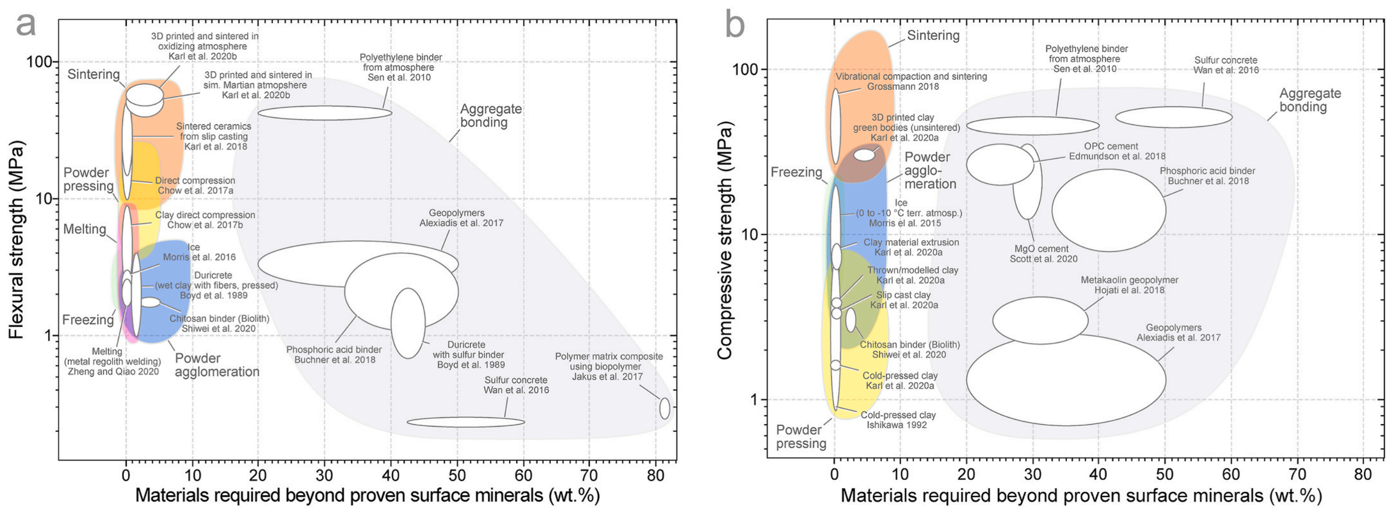

Fig. 31. (a) Flexural strength and (b) compressive strength over additional materials required (besides directly accessible proven surface minerals on Mars) for all ISRU studies using Martian simulants found in the literature (studies employing lunar simulants not included). All studies have been grouped using color-marked fields according to the different bonding concepts introduced in this work; each study mentioned is referenced in the preceding sections. (For interpretation of the references to color in this figure legend, the reader is referred to the Web version of this article.)

done by Liu et al. using a Chinese simulant [193]. They dispersed wet-ground CLRS-2 lunar simulant (45 vol% solid loading) in photocurable resin and DLP printed with layer thicknesses from 25 μm to 100 μm. Subsequently, samples were pyrolyzed at 450 °C for 2 h to remove the polymer binder and sintered at 1150 °C for 4 h (all with the slow heating rate of 2 °C/min typical for parts with high polymer content). Liu et al. reported remarkably high strength values with average compressive strength and flex strength of the sintered samples at 285–428 MPa and 60–129 MPa, respectively. Even assuming the strength values to be correct, the use of sacrificial polymer in excess of 55 vol% makes vat photopolymerization technology in general largely unfeasible for regolith ISRU, except for small demanding components.

6. Feasibility evaluation of bonding concept and AM for early ISRU on Mars

6.1. Comprehensive comparison of material and bonding concepts in ISRU research for Mars

Due to the harsh climate, atmosphere and radiation conditions, construction materials for habitats, greenhouses, landing pads and equipment building would be among the earliest ISRU concerns. The most relevant property for such structural materials is their mechanical strength. Fig. 31 gives an overview of the mechanical property values (flexural and compression strength) reported in ISRU studies for different material and bonding concepts coupled with the feedstock availability on the surface of Mars.

For industrialized societies on Earth, the building material of choice is concrete, and many attempts have been made to develop concrete-like materials for ISRU, as evidenced by the high number of aggregate bonding studies in Fig. 31. However, early Mars missions are not industrialized undertakings as such, and all aggregate bonding concepts currently discussed in the literature would require 20–50 wt% (or more) of raw materials that are not directly available on Mars. It could be argued that by using large amounts of energy, all basic building blocks could be ISRU produced. However, making such raw materials as Sulfur, Magnesium, or Kaolin available on a larger scale would require massive amounts of energy. In general, homogenization or transformation steps might be unnecessary as excellent alternative bonding concepts are available. This is illustrated by the fact that all non-aggregate bonding concepts use 90–100 wt% materials that have been proven to exist on the Martian surface.

Table 12
Overview of bonding concepts applicability in the Martian environment. The table is typographically coded as follows: **positive characteristics in bold**, *negative characteristics cursive* and remarks in the standard format.

Regolith bonding concept	Vacuum/low pressure	Gravity	Temperature	Remarks (Energy, feedstock)
Sintering	**Sintering might lead to higher densities;** *dense-sintering could be challenging due to sudden volatiles release.*	**Diffusion processes might be influenced.**	**Higher temperatures support the sintering process**; *low temperatures need to be overcome.*	*High amounts of energy are required* - a widely used approach for durable and resistant building materials (and tools) on Earth. Gas-tight materials are possible at higher sintering temperatures.
Melting	*Extreme volatile release is more likely;* **slow cooling might be favorable due to the release of processing tensions (annealing).**	*During cooling, the liquid-solid transformation might be different from on Earth.*	**Higher temperatures support the process**; *low temperatures need to be overcome.*	*Very high amounts of energy are required.* **Durable and gas-tight end products are possible.**
Powder pressing	*Low humidity conditions could be an issue for pressed body stability*	*Powder movement harder, gravity is missing*	No immediate impact on dry-pressing; **higher temperatures are favorable for hot-pressing or cold sintering.**	**Relatively low energy is required for dry-pressing, but yield in compressive strength is low.** *Cold sintering-like approaches require very high pressures.*
Powder agglomeration	*Low relative humidity could reduce agglomeration behavior; wet-processing only under liquid-phase conditions for specific colloid*	**Less sedimentation for wet-processing, colloids would require less natural or synthetic stabilizers.**	*Wet-processing requires liquid-phase conditions; stable temperature conditions are important.*	**Little energy is required; the process could be coupled with freezing bonding and or sintering.**
Aggregate bonding	*Atmosphere needed for many liquid systems; liquid-phase conditions especially for concrete approaches needed (also continued wetting needed).*	*Casting might be influenced.* **Less segregation during casting.** *Entrapped gas from mixing might be hard to get rid of.*	*Liquid-phase conditions are necessary for many material systems. Stabil temperature conditions are important.*	*Bonding material (sulfur, concrete, polymers) is not directly available; high effort is required to produce them.*
Chemical fusion	*Reduced pressure could have an impact on chemical reactions*	*Reactions might behave differently than in Earth's gravity.*	**High temperatures would support the processes.**	*Either reactant grade feedstocks are required, or very high energies are required.* **The process could yield cleaned feedstocks for secondary processes.**
Freezing	*The processing system needs to be able to cross phase boundaries (liquid to solid)*	The freezing direction might be influenced.	**For low temperatures, there is no energy needed to keep materials frozen.** *High temperatures might make the approach unfeasible.*	**A good system for early ISRU if water is available. When temperature conditions are ideal, very low energy is required.**

In detail, sintering studies produced the highest strength values for flex and compression and can be considered the gold standard if larger amounts of energy are available. For flexural strength, this is followed by powder pressing, melting, powder agglomeration and freezing. For compressive strength, which is essential for building materials, powder agglomeration is followed by freezing and powder pressing. Fig. 31 makes it clear that clay minerals are an excellent primary feedstock for many of the fusion concepts, not exclusively but also for approaches that require minimal energy and processing effort. A similar observation can be made for Earth, where the ubiquitous building material for 'pre-concrete' societies is clay earth [84].

6.2. *Assessment of bonding concepts applicability to the space environment*

Table 12 gives an overview of the effects that can be expected when the different bonding concepts are used in a general space environment.

While mechanical properties of the different bonding concepts are somewhat available in the current ISRU literature (or can be implied from similar materials concepts on Earth), one of the biggest challenges for the future is the transfer of processing from terrestrial environment conditions to simulated Martian conditions. The specific energies requirements for each bonding concept are sketched in Table 12; however, for an overall evaluation of their ISRU suitability, a comprehensive comparison for each approach is missing that should start with excavation and take into account the whole process chain until the parts are finished.

6.3. *Assessment of AM technologies in the space environment*

An assessment of AM technologies in space ISRU is provided in Table 13, outlining positive and negative aspects of the different space AM technologies.

Material extrusion can be well suited for low-pressure and low gravity environments and has excellent scalability, making it the most suited AM technology for direct regolith ISRU, as discussed by Mueller et al. [166]. This is followed by powder bed fusion, directed energy deposition and possibly binder jetting, which all have the potential to be adapted to the Martian environment, while vat photopolymerization, binder jetting, and sheet lamination can be considered non-suitable for the production of large structures from unrefined Martian regolith.

Much work is needed to verify the specific AM approaches in the space environment, with some early work on gravity already underway. For the International Space Station (ISS), the use of a material extrusion 3D printer in zero gravity has been widely reported [195]. Other AM approaches have been used or planned on the ISS, such as a Bio-Fabrication Facility from Techshot or the Vulcan unit (derived from the wire-feed welding process) and vat photopolymerization setup both from Made in Space [196,197]. Other efforts have been undertaken in microgravity on Zero-G flights for powder bed fusion either in the concept stage [198] or the production of high-quality parts [199] or liquid droplet systems towards materials extrusion [200].

7. Evaluation, summary, and outstanding research questions

7.1. *Summary evaluation of martian regolith simulant development*

Major achievements regarding Martian regolith simulant development and availability are the continuing improvement of quality and complexity of simulants thanks to the evolving scientific knowledge of our neighbor planet, which is mirrored in the generational concept introduced in this work. Secondly, efforts to specific best-practice workflows for the development of simulants and efforts to indicate applicability to different ISRU study types such as the regolith simulant report cards [37]. Thirdly, Space agencies and others have started controlled efforts on curation (such as simulant libraries), broad

Table 13
Assessment of additive manufacturing technologies in a space environment. Expanded from Sgambatia et al. [194]. The table is typographically coded as follows: **positive characteristics in bold**, *negative characteristics cursive* and remarks in the standard format.

Technology	Vacuum/low pressure	Gravity	Temperature	Remarks
Material extrusion	**Lower porosity and better interlayer adhesion***Nozzle clogging*	**Microgravity effect on sedimentation and crystallization might strengthen prints**	*Materials tend to be temperature sensitive*	Judged as the most suited AM technology for direct regolith ISRU
Vatphotopolymerization	No effect, process uses enclosed volume	*Requires additional control tech. to maintain a flat liquid interface*	*Process is temperature sensitive*	Requires large amounts of sensitive polymers. Not feasible for direct regolith ISRU
Powder bed fusion	**Dry environment can increase powder flowability and powder oxidation is hindered**	*Powder deposition on Earth is facilitated by gravity; additional tech. needed for powder deposition*	Pre-heating and temperature control required	PBF produces unfavorable microstructure for direct regolith ISRU
Material jetting	*Liquid droplet ejection might be problematic*	*Precise droplet deposition in low gravity questionable; would need add. controls*	*Materials are temp. sensitive* Temperature control for process required	Not ideally suited for the space environment
Binder jetting	**Dry environment can increase powder flowability** *Liquid droplet ejection might be problematic*	*Powder deposition on Earth is facilitated by gravity; additional tech. needed for powder deposition*	*Binder materials and deposition process can be temperature sensitive*	Even though challenging on Moon and Mars, some aspects of the technology could be feasible for building large structures
Sheet lamination	**No oxidation between sheets**	**Not affected**	Temperature control can be useful	Large amount of garbage/unused feedstock; older technology from prototyping age of AM
Directed energydeposition	**Electron beam fusion and laser energy requires/is preferred (in) vacuum**	**Microgravity effect on sedimentation and crystallization can have positive effects on prints**	Cooling system required to regulate excessive heating	Feasible technology for ISRU once refined materials/metals are available

availably and finally databases for simulants such as the simulant database [31]. In the future, site-specific simulants (instead of global simulants) can be expected, facilitating the preparation and training of individual missions going to specific landing sites.

7.2. Summary evaluation of the state of the art regolith particle bonding concepts

Major achievements in particle bonding concepts are first that all major bonding approaches used on Earth have been tried with regolith simulants. Secondly, these studies could generally produce similar mechanical properties to the typical terrestrial processes using such simulants. However, thirdly the authors feel there is a tendency in ISRU research, where bonding approaches that are unique or different (but have a very low TRL on Earth) are chosen to conduct studies or even financed. The ISRU community should try to develop a best practice approach to develop standardized criteria to assess the feasibility of different material bonding concepts. Such criteria depend to a large degree on the largely unresearched field of processing in simulated Martian conditions. From the collection, storage, handling and preparation of feedstock materials to the processing via the different proposed bonding concepts, the whole process chains need to be examined in Martian conditions regarding ISRU feasibility. One of the major challenges of early ISRU is that feedstocks ideally should require minimal preprocessing effort and would best be used directly without energy-intensive homogenization or transformation steps.

What is more, one of the major focus areas of structural ISRU materials research is mechanical properties. Properties such as radiation protection, thermal conductivity, (light) energy absorption and thermal shock have seldomly been examined. Similarly, almost no research exists on simulated Martian material structures' long-term behavior and stability in the appropriate environment.

7.3. Summary evaluation of additive manufacturing for ISRU state of the art

Major achievements in additive manufacturing for ISRU are first that for all major AM categories, proof of concept studies with (often lunar) simulants have been reported. Secondly, the NASA habitat print challenge (between other things) generated significant interest in the topic, and a larger number of researchers joined the field (however, often for one-off studies along the lines of proof of concept). Thirdly, some large-scale building efforts have been started to determine the feasibility of habitat printing (currently in a terrestrial environment), such as using concrete materials systems in material extrusion AM (mostly by NASA). For the future, major outstanding research questions are to move the processing from terrestrial environment conditions to simulated Martian conditions and generally along the lines of open questions discussed for bonding concepts in the previous section.

Data availability

The raw data required to reproduce these findings will be made available on request.

Author statement

David Karl: Conceptualization, Methodology, Writing - Original Draft, Writing - Review & Editing, Visualization.

Kevin M. Cannon: Writing - Review & Editing.

Aleksander Gurlo: Conceptualization, Writing - Review & Editing, Supervision.

Acknowledgments

We thank Advenit Makaya (ESA-ESTEC) for his feedback on an earlier version of this manuscript. We acknowledge support by the German Research Foundation and the Open Access Publication Fund of TU Berlin.

References

[1] E. Howell, N. Booth, The Search for Life on Mars: the Greatest Scientific Detective Story of All Time, Arcade Publishing, New York, 2020, ISBN 9781950691395.

[2] D. Rapp, Human Missions to Mars: Enabling Technologies for Exploring the Red Planet, Springer, Berlin, Chichester, UK, 2008, ISBN 9781281117847. Published in association with Praxis.

[3] M.S. Dodd, D. Papineau, T. Grenne, J.F. Slack, M. Rittner, F. Pirajno, J. O'Neil, C. T.S. Little, Evidence for early life in Earth's oldest hydrothermal vent precipitates, Nature 543 (2017) 60–64, https://doi.org/10.1038/nature21377.

[4] D.D. Sasselov, J.P. Grotzinger, J.D. Sutherland, The origin of life as a planetary phenomenon, Sci. Adv. 6 (2020), https://doi.org/10.1126/sciadv.aax3419 eaax3419.
[5] D. Banfield (Ed.), Mars Science Goals, Objectives, Investigations, and Priorities: 2020 Version: 89 P. White Paper Posted by the Mars Exploration Program Analysis Group (MEPAG), 2020. https://mepag.jpl.nasa.gov/reports.cfm. (Accessed 12 August 2021).
[6] R. Zubrin, R. Wagner, The Case for Mars: the Plan to Settle the Red Planet and Why We Must, Free Press, New York, 1996, ISBN 9780684835501.
[7] M. Roach, Packing for Mars: the Curious Science of Life in the Void, W.W. Norton & Company, New York, 2011, 1611293758.
[8] S.L. Petranek, How We'll Live on Mars, First TED Books hardcover edition, TED Books, Simon & Schuster, New York, NY, 2015, 1476784760.
[9] C. Impey, Beyond: Our Future in Space, first ed., W.W. Norton & Company, New York, 2015, 0393239306.
[10] A.A. Menezes, J. Cumbers, J.A. Hogan, A.P. Arkin, Towards synthetic biological approaches to resource utilization on space missions, J. R. Soc. Interface 12 (2015), 20140715, https://doi.org/10.1098/rsif.2014.0715.
[11] K. Sacksteder, G. Sanders, In-situ resource utilization for lunar and Mars exploration, in: 45th AIAA Aerospace Sciences Meeting and Exhibit, 2007, ISBN 978-1-62410-012-3, https://doi.org/10.2514/6.2007-345. Reno, Nevada.
[12] D. Rapp, Use of Extraterrestrial Resources for Human Space Missions to Moon or Mars: Mars ISRU, second ed., Springer, Cham, Switzerland, 2018, 9783319726939.
[13] NASA Mars architecture steering group, in: Bret G. Drake (Ed.), Human Exploration of Mars Design Reference Architecture 5.0, 2009. http://www.nasa.gov/pdf/373665main_NASA-SP-2009-566.pdf. (Accessed 20 July 2021).
[14] G.B. Sanders, M. Duke, et al., Capability road map (CRM) 13: in-situ resource utilization (ISRU), in: R. Willcoxon, H. Thronson, G. Varsi, R. Mueller, V. Regenie, T. Inman, et al. (Eds.), NASA Capability Roadmaps Executive Summary, 2005, pp. 264–291. https://ntrs.nasa.gov/citations/20050204002. (Accessed 12 August 2021).
[15] L.J. Wittenberg, In-situ extraction of lunar soil volatiles, in: R.G. Galloway, S. Lokaj (Eds.), Engineering, Construction, and Operations in Space IV: Proceedings of Space 94, American Society of Civil Engineers, New York, N.Y., 1994, pp. 687–696, 9780872629370.
[16] Design of a lunar colony, in: C. Dalton, E. Hohmann (Eds.), Houston Univ., Rice Univ., and NASA, 1972. Manned Spacecraft Center, Report Nr. CR-129164, https://ntrs.nasa.gov/search.jsp?R=19730002509. (Accessed 12 August 2021).
[17] C.C. Allen, K.M. Jager, R.V. Morris, D.J. Lindstrom, M.M. Lindstrom, J. P. Lockwood, Martian soil simulant available for scientific, educational study, Eos Trans. AGU 79 (1998) 405, https://doi.org/10.1029/98EO00309.
[18] A. Meurisse, J.C. Beltzung, M. Kolbe, A. Cowley, M. Sperl, Influence of mineral composition on sintering lunar regolith, J. Aero. Eng. 30 (2017), 4017014, https://doi.org/10.1061/(ASCE)AS.1943-5525.0000721.
[19] M. Fateri, A. Meurisse, M. Sperl, D. Urbina, H.K. Madakashira, S. Govindaraj, J. Gancet, B. Imhof, W. Hoheneder, et al., Solar sintering for lunar additive manufacturing, J. Aero. Eng. 32 (2019), 4019101, https://doi.org/10.1061/(ASCE)AS.1943-5525.0001093.
[20] S.L. Taylor, A.E. Jakus, K.D. Koube, A.J. Ibeh, N.R. Geisendorfer, R.N. Shah, D. C. Dunand, Sintering of micro-trusses created by extrusion-3D-printing of lunar regolith inks, Acta Astronaut. 143 (2018) 1–8, https://doi.org/10.1016/j.actaastro.2017.11.005.
[21] R. Dou, W.Z. Tang, L. Wang, S. Li, W.Y. Duan, M. Liu, Y.B. Zhang, G. Wang, Sintering of lunar regolith structures fabricated via digital light processing, Ceram. Int. 45 (2019) 17210–17215, https://doi.org/10.1016/j.ceramint.2019.05.276.
[22] D. Karl, F. Kamutzki, P. Lima, A. Gili, T. Duminy, A. Zocca, J. Günster, A. Gurlo, Sintering of ceramics for clay in situ resource utilization on Mars, Open Ceramics 2 (2020), 100008, https://doi.org/10.1016/j.oceram.2020.100008.
[23] N.A. Cabrol, G. Chong-Diaz, C.R. Stoker, V.C. Gulick, R. Landheim, P. Lee, T. L. Roush, A.P. Zent, C.H. Lameli, et al., Nomad rover field experiment, Atacama desert, Chile: 1. Science results overview, J. Geophys. Res. 106 (2001) 7785–7806, https://doi.org/10.1029/1999JE001166.
[24] T.P. Gouache, N. Patel, C. Brunskill, G.P. Scott, C.M. Saaj, M. Matthews, L. Cui, Soil simulant sourcing for the ExoMars rover testbed, Planet. Space Sci. 59 (2011) 779–787, https://doi.org/10.1016/j.pss.2011.03.006.
[25] J.J. Marlow, Z. Martins, M.A. Sephton, Mars on earth: soil analogues for future Mars missions, Astron. Geophys. 49 (2008) 2.20–2.23, https://doi.org/10.1111/j.1468-4004.2008.49220.x.
[26] K.M. Cannon, D.T. Britt, T.M. Smith, R.F. Fritsche, D. Batcheldor, Mars global simulant MGS-1: a Rocknest-based open standard for basaltic martian regolith simulants, Icarus 317 (2019) 470–478, https://doi.org/10.1016/j.icarus.2018.08.019.
[27] J.J. Wray, Diverse surface mineralogy of Mars from hyperspectral sensing, in: IGARSS 2019 - 2019 IEEE International Geoscience and Remote Sensing Symposium, 28.07-02.08.2019 Yokohama, Japan, 2019, pp. 4908–4910, https://doi.org/10.1109/IGARSS.2019.8900545, 978-1-5386-9154-0.
[28] U. Böttger, J.-P. de Vera, J. Fritz, I. Weber, H.-W. Hübers, D. Schulze-Makuch, Optimizing the detection of carotene in cyanobacteria in a martian regolith analogue with a Raman spectrometer for the ExoMars mission, Planet. Space Sci. 60 (2012) 356–362, https://doi.org/10.1016/j.pss.2011.10.017.
[29] D.T. Britt, K.M. Cannon, K. Donaldson Hanna, J. Hogancamp, O. Poch, P. Beck, D. Martin, J. Escrig, L. Bonal, et al., Simulated asteroid materials based on carbonaceous chondrite mineralogies, Meteoritics Planet Sci. 89 (2019) 4059, https://doi.org/10.1111/maps.13345.
[30] N.K. Ramkissoon, V.K. Pearson, S.P. Schwenzer, C. Schröder, T. Kirnbauer, D. Wood, R.G. Seidel, M.A. Miller, K. Olsson-Francis, New simulants for martian regolith: controlling iron variability, Planet. Space Sci. (2019), 104722, https://doi.org/10.1016/j.pss.2019.104722.
[31] K.M. Cannon, Planetary simulant database: free resource for regolith simulant information. https://simulantdb.com/, 2020. (Accessed 12 August 2021).
[32] Z. Martins, H. Cottin, J.M. Kotler, N. Carrasco, C.S. Cockell, R. de la Torre Noetzel, R. Demets, J.-P. de Vera, L. d'Hendecourt, et al., Earth as a tool for astrobiology—a European perspective, Space Sci. Rev. 209 (2017) 43–81, https://doi.org/10.1007/s11214-017-0369-1.
[33] A. Witze, Why planetary scientists want better fake space dirt: (Published in print with the title: NASA seeks better fake space dirt), Nature 547 (2017) 146–147, https://doi.org/10.1038/nature.2017.22228.
[34] L. Taylor (Ed.), For the Simulant Working Group, Status of Lunar Regolith Simulants and Demand for Apollo Lunar Samples, 2010. https://www.lpi.usra.edu/lunar/samples/LEAG-SIM-SAT2010_LunarRegolithSimulants.pdf. (Accessed 12 August 2021).
[35] C.M. Schrader, D.L. Rickman, C.A. McLemore, J.C. Fikes, Lunar Regolith Simulant User's Guide: NASA/TM-2010-216446, NASA, marshall space flight center, Alabama. https://www.nasa.gov/sites/default/files/atoms/files/nasa_tm_2010_216446_simuserg.pdf, 2010. (Accessed 27 August 2021).
[36] P.T. Metzger, D.T. Britt, S. Covey, C. Schultz, K.M. Cannon, K.D. Grossman, J. G. Mantovani, R.P. Mueller, Measuring the fidelity of asteroid regolith and cobble simulants, Icarus 321 (2019) 632–646, https://doi.org/10.1016/j.icarus.2018.12.019.
[37] S. Deitrick, K.M. Cannon, Regolith simulant report cards: a user friendly simulant certification system, in: Proceedings of the 11th Joint Planetary and Terrestrial Mining Sciences Symposium and Space Resources Roundtable (PTMSS/SRR), June 8-11, 2021 (Virtual), 2021. https://www.ptmss.ca/archive. (Accessed 27 August 2021).
[38] L.A. Taylor, Y. Liu, Important considerations for lunar soil simulants, in: Earth and Space 2010: Engineering, Science, Construction, and Operations in Challenging Environments, 2010, pp. 106–118, https://doi.org/10.1061/41096(366)14.
[39] L.A. Taylor, C.M. Pieters, D. Britt, Evaluations of lunar regolith simulants, Planet. Space Sci. 126 (2016) 1–7, https://doi.org/10.1016/j.pss.2016.04.005.
[40] L. Taylor, H. Schmitt, W. Carrier, M. Nakagawa, in: Lunar Dust Problem: from Liability to Asset, 1st Space Exploration Conference: Continuing the Voyage of Discovery, Held 30 January 2005 - 01, February 2005, https://doi.org/10.2514/6.2005-2510. Orlando, Florida.
[41] J.J. Marlow, Z. Martins, M.A. Sephton, Organic host analogues and the search for life on Mars, Int.Jnl Astrobiol. 10 (2011) 31–44, https://doi.org/10.1017/S1473550410000303.
[42] CLASS Exolith Lab, in: Kevin M. Cannon, Mike Conroy, Daniel T. Britt (Eds.), Datasheet for MGS-1 Mars global simulant, University of Central Florida, USA, March 2019. https://sciences.ucf.edu/class/simulant_marsglobal. (Accessed 12 August 2021).
[43] R. Navarro-González, F.A. Rainey, P. Molina, D.R. Bagaley, B.J. Hollen, J. de La Rosa, A.M. Small, R.C. Quinn, F.J. Grunthaner, et al., Mars-like soils in the Atacama Desert, Chile, and the dry limit of microbial life, Science (New York, N.Y.) 302 (2003) 1018–1021, https://doi.org/10.1126/science.1089143.
[44] L.L. Baker, D.J. Agenbroad, S.A. Wood, Experimental hydrothermal alteration of a martian analog basalt: implications for martian meteorites, Meteoritics Planet Sci. 35 (2000) 31–38, https://doi.org/10.1111/j.1945-5100.2000.tb01971.x.
[45] CLASS Exolith Lab, in: Kevin M. Cannon, Mike Conroy, Daniel T. Britt (Eds.), Datsheet for MGS-1C clay ISRU, University of Central Florida, USA, November 2018. https://sciences.ucf.edu/class/simulant_mgs1c. (Accessed 12 August 2021).
[46] D. Fernández-Remolar, J. Gómez-Elvira, F. Gómez, E. Sebastian, J. Martıin, J. A. Manfredi, J. Torres, C. González Kesler, R. Amils, The Tinto River, an extreme acidic environment under control of iron, as an analog of the Terra Meridiani hematite site of Mars, Planet. Space Sci. 52 (2004) 239–248, https://doi.org/10.1016/j.pss.2003.08.027.
[47] Orbitec, JSC Mars-1A Martian regolith simulant material safety datasheet. www.orbitec.com, 2008. (Accessed 12 August 2021). https://web.archive.org/web/20160331191710/http://orbitec.com/store/JSC_Mars-1A_Material_Safety_Datasheet.pdf.
[48] A.C. Schuerger, D.C. Golden, D.W. Ming, Biotoxicity of Mars soils: 1. Dry deposition of analog soils on microbial colonies and survival under Martian conditions, Planet. Space Sci. 72 (2012) 91–101, https://doi.org/10.1016/j.pss.2012.07.026.
[49] CLASS Exolith Lab, in: Kevin M. Cannon, Mike Conroy, Daniel T. Britt (Eds.), Datsheet for MGS-1S sulfate ISRU, University of Central Florida, USA, January 2021. https://sciences.ucf.edu/class/simulant_mgs1s/. (Accessed 12 August 2021).
[50] M.A. Chan, B. Beitler, W.T. Parry, J. Ormö, G. Komatsu, A possible terrestrial analogue for haematite concretions on Mars, Nature 429 (2004) 731–734, https://doi.org/10.1038/nature02600.
[51] G.H. Peters, W. Abbey, G.H. Bearman, G.S. Mungas, J.A. Smith, R.C. Anderson, S. Douglas, L.W. Beegle, Mojave Mars simulant - characterization of a new geologic Mars analog, Icarus 197 (2008) 470–479, https://doi.org/10.1016/j.icarus.2008.05.004.
[52] X. Zeng, X. Li, S. Wang, S. Li, N. Spring, H. Tang, Y. Li, J. Feng, JMSS-1: a new Martian soil simulant, Earth Planets Space 67 (2015), https://doi.org/10.1186/s40623-015-0248-5.

[53] CLASS Exolith Lab, in: Kevin M. Cannon, Mike Conroy, Daniel T. Britt (Eds.), Datasheet for JEZ-1 Mars global simulant, University of Central Florida, USA, February 2019. https://sciences.ucf.edu/class/simulant_jez1/. (Accessed 12 August 2021).
[54] K. Benison, B. Bowen, Acid saline lake systems give clues about past environments and the search for life on Mars, Icarus 183 (2006) 225–229, https://doi.org/10.1016/j.icarus.2006.02.018.
[55] The Martian Garden, Safety data sheet: MMS-1, revised, https://www.themartiangarden.com/s/SDS-MMS-1-Mars-Regolith-Simulant.pdf, April 2019. (Accessed 12 August 2021).
[56] A.N. Scott, C. Oze, Y. Tang, A. O'Loughlin, Development of a Martian regolith simulant for in-situ resource utilization testing, Acta Astronaut. 131 (2017) 45–49, https://doi.org/10.1016/j.actaastro.2016.11.024.
[57] J. Clarke, D. Willson, D. Cooper, In-situ resource utilisation through water extraction from hydrated minerals–relevance to Mars missions and an Australian analogue, in: 2006, Proceedings of the 6th Australian Mars Exploration Conference, Mars Society Australia, Victorian Space Science Education Centre, Melbourne, July. 2006. http://cmapspublic3.ihmc.us/rid=1P89G8N0M-8ZRB03-17QJ/Water%20Requirements.pdf. (Accessed 12 August 2021).
[58] P. Nørnberg, H.P. Gunnlaugsson, J.P. Merrison, A.L. Vendelboe, Salten Skov I: a Martian magnetic dust analogue, Planet. Space Sci. 57 (2009) 628–631, https://doi.org/10.1016/j.pss.2008.08.017.
[59] A.H. Stevens, E. Steer, A. McDonald, E.S. Amador, C.S. Cockell, Y-Mars: An Astrobiological analogue of martian mudstone, Earth Space Sci. 5 (2018) 163–174, https://doi.org/10.1002/2017EA000318.
[60] Z. Peeters, R. Quinn, Z. Martins, M.A. Sephton, L. Becker, M. van Loosdrecht, J. Brucato, F. Grunthaner, P. Ehrenfreund, Habitability on planetary surfaces: interdisciplinary preparation phase for future Mars missions, Int.Jnl Astrobiol. 8 (2009) 301–315, https://doi.org/10.1017/S1473550409990140.
[61] J.E. Valdivia-Silva, R. Navarro-González, F. Ortega-Gutierrez, L.E. Fletcher, S. Perez-Montaño, R. Condori-Apaza, C.P. McKay, Multidisciplinary approach of the hyperarid desert of Pampas de La Joya in southern Peru as a new Mars-like soil analog, Geochem. Cosmochim. Acta 75 (2011) 1975–1991, https://doi.org/10.1016/j.gca.2011.01.017.
[62] G. Scott, C. Saaj, Measuring and simulating the effect of variations in soil properties on microrover trafficability, in: SPACE Conferences and Exposition: AIAA SPACE 2009 Conference & Exposition, Pasadena, California, 2009, https://doi.org/10.2514/6.2009-6468, 978-1-60086-980-8.
[63] G.P. Scott, C.M. Saaj, The development of a soil trafficability model for legged vehicles on granular soils, J. Terramechanics 49 (2012) 133–146, https://doi.org/10.1016/j.jterra.2011.12.002.
[64] S.J. Kang, Development and Characterization of Korean Mars Simulant for in Situ Resource Utilization: Master Thesis, Hanyang University, 2018. http://repository.hanyang.ac.kr/handle/20.500.11754/69046. (Accessed 12 August 2021).
[65] L.K. Tamppari, R.M. Anderson, P.D. Archer, S. Douglas, S.P. Kounaves, C. P. McKay, D.W. Ming, Q. Moore, J.E. Quinn, et al., Effects of extreme cold and aridity on soils and habitability: McMurdo Dry Valleys as an analogue for the Mars Phoenix landing site, Antarct. Sci. 24 (2012) 211–228, https://doi.org/10.1017/S0954102011000800.
[66] J. Gaier, P. de Leon, P. Lee, T. McCue, E. Hodgson, J. Thrasher, Preliminary testing of a pressurized space suit and candidate fabrics under simulated Mars dust storm and dust devil conditions, in: International Conference on Environmental Systems (ICES): 40th International Conference on Environmental Systems, Barcelona, Spain, 2010, https://doi.org/10.2514/6.2010-6247, 978-1-60086-957-0.
[67] J. Guan, A. Liu, K. Xie, Z. Shi, B. Kubikova, Preparation and characterization of Martian soil simulant NEU Mars-1, Trans. Nonferrous Metals Soc. China 30 (2020) 212–222, https://doi.org/10.1016/S1003-6326(19)65193-9.
[68] S.M. Perl, B.K. Baxter, Great salt lake as an astrobiology analogue for ancient martian hypersaline aqueous systems, in: B.K. Baxter, J.K. Butler (Eds.), Great Salt Lake Biology, Springer International Publishing, Cham, 2020, pp. 487–514, https://doi.org/10.1007/978-3-030-40352-2_16, 978-3-030-40351-5.
[69] C. Brunskill, N. Patel, T.P. Gouache, G.P. Scott, C.M. Saaj, M. Matthews, L. Cui, Characterisation of martian soil simulants for the ExoMars rover testbed, J. Terramechanics 48 (2011) 419–438, https://doi.org/10.1016/j.jterra.2011.10.001.
[70] H.A. Oravec, V.M. Asnani, C.M. Creage, S.J. Moreland, Geotechnical review of existing Mars soil simulants for surface mobility, in: Earth and Space, vol. 2021, 2021, pp. 157–170, https://doi.org/10.1061/9780784483374.016.
[71] H.A. Perko, J.D. Nelson, J.R. Green, Mars soil mechanical properties and suitability of Mars soil simulants, J. Aero. Eng. 19 (2006) 169–176, https://doi.org/10.1061/(ASCE)0893-1321(2006)19:3(169).
[72] D. Vaniman, M.D. Dyar, R. Wiens, A. Ollila, N. Lanza, J. Lasue, J.M. Rhodes, S. Clegg, H. Newsom, Ceramic ChemCam calibration targets on Mars science laboratory, Space Sci. Rev. 170 (2012) 229–255, https://doi.org/10.1007/s11214-012-9886-0.
[73] M.R. El-Maarry, A. Pommerol, N. Thomas, Desiccation of phyllosilicate-bearing samples as analog for desiccation cracks on Mars: experimental setup and initial results, Planet. Space Sci. 111 (2015) 134–143, https://doi.org/10.1016/j.pss.2015.03.021.
[74] The Martian Garden, Safety data sheet: MMS-2, revised, https://www.themartiangarden.com/s/MMS-2-SDS.pdf, July 2019. (Accessed 12 August 2021).
[75] S.J. Knak Jensen, J. Skibsted, H.J. Jakobsen, I.L. ten Kate, H.P. Gunnlaugsson, J. P. Merrison, K. Finster, E. Bak, J.J. Iversen, et al., A sink for methane on Mars? The answer is blowing in the wind, Icarus 236 (2014) 24–27, https://doi.org/10.1016/j.icarus.2014.03.036.
[76] J.V. Hogancamp, P.D. Archer, J. Gruener, D.W. Ming, V. Tu, JSC-rocknest: a large-scale Mojave Mars simulant (MMS) based soil simulant for in-situ resource utilization water-extraction studies: 50th lunar and planetary science conference 2019 (LPI contrib. No. 2132), https://ntrs.nasa.gov/archive/nasa/casi.ntrs.nasa.gov/20190001833.pdf, 2019. (Accessed 12 August 2021).
[77] J.V. Clark, P.D. Archer, J.E. Gruener, D.W. Ming, V.M. Tu, P.B. Niles, S. A. Mertzman, JSC-Rocknest: A large-scale Mojave Mars Simulant (MMS) based soil simulant for in-situ resource utilization water-extraction studies, Icarus (2020), 113936, https://doi.org/10.1016/j.icarus.2020.113936.
[78] W. Zheng, G. Qiao, Mechanical behavior of the metal parts welded with extraterrestrial regolith simulant by the solar concentrator in ISRU & ISRF application, Adv. Space Res. 65 (2020) 2303–2314, https://doi.org/10.1016/j.asr.2020.02.008.
[79] N. Bost, F. Westall, C. Ramboz, F. Foucher, D. Pullan, A. Meunier, S. Petit, I. Fleischer, G. Klingelhöfer, et al., Missions to Mars: characterisation of Mars analogue rocks for the international space analogue rockstore (ISAR), Planet. Space Sci. 82–83 (2013) 113–127, https://doi.org/10.1016/j.pss.2013.04.006.
[80] E.A. Cloutis, P. Mann, M.R. Izawa, D.M. Applin, C. Samson, R. Kruzelecky, T. D. Glotch, S.A. Mertzman, K.R. Mertzman, et al., The Canadian space agency planetary analogue materials suite, Planet. Space Sci. 119 (2015) 155–172, https://doi.org/10.1016/j.pss.2015.09.001.
[81] C.L. Smith, D. Martin, S.-J. Gill, K. Manick, C.G. Miller, C. Jones, et al., The European space agency exploration sample analogue collection (ESA2C) and curation facility - update, in: Ninth International Conference on Mars, 2019. Held 22-25 July, 2019 in Pasadena, California. LPI Contribution No. 2089, id.6196, https://ui.adsabs.harvard.edu/abs/2019LPICo2089.6196S/abstract. (Accessed 12 August 2021).
[82] A.G. Caporale, S. Vingiani, M. Palladino, C. El-Nakhel, L.G. Duri, A. Pannico, Y. Rouphael, S. de Pascale, P. Adamo, Geo-mineralogical characterisation of Mars simulant MMS-1 and appraisal of substrate physico-chemical properties and crop performance obtained with variable green compost amendment rates, Sci. Total Environ. 720 (2020), 137543, https://doi.org/10.1016/j.scitotenv.2020.137543.
[83] M. Baqué, C. Verseux, U. Böttger, E. Rabbow, J.-P.P. de Vera, D. Billi, Preservation of biomarkers from cyanobacteria mixed with mars-like regolith under simulated martian atmosphere and UV flux, Orig. life Evol. Biosphere J. Int. Soc. Stud. Orig. Life 46 (2016) 289–310, https://doi.org/10.1007/s11084-015-9467-9.
[84] D. Karl, T. Duminy, P. Lima, F. Kamutzki, A. Gili, A. Zocca, J. Günster, A. Gurlo, Clay in situ resource utilization with Mars global simulant slurries for additive manufacturing and traditional shaping of unfired green bodies, Acta Astronaut. 174 (2020) 241–253, https://doi.org/10.1016/j.actaastro.2020.04.064.
[85] A. Abbud-Madrid, D. Beaty, D. Boucher, B. Bussey, R. Davis, L. Gertsch, et al., Mars water in-situ resource utilization (ISRU) planning (M-WIP) study: 90 p, posted April, California Insitute of Technology, https://mepag.jpl.nasa.gov/reports/Mars_Water_ISRU_Study.pdf, 2016. (Accessed 12 August 2021).
[86] J.F. Mustard, S.L. Murchie, S.M. Pelkey, B.L. Ehlmann, R.E. Milliken, J.A. Grant, J.-P. Bibring, F. Poulet, J. Bishop, et al., Hydrated silicate minerals on Mars observed by the Mars reconnaissance orbiter CRISM instrument, Nature 454 (2008) 305, https://doi.org/10.1038/nature07097.
[87] C.C. Allen, R.V. Morris, K.M. Jager, D.C. Golden, D.J. Lindstrom, M.M. Lindstrom, et al., Martian regolith simulant JSC Mars-1, in: 1997, 28th Annual Lunar and Planetary Science Conference, March, vols. 17–21, 1997, p. 27. Houston, TX, https://ui.adsabs.harvard.edu/abs/1997LPI…28…27A/abstract. (Accessed 12 August 2021).
[88] L.A. Leshin, P.R. Mahaffy, C.R. Webster, M. Cabane, P. Coll, P.G. Conrad, P. D. Archer, S.K. Atreya, A.E. Brunner, et al., Volatile, isotope, and organic analysis of martian fines with the Mars Curiosity rover, Science (New York, N.Y.) 341 (2013), 1238937, https://doi.org/10.1126/science.1238937.
[89] A. Eichler, N. Hadland, D. Pickett, D. Masaitis, D. Handy, A. Perez, D. Batcheldor, B. Wheeler, A. Palmer, Challenging the agricultural viability of Martian regolith simulants, Icarus (2020), 114022, https://doi.org/10.1016/j.icarus.2020.114022.
[90] G.W.W. Wamelink, J.Y. Frissel, W.H.J. Krijnen, M.R. Verwoert, P.W. Goedhart, Can plants grow on Mars and the moon: a growth experiment on Mars and moon soil simulants, PLoS One 9 (2014), e103138, https://doi.org/10.1371/journal.pone.0103138.
[91] C. Raúl, G. Martian, Soil as a potential source of nanoparticles: study using martian regolith simulant, Front. Nanosci. Nanotech. 2 (2016) 91–99, https://doi.org/10.15761/FNN.1000115.
[92] The Martian Garden, MMS-2 XRF analysis, https://www.themartiangarden.com/s/MMS-2-SDS.pdf (accessed 12 August 2021).
[93] T. Fujikawa, T. Newson, A. Ahmed, M. Safdar, Assessment of the geo-mechanical properties of Mojave Mars simulant-1 (MMS-1) soil, in: Geotechnical Engineering in the XXI Century: Lessons Learned and Future Challenges: Proceedings of the XVI Pan-American Conference on Soil Mechanics and Geotechnical Engineering (XVI PCSMGE), 17-20 November 2019, Cancun, Mexico, 2019, p. 268, https://doi.org/10.3233/STAL190049, 1643680315.
[94] F. Hanke, in: Evaluation of Techniques for Handling Luminescence in Raman Spectroscopy for Space Application in Regard to the Search for Extraterrestrial Life, 2020, https://doi.org/10.18452/21092.
[95] F. Poulet, J.-P. Bibring, J.F. Mustard, A. Gendrin, N. Mangold, Y. Langevin, R. E. Arvidson, B. Gondet, C. Gomez, et al., Phyllosilicates on Mars and implications for early martian climate, Nature 438 (2005) 623–627, https://doi.org/10.1038/nature04274.
[96] J. Schirmack, M. Alawi, D. Wagner, Influence of Martian regolith analogs on the activity and growth of methanogenic archaea, with special regard to long-term

desiccation, Front. Microbiol. 6 (2015) 210, https://doi.org/10.3389/fmicb.2015.00210.
[97] D. Maus, J. Heinz, J. Schirmack, A. Airo, S.P. Kounaves, D. Wagner, D. Schulze-Makuch, Methanogenic archaea can produce methane in deliquescence-driven Mars analog environments, Sci. Rep. 10 (2020) 6, https://doi.org/10.1038/s41598-019-56267-4.
[98] The Martian Garden, MMS-1 XRF analysis, https://www.themartiangarden.com/s/SDS-MMS-1-Mars-Regolith-Simulant.pdf (accessed 12 August 2021).
[99] T.F. Bristow, E.B. Rampe, C.N. Achilles, D.F. Blake, S.J. Chipera, P. Craig, J. A. Crisp, D.J. Des Marais, R.T. Downs, et al., Clay mineral diversity and abundance in sedimentary rocks of Gale crater, Mars, Sci. Adv. 4 (2018), https://doi.org/10.1126/sciadv.aar3330 eaar3330.
[100] A.A. Hansen, J. Merrison, P. Nørnberg, B.A. Lomstein, K. Finster, Activity and stability of a complex bacterial soil community under simulated Martian conditions, Int.Jnl Astrobiol. 4 (2005) 135, https://doi.org/10.1017/S1473550405002557.
[101] O.B. Toon, J.B. Pollack, C. Sagan, Physical properties of the particles composing the Martian dust storm of 1971–1972, Icarus 30 (1977) 663–696, https://doi.org/10.1016/0019-1035(77)90088-4.
[102] C.N. Achilles, R.T. Downs, D.W. Ming, E.B. Rampe, R.V. Morris, A.H. Treiman, S. M. Morrison, D.F. Blake, D.T. Vaniman, et al., Mineralogy of an active eolian sediment from the Namib dune, Gale crater, Mars, J. Geophys. Res. Planets 122 (2017) 2344–2361, https://doi.org/10.1002/2017JE005262.
[103] A. Scott, C. Oze, M.W. Hughes, Magnesium-based cements for martian construction, J. Aero. Eng. 33 (2020), 4020019, https://doi.org/10.1061/(ASCE)AS.1943-5525.0001132.
[104] A. Buch, D.P. Glavin, R. Sternberg, C. Szopa, C. Rodier, R. Navarro-González, F. Raulin, M. Cabane, P.R. Mahaffy, A new extraction technique for in situ analyses of amino and carboxylic acids on Mars by gas chromatography mass spectrometry, Planet. Space Sci. 54 (2006) 1592–1599, https://doi.org/10.1016/j.pss.2006.05.041.
[105] D. Meunier, R. Sternberg, F. Mettetal, A. Buch, D. Coscia, C. Szopa, C. Rodier, P. Coll, M. Cabanec, et al., A laboratory pilot for in situ analysis of refractory organic matter in Martian soil by gas chromatography–mass spectrometry, Adv. Space Res. 39 (2007) 337–344, https://doi.org/10.1016/j.asr.2005.05.008.
[106] G. Klingelhöfer, R.V. Morris, B. Bernhardt, C. Schröder, D.S. Rodionov, P.A. de Souza, A. Yen, R. Gellert, E.N. Evlanov, et al., Jarosite and hematite at meridiani planum from opportunity's mossbauer spectrometer, Science (New York, N.Y.) 306 (2004) 1740–1745, https://doi.org/10.1126/science.1104653.
[107] D.A. Ramírez, J. Kreuze, W. Amoros, J.E. Valdivia-Silva, J. Ranck, S. Garcia, E. Salas, W. Yactayo, Extreme salinity as a challenge to grow potatoes under Mars-like soil conditions: targeting promising genotypes, Int.Jnl Astrobiol. 18 (2019) 18–24, https://doi.org/10.1017/S1473550417000453.
[108] S.T. Stroble, K.M. McElhoney, S.P. Kounaves, Comparison of the Phoenix Mars lander WCL soil analyses with Antarctic dry valley soils, Mars meteorite EETA79001 sawdust, and a Mars simulant, Icarus 225 (2013) 933–939, https://doi.org/10.1016/j.icarus.2012.08.040.
[109] J. Green, The geology of a Lunar base, Ann. N. Y. Acad. Sci. 105 (1963) 491–625, https://doi.org/10.1111/j.1749-6632.1963.tb42992.x.
[110] W. Phinney, D. Criswell, Lunar resources and their utilization, in: 3rd Conference on Space Manufacturing Facilities, 09-12 May 1977, U.S.A, Princeton, NJ, 1977, https://doi.org/10.2514/6.1977-537.
[111] J.A. Happel, Indigenous materials for lunar construction, Appl. Mech. Rev. 46 (1993) 313, https://doi.org/10.1115/1.3120360.
[112] G. Scheerbaum, In-situ manufacture of martian construction materials, in: Space 2000, Albuquerque, New Mexico, United States, 2000, pp. 934–940, https://doi.org/10.1061/40479(204)111, 9780784404799.
[113] S. Lim, V.L. Prabhu, M. Anand, L.A. Taylor, Extra-terrestrial construction processes – Advancements, opportunities and challenges, Adv. Space Res. 60 (2017) 1413–1429, https://doi.org/10.1016/j.asr.2017.06.038.
[114] M.Z. Naser, Extraterrestrial construction materials, Prog. Mater. Sci. 105 (2019), 100577, https://doi.org/10.1016/j.pmatsci.2019.100577.
[115] M.Z. Naser, Space-native construction materials for earth-independent and sustainable infrastructure, Acta Astronaut. 155 (2019) 264–273, https://doi.org/10.1016/j.actaastro.2018.12.014.
[116] M.Z. Naser, A.I. Chehab, Materials and design concepts for space-resilient structures, Prog. Aero. Sci. 98 (2018) 74–90, https://doi.org/10.1016/j.paerosci.2018.03.004.
[117] C.H. Simonds, Sintering and hot pressing of Fra Mauro composition glass and the lithification of lunar breccias, Am. J. Sci. 273 (1973) 428–439, https://doi.org/10.2475/ajs.273.5.428.
[118] C.C. Allen, J.C. Graf, D.S. McKay, Sintering bricks on the moon, in: R.G. Galloway, S. Lokaj (Eds.), Engineering, Construction, and Operations in Space IV: Proceedings of Space 94, American Society of Civil Engineers, New York, N.Y., 1994, pp. 1220–1229, 9780872629370.
[119] P.E. Hintze, Building a vertical take off and landing pad using in situ materials, Space manufacturing 14: critical technologies for space settlement - space studies institute october 29-31, http://ssi.org/2010/SM14-proceedings/Building-a-Vertical-Take-Off-and-Landing-Pad-using-in-situ-Materials-Hintze.pdf, 2010. (Accessed 12 August 2021).
[120] K. Grossman, Regolith-Based Construction Materials for Lunar and Martian Colonies, Supervisor: Sudipta Seal, University of Central Florida, Orlando, Dissertation, 2018. https://stars.library.ucf.edu/etd/6165. (Accessed 12 August 2021).
[121] D. Karl, F. Kamutzki, A. Zocca, O. Goerke, J. Guenster, A. Gurlo, Towards the colonization of Mars by in-situ resource utilization: slip cast ceramics from Martian soil simulant, PLoS One 13 (2018), e0204025, https://doi.org/10.1371/journal.pone.0204025.
[122] T.T. Meek, D.T. Vaniman, R.D. Blake, M.J. Godbole, Sintering of lunar soil simulants using 2.45 GHz microwave radiation. http://articles.adsabs.harvard.edu/full/1987LPI…18.635M, 1987. (Accessed 12 August 2021).
[123] L.A. Taylor, T.T. Meek, Microwave sintering of lunar soil: properties, theory, and practice, J. Aero. Eng. 18 (2005) 188–196, https://doi.org/10.1061/(ASCE)0893-1321(2005)18:3(188).
[124] R.R. Menezes, P.M. Souto, R.H. Kiminami, Microwave hybrid fast sintering of porcelain bodies, J. Mater. Process. Technol. 190 (2007) 223–229, https://doi.org/10.1016/j.jmatprotec.2007.02.041.
[125] C. Vakifahmetoglu, L. Karacasulu, Cold sintering of ceramics and glasses: a review, Curr. Opin. Solid State Mater. Sci. 24 (2020), 100807, https://doi.org/10.1016/j.cossms.2020.100807.
[126] B.J. Chow, T. Chen, Y. Zhong, Y. Qiao, Direct Formation of structural components using a martian soil simulant, Sci. Rep. 7 (2017) 317, https://doi.org/10.1038/s41598-017-01157-w.
[127] J.D. Blacic, Mechanical properties of lunar materials under anhydrous, hard vacuum conditions: applications of lunar glass structural components, in: W. W. Mendell (Ed.), Lunar Bases and Space Activities of the 21st Century, Washington, DC (USA), 1985, pp. 487–495. https://www.lpi.usra.edu/publications/books/lunar_bases/. (Accessed 12 August 2021).
[128] P. Carpenter, L. Sebille, W. Boles, M. Chadwell, L. Schwarz, JSC mars-1 martian soil simulant: melting experiments and electron microprobe studies, Microsc. Microanal. 9 (2003) 30–31, https://doi.org/10.1017/S1431927603440701.
[129] C.S. Ray, N. Ramachandran, J. Rogers, Developing glassy magnets from simulated composition of moon/mars regolith for exploration applications, MRS Proc 851 (2004), https://doi.org/10.1557/PROC-851-NN10.5.
[130] C.S. Ray, S.T. Reis, W.M. Pontuschka, J.B. Yang, F.F. Sene, J.M. Giehl, C.W. Kim, S. Sen, Mössbauer and EPR spectra for glasses and glass-ceramics prepared from simulated compositions of Lunar and Martian soils, J. Non-Cryst. Solids 352 (2006) 3677–3684, https://doi.org/10.1016/j.jnoncrysol.2006.02.117.
[131] C.S. Ray, S.T. Reis, S. Sen, Characterization and glass formation of JSC-1 lunar and martian soil simulants, AIP Conf. Proc. 969 (2008) 908, https://doi.org/10.1063/1.2845057.
[132] J. Schleppi, J. Gibbons, A. Groetsch, J. Buckman, A. Cowley, N. Bennett, Manufacture of glass and mirrors from lunar regolith simulant, J. Mater. Sci. 54 (2019) 3726–3747, https://doi.org/10.1007/s10853-018-3101-y.
[133] R. Boyd, P. Thomson, B. Clark, Duricrete and composites construction on Mars, in: C.R. Stoker (Ed.), The Case for Mars III: Strategies for Exploration - General Interest and Overview: Proceedings of the Third Case for Mars Conference Held July 18-22, 1987, at the University of Colorado, Published by, Univelt for the American Astronautical Society, 1989, 0877033048.
[134] Y. Ishikawa, Utilization of regolith for manufacturing construction material on Mars, chapter 19.1 - habitat on Mars, in: V. Badescu (Ed.), Mars: Prospective Energy and Material Resources, Springer, Berlin, Heidelberg, 2009, pp. 543–550, https://doi.org/10.1007/978-3-642-03629-3_19, 978-3-642-03629-3.
[135] B.J. Chow, T. Chen, Y. Zhong, M. Wang, Y. Qiao, Compaction of montmorillonite in ultra-dry state, Adv. Space Res. 60 (2017) 1443–1452, https://doi.org/10.1016/j.asr.2017.07.001.
[136] A. Heath, D. Maskell, P. Walker, M. Lawrence, C. Fourie, Modern earth masonry: structural properties and structural design. 2012, Struct. Eng. 90 (2012) 38–44. http://www.istructe.org/webtest/files/60/6093d338-aa24-4ff8-8de5-99bc757940f8.pdf. (Accessed 20 December 2019).
[137] L.A. Beyer, Lunarcrete - a novel approach to extraterrestrial construction, in: B. Faughnan, G. Maryniak (Eds.), Space Manufacturing V: Engineering with Lunar and Asteroidal Materials: Proceedings of the 7th Princeton/AIAA/SSI Conference. Space Studies Institute, Princeton, and AIAA, New York, American Institute of Aeronautics and Astronautics, New York, 1985, pp. 8–11, 093040307X.
[138] D. Karl, A. Gurlo, Synthetic H2O weathering of simple feldspar lunar regolith simulants aiming to build high strength 'sandcastles' using fusion drying, in: 17th Biennial International Conference on Engineering, Science, Construction, and Operations in Challenging Environments, Virtual Conference, 2021, pp. 958–969, https://doi.org/10.1061/9780784483374.087, 9780784483374.
[139] D.S. McKay, B.L. Cooper, L.A. Taylor, J.T. James, K. Thomas-Keprta, C.M. Pieters, S.J. Wentworth, W.T. Wallace, T.S. Lee, Physicochemical properties of respirable-size lunar dust, Acta Astronaut. 107 (2015) 163–176, https://doi.org/10.1016/j.actaastro.2014.10.032.
[140] T.D. Lin, H. Love, D. Stark, Physical properties of concrete made with Apollo 16 lunar soil sample, in: W. Mendell (Ed.), The Second Conference on Lunar Bases and Space Activities of the 21st Century, Proceedings from a Conference Held in Houston, TX, April 5-7, 1988, NASA Conference Publication 3166, NASA, 1992, p. 159. https://space.nss.org/the-second-conference-on-lunar-bases-and-space-activities-of-the-21st-century/. (Accessed 12 August 2021).
[141] D.S. McKay, C.C. Allen, Concrete — a practical construction material for Mars, in: Engineering, Construction, and Operations in Space V, Albuquerque, New Mexico, United States, 1996, pp. 566–570, https://doi.org/10.1061/40177(207)78, 9780784401774.
[142] C.S. Desai, K. Girdner, Structural materials from lunar simulants through thermal liquefaction, in: W.Z. Sadeh, S. Sture, R. Miller (Eds.), Engineering, Construction, and Operations in Space III: Space '92 Proceedings of the Third International Conference, Denver, Colorado, 31 May-4 June 1992, American Society of Civil Engineers, New York, 1992, pp. 528–536, 9780872628687.
[143] R.N. Grugel, Sulfur Concrete for Lunar Applications-Environmental Considerations, Marshall Space Flight Center, Alabama, 2008. NASA/

TM—2008–215250, https://ntrs.nasa.gov/archive/nasa/casi.ntrs.nasa.gov/20080022947.pdf. (Accessed 12 August 2021).
[144] L. Wan, R. Wendner, G. Cusatis, A novel material for in situ construction on Mars: experiments and numerical simulations, Construct. Build. Mater. 120 (2016) 222–231, https://doi.org/10.1016/j.conbuildmat.2016.05.046.
[145] M. Troemner, G. Cusatis, Martian material sourcing challenges propel earth construction opportunities, Matter 1 (2019) 547–549, https://doi.org/10.1016/j.matt.2019.07.023.
[146] H.B. Franz, P.L. King, F. Gaillard, Sulfur on Mars from the atmosphere to the core, in: Volatiles in the Martian Crust, Elsevier, 2019, ISBN 9780128041918, pp. 119–183, https://doi.org/10.1016/B978-0-12-804191-8.00006-4.
[147] A. Alexiadis, F. Alberini, M.E. Meyer, Geopolymers from lunar and Martian soil simulants, Adv. Space Res. 59 (2017) 490–495, https://doi.org/10.1016/j.asr.2016.10.003.
[148] C. Montes, K. Broussard, M. Gongre, N. Simicevic, J. Mejia, J. Tham, E. Allouche, G. Davis, Evaluation of lunar regolith geopolymer binder as a radioactive shielding material for space exploration applications, Adv. Space Res. 56 (2015) 1212–1221, https://doi.org/10.1016/j.asr.2015.05.044.
[149] N. Shiwei, S. Dritsas, J.G. Fernandez, Martian biolith: a bioinspired regolith composite for closed-loop extraterrestrial manufacturing, PLoS One 15 (2020), e0238606, https://doi.org/10.1371/journal.pone.0238606.
[150] S. Sen, S. Carranza, S. Pillay, Multifunctional Martian habitat composite material synthesized from in situ resources, Adv. Space Res. 46 (2010) 582–592, https://doi.org/10.1016/j.asr.2010.04.009.
[151] E.J. Faierson, K.V. Logan, B.K. Stewart, M.P. Hunt, Demonstration of concept for fabrication of lunar physical assets utilizing lunar regolith simulant and a geothermite reaction, Acta Astronaut. 67 (2010) 38–45, https://doi.org/10.1016/j.actaastro.2009.12.006.
[152] G. Corrias, R. Licheri, R. Orrù, G. Cao, Self-propagating high-temperature reactions for the fabrication of Lunar and Martian physical assets, Acta Astronaut. 70 (2012) 69–76, https://doi.org/10.1016/j.actaastro.2011.07.022.
[153] B.A. Lomax, M. Conti, N. Khan, N.S. Bennett, A.Y. Ganin, M.D. Symes, Proving the viability of an electrochemical process for the simultaneous extraction of oxygen and production of metal alloys from lunar regolith, Planet. Space Sci. (2019), 104748, https://doi.org/10.1016/j.pss.2019.104748.
[154] S.S. Schreiner, Molten Regolith Electrolysis Reactor Modeling and Optimization of In-Situ Resource Utilization Systems, Massachusetts Institute of Technology (MIT), Master thesis at the Department of Aeronautical and Astronautical Engineering, 2015. https://dspace.mit.edu/bitstream/handle/1721.1/98589/921147148-MIT.pdf?sequence=1. (Accessed 12 August 2021).
[155] K.D. Grossman, T.S. Sakthivel, L. Sibille, J.G. Mantovani, S. Seal, Regolith-derived ferrosilicon as a potential feedstock material for wire-based additive manufacturing, Adv. Space Res. 63 (2019) 2212–2219, https://doi.org/10.1016/j.asr.2018.12.002.
[156] P.H. Smith, L.K. Tamppari, R.E. Arvidson, D. Bass, D. Blaney, W.V. Boynton, A. Carswell, D.C. Catling, B.C. Clark, et al., H2O at the Phoenix landing site, Science (New York, N.Y.) 325 (2009) 58–61, https://doi.org/10.1126/science.1172339.
[157] N. Ishikawa, H. Kanamori, T. Okada, The possibility of concrete production on the Moon, in: W. Mendell (Ed.), The Second Conference on Lunar Bases and Space Activities of the 21st Century, Proceedings from a Conference Held in Houston, TX, April 5-7, 1988, NASA Conference Publication 3166, NASA, 1992. https://space.nss.org/the-second-conference-on-lunar-bases-and-space-activities-of-the-21st-century/. (Accessed 12 August 2021).
[158] M. Morris, C. Ciardullo, K. Lents, J. Montes, O. Rudakevych, M. Sono, Y. Sono, M. Yashar, Mars ice house: using the physics of phase change in 3D printing a habitat with H2O, in: AIAA Space 2016, Long Beach, California, American Institute of Aeronautics and Astronautics, 2016, p. 211, https://doi.org/10.2514/6.2016-5528, 978-1-62410-427-5.
[159] J.J. Petrovic, Review Mechanical properties of ice and snow, J. Mater. Sci. 38 (2003) 1–6, https://doi.org/10.1023/A:1021134128038.
[160] B. Khoshnevis, R. Dutton, Innovative rapid prototyping process makes large sized, smooth surfaced complex shapes in a wide variety of materials, Mater. Technol. 13 (1998) 53–56, https://doi.org/10.1080/10667857.1998.11752766.
[161] I. Gibson, D. Rosen, B. Stucker, Additive Manufacturing Technologies: 3D Printing, Rapid Prototyping, and Direct Digital Manufacturing, second ed., vol. 2015, Springer New York, New York NY, 2015, 978-1-4939-2113-3.
[162] A. Gebhardt, J.-S. Hötter, Additive Manufacturing: 3D Printing for Prototyping and Manufacturing, Carl Hanser Fachbuchverlag, Munich, Cincinnati, OH, 2016, https://doi.org/10.3139/9781569905838, 9781569905821.
[163] A. Bandyopadhyay, S. Bose, Additive Manufacturing, CRC Press, Boca Raton, 2016, https://doi.org/10.1201/b18893, 1523107588.
[164] ISO, Additive Manufacturing - General Principles - Part 1: Terminology, 2015th ed.(52900), 2016.
[165] ISO, Additive Manufacturing - General Principles - Part 2: Overview of Process Categories and Feedstock, second ed.(17296-2), 2015.
[166] R.P. Mueller, S. Howe, D. Kochmann, H. Ali, C. Andersen, H. Burgoyne, W. Chambers, R. Clinton, X. de Kestellier, et al., Automated additive construction (AAC) for earth and space using in situ resources, in: Earth and Space 2018, Cleveland, Ohio, 2018, pp. 354–377, https://doi.org/10.1061/9780784479971.036, 9780784481899.
[167] B. Khoshnevis, Automated construction by contour crafting—related robotics and information technologies, Autom. ConStruct. 13 (2004) 5–19, https://doi.org/10.1016/j.autcon.2003.08.012.
[168] B. Khoshnevis, M. Bodiford, K. Burks, E. Ethridge, D. Tucker, W. Kim, H. Toutanji, M. Fiske, Lunar contour crafting - a novel technique for ISRU-based habitat development, in: 43rd AIAA Aerospace Sciences Meeting and Exhibit, Nevada, Reno, 2005, https://doi.org/10.2514/6.2005-538, 978-1-62410-064-2.
[169] J.E. Edmunson, M.R. Fiske, R.P. Mueller, H.S. Alkhateb, A.K. Akhnoukh, H. C. Morris, I.I. Townsend, J.C. Fikes, M.M. Johnston, Additive construction with mobile emplacement: multifaceted planetary construction materials development, in: Earth and Space 2018, Cleveland, Ohio, 2018, pp. 782–792, https://doi.org/10.1061/9780784481899.074, 9780784481899.
[170] B. Khoshnevis, X. Yuan, B. Zahiri, J. Zhang, B. Xia, Construction by Contour Crafting using sulfur concrete with planetary applications, Rapid Prototyp. J. 22 (2016) 848–856, https://doi.org/10.1108/RPJ-11-2015-0165.
[171] M.R. Fiske, J.E. Edmunson, Additive Construction with Mobile Emplacement (ACME) 3D Printing Structures with In-Situ Resources, University of Alabama Presentation, 2017. Document ID: 20170011110, https://ntrs.nasa.gov/search?q=20170011110. (Accessed 12 August 2021).
[172] M. Hojati, S. Nazarian, J.P. Duarte, A. Radlinska, N. Ashrafi, F. Craveiro, S. Bilen, 3D printing of concrete: a continuous exploration of mix design and printing process, in: Proceedings of the 42nd IAHS World Congress on the Housing for the Dignity of Mankind, Naples, Italy, 2018, p. 124, 10-13th April, https://www.researchgate.net/publication/325076823_3D_Printing_of_Concrete_a_Continuous_Exploration_of_Mix_Design_and_Printing_Process. (Accessed 12 August 2021).
[173] S. Pilehvar, M. Arnhof, R. Pamies, L. Valentini, A.-L. Kjøniksen, Utilization of urea as an accessible superplasticizer on the moon for lunar geopolymer mixtures, J. Clean. Prod. (2019), 119177, https://doi.org/10.1016/j.jclepro.2019.119177.
[174] A.E. Jakus, K.D. Koube, N.R. Geisendorfer, R.N. Shah, Robust and elastic lunar and martian structures from 3D-printed regolith inks, Sci. Rep. 7 (2017), 44931, https://doi.org/10.1038/srep44931.
[175] C. Buchner, R.H. Pawelke, T. Schlauf, A. Reissner, A. Makaya, A new planetary structure fabrication process using phosphoric acid, Acta Astronaut. 143 (2018) 272–284, https://doi.org/10.1016/j.actaastro.2017.11.045.
[176] M.C. Leu, W. Zhang, G. Sui, An experimental and Analytical study of ice Part Fabrication with rapid freeze prototyping, CIRP Annals 49 (2000) 147–150, https://doi.org/10.1016/S0007-8506(07)62916-3.
[177] T. Huang, M.S. Mason, X. Zhao, G.E. Hilmas, M.C. Leu, Aqueous-based freeze-form extrusion fabrication of alumina components, Rapid Prototyp. J. 15 (2009) 88–95, https://doi.org/10.1108/13552540910943388.
[178] M. Fateri, M. Khosravi, On-site additive manufacturing by selective laser melting of composite objects, Concepts and Approaches for Mars Exploration, held June 12-14, 2012 in Houston, Texas. LPI Contribution No. 1679, id.4368, https://ui.adsabs.harvard.edu/abs/2012LPICo1679.4368F/abstract, 2012. (Accessed 12 August 2021).
[179] M. Fateri, A. Gebhardt, Process parameters development of selective laser melting of lunar regolith for on-site manufacturing applications, Int. J. Appl. Ceram. Technol. 12 (2015) 46–52, https://doi.org/10.1111/ijac.12326.
[180] A. Goulas, J.G. Binner, R.A. Harris, R.J. Friel, Assessing extraterrestrial regolith material simulants for in-situ resource utilisation based 3D printing, Appl. Mater. Today 6 (2017) 54–61, https://doi.org/10.1016/j.apmt.2016.11.004.
[181] A. Goulas, J.G.P. Binner, D.S. Engstrøm, R.A. Harris, R.J. Friel, Mechanical behaviour of additively manufactured lunar regolith simulant components, Proc. IMechE 233 (2019) 1629–1644, https://doi.org/10.1177/1464420718777932.
[182] L. Caprio, A.G. Demir, B. Previtali, B.M. Colosimo, Determining the feasible conditions for processing lunar regolith simulant via laser powder bed fusion, Addit. Manuf. 32 (2020), 101029, https://doi.org/10.1016/j.addma.2019.101029.
[183] P. Hintze, J. Curran, T. Back, Lunar surface stabilization via sintering or the use of heat cured polymers, in: 47th AIAA Aerospace Sciences Meeting Including the New Horizons Forum and Aerospace Exposition, Orlando, Florida, 2009, https://doi.org/10.2514/6.2009-1015, 978-1-60086-973-0.
[184] P.E. Hintze, S. Quintana, Building a lunar or martian launch pad with in situ materials: recent laboratory and field studies, J. Aero. Eng. 26 (2013) 134–142, https://doi.org/10.1061/(ASCE)AS.1943-5525.0000205.
[185] H.R. Fischer, In-situ resource utilization–feasibility of the use of lunar soil to create structures on the moon via sintering based additive manufacturing technology, AAOAJ 2 (2018), https://doi.org/10.15406/aaoaj.2018.02.00056.
[186] A. Meurisse, A. Makaya, C. Willsch, M. Sperl, Solar 3D printing of lunar regolith, Acta Astronaut. 152 (2018) 800–810, https://doi.org/10.1016/j.actaastro.2018.06.063.
[187] G. Cesaretti, E. Dini, X. de Kestelier, V. Colla, L. Pambaguian, Building components for an outpost on the Lunar soil by means of a novel 3D printing technology, Acta Astronaut. 93 (2014) 430–450, https://doi.org/10.1016/j.actaastro.2013.07.034.
[188] S.A. Walling, J.L. Provis, Magnesia-based cements: a journey of 150 Years, and cements for the future? Chem. Rev. 116 (2016) 4170–4204, https://doi.org/10.1021/acs.chemrev.5b00463.
[189] V.K. Balla, L.B. Roberson, G.W. O'Connor, S. Trigwell, S. Bose, A. Bandyopadhyay, First demonstration on direct laser fabrication of lunar regolith parts, Rapid Prototyp. J. 18 (2012) 451–457, https://doi.org/10.1108/13552541211271992.
[190] B. Khoshnevis, J. Zhang, Selective separation sintering (SSS) - an additive manufacturing approach for fabrication of ceramic and metallic parts with application in planetary construction, in: AIAA SPACE 2015 Conference and Exposition, Pasadena, California, 2015, p. 204, https://doi.org/10.2514/6.2015-4450, 978-1-62410-334-6.
[191] M. Schwentenwein, J. Homa, A. Makaya, 3D-printed ceramic parts made from lunar regolith. ESA, http://www.esa.int/ESA_Multimedia/Images/2018/11/3D-printed_ceramic_parts_made_from_lunar_regolith (accessed 12 August 2021).

[192] A.A. Altun, F. Ertl, M. Marechal, A. Makaya, A. Sgambati, M. Schwentenwein, Additive manufacturing of lunar regolith structures, Open Ceramics 5 (2021), 100058, https://doi.org/10.1016/j.oceram.2021.100058.
[193] M. Liu, W. Tang, W. Duan, S. Li, R. Dou, G. Wang, B. Liu, L. Wang, Digital light processing of lunar regolith structures with high mechanical properties, Ceram. Int. 45 (2019) 5829–5836, https://doi.org/10.1016/j.ceramint.2018.12.049.
[194] A. Sgambatia, M. Berga, F. Rossia, A. Daurskikhb, B. Imhofc, R. Davenportc, P. Weiss, M. Peer, T. Gobert, et al., URBAN: conceiving a lunar base using 3D printing technologies, IAC-18.D3.3.7x42605, in: Proceedings of the 69th International Astronautical Congress (IAC 2018), Bremen, Germany, 2018. https://www.academia.edu/37564343/URBAN_conceiving_a_lunar_base_using_3D_printing_technologies. (Accessed 12 August 2021).
[195] W.J. O'Hara, J.M. Kish, M.J. Werkheiser, Turn-key use of an onboard 3D printer for international space station operations, Addit. Manuf. 24 (2018) 560–565, https://doi.org/10.1016/j.addma.2018.10.029.
[196] T. Prater, M. Moraguez, In-space manufacturing: the gateway to the high frontier and an enabling technology for human space exploration: Tennessee valley interstellar workshop. https://ntrs.nasa.gov/api/citations/20200000035/downloads/20200000035.pdf, 2019. (Accessed 30 September 2021).
[197] J. Peels, Made in space to launch ceramic SLA 3D printer to ISS. https://3dprint.com/273236/made-in-space-to-launch-ceramic-sla-3d-printer-to-iss/, 2020. (Accessed 29 September 2021).
[198] O. D'Angelo, F. Kuthe, S.-J. Liu, R. Wiedey, J.M. Bennett, M. Meisnar, et al., A gravity-independent powder-based additive manufacturing process tailored for space applications. http://arxiv.org/pdf/2102.09815v1, 2021. (Accessed 29 September 2021).
[199] A. Zocca, J. Lüchtenborg, T. Mühler, J. Wilbig, G. Mohr, T. Villatte, F. Léonard, G. Nolze, M. Sparenberg, et al., Enabling the 3D printing of metal components in μ-gravity, Adv. Mater. Technol. 4 (2019), 1900506, https://doi.org/10.1002/admt.201900506.
[200] W. Li, D. Lan, Y. Wang, Exploration of direct-ink-write 3D printing in space: droplet dynamics and patterns formation in microgravity, Microgravity Sci. Technol. 32 (2020) 935–940, https://doi.org/10.1007/s12217-020-09820-0.